ISSN:0000-0000

ENOCH PUBLISHING CORPORATION

Lipid and Cardiovascular Research

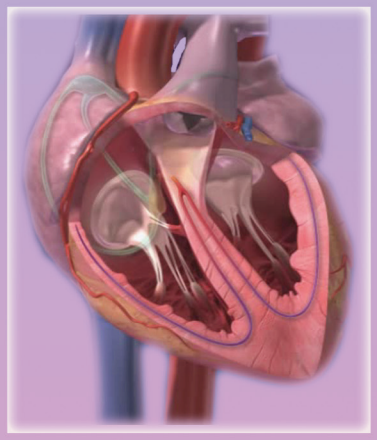

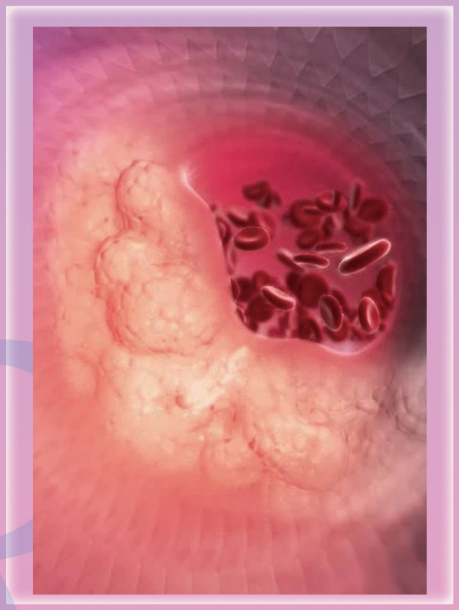

LCR:Vol 1,No 1(2015)

Lipid and Cardiovascular Research

About the Journal

Lipid and Cardiovascular Research (LCR) is an open access, peer-reviewed, international journal available in print and online, aiming to the rapid dissemination of novel and significant studies in all areas of lipids and cardiovascular diseases. Issues of LCR are published quarterly by Enoch Publishing Corporation, Georgia, USA, and the journal's full text is available online at http://www.enochpublisher.com/lcr. LCR is currently working towards being indexed (Science Citation IndexExpanded, Medline (PubMed), BIOSIS, Scopus).

Scope of the Journal

The journal publishes original articles, reviews, editorials, letters to the editor, rapid communications and case reports in English, focusing on basic, translational and clinical research in the fields of lipids and cardiovascular diseases. Areas that are covered include, but are not limited to molecular biology, cell biology, pathophysiology, immunology, genetics, pharmacology, pathogenesis, epidemiology and surgical techniques that are in the lines of the prevention, diagnosis, therapy of lipids and cardiovascular diseases, as well as their complications.

Target Audience/Readers

Target readers include medical associates, technologists, students, intern or resident physicians, clinical fellows, specialists in cardiology, as well as scientists who are interested in the field of lipids and cardiology, and employees of pharmaceutical entities.

THE EDITORIAL BOARD OF LIPID AND CARDIOVASCULAR RESEARCH

THE EDITORIAL BOARD OF LIPID AND CARDIOVASCULAR RESEARCH

CONTENTS

Lipid and Cardiovascular Research. 2015;**01**(1):01
http://www.enochpublisher.com/LCR

ENOCH PUBLISHING CORPORATION

Introducing the Lipid and Cardiovascular Research

Jian-Jun Li, M.D., Ph.D., FESC, FACC
Professor, Cardiology
Director, Center for Dyslipidemia&CVD

Cardiovascular disease (CVD) is one of the most common diseases seriously harmful to human health. The death toll associated with CVD has surpassed that of other diseases, including cancer and respiratory disease, and continues to increase. Atherosclerosis (AS) is the leading cause of the occurrence and development of CVD. AS may arise in blood vessels throughout the body and may promote the development of other diseases. The narrowing of the arteries due to cholesterol buildup in the blood vessel walls is largely responsible for AS. Abnormal blood lipid levels, especially hypercholesterolemia, have been regarded as a leading cause of cardiovascular events. In addition, abnormal lipid metabolism can also lead to hyperlipidemia, nonalcoholic fatty liver disease (NAFLD), cancer, and neurodegenerative diseases, among other diseases. However, abnormalities in cholesterol metabolism are extremely complex, and a number of different associated aspects require further examination. In addition, more research is needed on the treatment or prevention of AS and CVD. Forums for sharing research results and exchanging information are thus especially welcome.

I am delighted to hereby introduce *Lipid and Cardiovascular Research*, a newly launched, open access, peer-reviewed, international journal available in print and online, with the aim of providing a global forum for the rapid dissemination of significant, original research results related to all aspects of lipids and CVD. Target readers of this journal include, but are not limited to, medical associates, technologists, students, intern or resident physicians, clinical fellows, specialists in cardiology, as well as scientists who are interested in the field of lipids and cardiology, and employees of pharmaceutical entities.

We are currently in the process of building an outstanding international Editorial Board comprised of clinicians, teachers, and investigators from around the world, who seek to ensure that our journal is of superior quality and meets the needs of contributors and readers. The editorial board and its members aspire to provide prompt, impartial, high-quality service to all contributors and readers at all times.

Original articles, reviews, editorials, letters to the editor, rapid communications, and case reports in English, covering basic, translational, and clinical research in the fields of lipids and CVD, will be considered. We look forward to your submissions to *Lipid and Cardiovascular Research*.

Division of Dyslipidemia, State Key Laboratory of Cardiovascular Disease, Fu Wai Hospital, National Center for CVDs, Chinese Academy of Medical Sciences, Peking Union Medical College, Beijing 100037, China; Tel: +86-10-88396077; E-mail: lijianjun938@126.com

Lipid and Cardiovascular Research. 2015;**01**(1):02-11
http://www.enochpublisher.com/LCR

REVIEW

Endoplasmic Reticulum Stress Signaling in Atherosclerosis

Wen-Cheng Nie, Hui Yan, Shan Li, Wei-Guo Zhu, Fang-Yan Fan*

Abstract

There is increasing evidence for the activation of endoplasmic reticulum (ER) stress signaling in the pathogenesis of atherosclerosis. The ER is one of the functional eukaryotic organelles and is responsible for the folding of immature proteins. Under ordinary conditions, misfolded or unfolded proteins can be recognized by the ER; however, abundant accumulation of unfolded proteins stimulated by various risk factors, such as oxidative stress and aberrant expression of folded proteins, will cause an ER stress response. The unfolded protein response (UPR) and induced reduction of unfolded proteins is such an initial response for ER stress. Nevertheless, once accumulated UPR exceeds the ER processing capacity, apoptosis-related signals are activated, thereby contributing to vascular dysfunction. This progress is mainly derived from incidents of damage by macrophages, endothelial cells, and smooth muscle cells. The progression of atherosclerosis is thereby linked to these ER-initiated events. This internal relation provides a prospect to explore comprehensive knowledge of the mechanisms underlying ER-stress-initiated molecular pathology in atherosclerosis, so as to search for new targets for medical and interventional treatments.

Keywords: endoplasmic reticulum stress, endothelial cells, vascular smooth muscle cell, macrophages

Introduction-Atherosclerosis and endoplasmic reticulum stress

Atherosclerotic vascular disease is increasingly developing into a major health burden on a global scale (1). As for the pathological process, retention of apolipoprotein B (apo B)-integrating lipoproteins in the local domain of the arterial subendothelium initiates the plaque formation that leads to atherogenesis (2, 3). These abnormal physiological states of lipoproteins might experience modification through enzymatic and oxidative patterns, and subsequently arouse a range of disadvantageous inflammatory responses (4-6). Among these inflammation-related responses, primary monocytes move to lipoprotein retention domains around endothelial cells, then the directional differentiation of macrophages occurs (7, 8). The generated macrophages focus on internalization of the enzymatically and oxidatively modified low density lipoproteins (LDLs) in the endothelium, thereby resulting in the formation of foam cells (9-11). In addition, the activated macrophages induce an inflammation reaction around retained lipoproteins by recruiting various inflammatory cells into the developing lesion. Moreover, the inflammatory reaction becomes continuously larger along with the continuing process of lipoprotein retention (12).

Generally, the comprehensive interaction between cell biological and physiological factors constitutes the initiation and development of atherosclerosis. Initially, harmful hematological and metabolic factors, such as diabetes (13), lipid metabolism disorders (14), high blood pressure (15), and poor lifestyle habits (16, 17), induce irritable enrichment of circulating apo B lipoproteins. Based on this event, atheromatous plaques in the arterial wall progress in response to hematologic systemic risk factors through a series of cellular and molecular metabolic processes, including controlling apo B lipoprotein modification; inflammation in endothelial cells (ECs), especially activated by macrophages; then, introduction of intimal vascular smooth muscle cell (VSMC) proliferation. On the other hand, the molecular pathology basis for this involves the activation of inflammatory factors, collagen biosynthesis, intimal cell apoptosis, and cell clearance. Accumulated evidence emphasizes that endoplasmic reticulum (ER) stress is activated during these pathological processes.

The ER is an organelle that functions as an essential regulator in multiple cellular processes, including the folding of secretory and membrane proteins, calcium homeostasis, and participating in lipid and glucose metabolism (18-20). A variety of harmful factors for atherogenesis can

Department of Cardiology, the First Affiliated Hospital of Zhejiang University, School of Medicine, Hangzhou 310003, China

* Corresponding author: Wen-Cheng Nie
Department of Cardiology, the First Affiliated Hospital of Zhejiang University, School of Medicine, No. 79, Qingchun Road, Hangzhou 310003, Zhejiang, China
Tel: +86-571-87236500; Fax: +86-571-87236794
E-Mail: jacky6665@zju.edu.cn

Received: 15 September 2015 / Accepted: 3 December 2015
Published online: 29 December 2015

disturb ER function, contributing to the increasing accumulation of unfolded and misfolded proteins in the ER. Upon this aggregation, ER transmembrane sensors are activated, thereby inducing the unfolded protein response (UPR) to adapt the cell to stress (21). Under normal, non-stress conditions, three transmembrane sensors, including protein kinase-like ER kinase (PERK), inositol-requiring kinase 1 (IRE1), and the transcriptional factor activating transcription factor 6 (ATF6) (22-24), are kept in inactivated states through interacting with the protein chaperone glucose-regulated protein 78 (GRP78)/BiP. Following the detection of unfolded proteins, sensors separate from GRP78, enter the activated state, and thereby induce initiation of the UPR. Proper UPR is beneficial for cell survival, however, when ER stress is prolonged, the cell will suffer programmed cell death (apoptosis). Recent studies have suggested that the UPR and ER-initiated apoptosis are implicated in the pathophysiology of various human diseases (25-27), and are especially closely correlated with the pathological process of cardiovascular disease (28). This review summarizes (1) the molecular mechanisms of the UPR and ER-initiated cellular function change; and (2) their involvement in the cellular pathophysiology of atherosclerosis.

Cell physiological basis of ER stress in Atherosclerosis

Prolonged ER stress that is derived from sustained dysfunction of protein folding, and other processes that contribute to chronic disturbances in ER, are recognized as the essential basis for the pathological process of atherosclerosis (29). This fact is related to morphological and molecular evidence that have been presented in the analysis of experimental formation of atherosclerotic lesions in animals and human atherosclerotic lesions, which have shown that ER stress promotes the formation and maintenance of atherosclerotic plaques (30). Furthermore, alleviation of ER stress-initiated atherosclerosis-related apoptotic and inflammatory signaling occurs (31, 32). Considering that the three cell types mentioned above (ECs, VSMC and macrophages) dominate the cellular basis of atherosclerotic pathogenesis, this review has been designed to elucidate the ER stress-related signaling pathway in the pathological activity in these cells (Figure 1).

Macrophages and atherosclerosis

Under their normal behavior, macrophages are responsible for taking in apo B-carrying lipoproteins and transporting them to the ER for subsequent cholesterol esterification. Evidence of the accumulation of massive amounts of unesterified or "free" cholesterol (FC) in advanced macrophage lesions is provided by studies that suggest that the formation of lesions is accompanied by possible failure of the biological process of cholesterol re-esterification (33, 34). In addition, atherosclerotic lesions generate abundant 7-ketocholesterol (7KC) (35), which associates with accumulated FC and can cause ER stress-induced macrophage death. Apoptotic cell debris is timely phagocytized by macrophages in early plaques (36), while macrophages in advanced plaques cannot efficiently clear dying cells and, thereby, plaques are transformed into inflammatory necrotic cores. This process is driven by anti-inflammatory cytokines such as transforming growth factor- β (TGF-) (37) and interleukin-10 (IL-10) (38).

VSMCs and atherosclerosis

It is considered that the presence of VSMCs within advanced atherosclerotic plaques is beneficial and protective, due to their pivotal role in the formation and sustenance of the fibrous cap that guards advanced lesions from plaque rupture and subsequent thrombosis (39). On the other, disadvantageous hand, VSMCs may undergo phenotypic

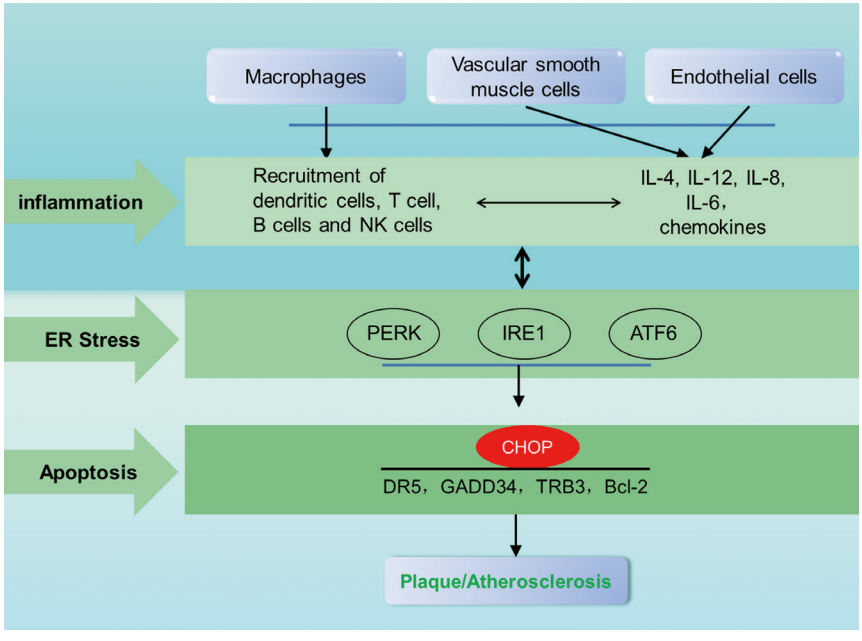

Figure 1. Cell physiological basis of endoplasmic reticulum (ER) stress in atherosclerosis. A basis underlying atherosclerosis is inflammation that occurs in cells of the artery and blood system, monocyte/macrophage recruitment that occurs on the arterial wall, and subsequent endoplasmic reticulum (ER) stress. CHOP is the pro-apoptotic bZIP transcription factor that is regulated mainly by PERK-, IRE1-, and ATF6-dependent pathways. CHOP has been shown to activate the transcription of several genes, including GADD34, TRB3, Bcl-2, and DR5, which may facilitate apoptosis.

modulation from a contractile to a synthetic phenotype, proliferation and intima-oriented migration, and transformation into foam cells, thereby promoting plaque development and bringing about atherogenesis (40, 41). Moreover, apoptosis of VSMCs in plaques destabilizes the lesion and subsequently decreases collagen production, resulting in failure of the formation of the protective fibrous cap (40). A potential mechanism underlying all of these progressions is correlated with ER stress due to identification of several inducers of ER stress in VSMCs. In in vitro cell studies, C/EBP homologous protein (CHOP), a mediator for ER stress-induced apoptosis, was significantly elevated in 7KC (42), unesterified cholesterol (43), homocysteine (44), or hepcidin (45) treated VSMCs. Although there may be increasing ER stress markers, such as UPR activation (46) and cholesterol overload (47) in VSMCs, which have been found in lesions of diabetic animal models or human hyperglycemia, there is little evidence focusing on a possible correlation between UPR activation and VSMC apoptosis. By using cultured VSMCs, activation of the IRE1 branch of the UPR is identified in studies using 7KC (48). Thus, further research is needed for the investigation of the mechanism of ER stress-induced apoptosis in VSMCs (49).

ECs and atherosclerosis

Activated ER stress has also been identified in endothelial cells both in in vitro cultured cells and in experimental animals (50, 51). ER stress induced by atherosclerosis-interrelated inducers in ECs can activate the IRE1 branch of the UPR, NF kappa B, and modified forms of LDL (52-54). These studies demonstrated that ECs were more inclined to alternate lipoprotein permeability and recruit inflammatory cells rather than undergo autologous apoptosis. The critical role of unbroken endothelium in the process of atherosclerosis is its isolating action between the atherosclerotic plaque and the vessel lumen. Nevertheless, Ampem et al. found that ER stress can induce apoptosis of ECs via controlling cellular calcium (Ca2+), independent of transient receptor potential canonical 3 (TRPC3) channels in in vitro cell culture (55). Apoptosis in ECs develops as an accident of procoagulant and pro-adhesiveness of platelets. The immediate consequence following this development is plaque erosion or rupture (56). To date, clear mechanisms addressing the causal relationship between ER stress and endothelial cell apoptosis, as well as between these occurrences, and atherosclerosis progress in vivo are not yet definitive and therefore imply a potential opportunity for further exploratory research in this field.

Multiple signals/mechanisms underlying ER stress-mediated Atherosclerosis

CHOP-mediated ER stress-induced cell death

Probably the most significant ER stress-induced apoptotic pathway is mediated through CHOP. CHOP functions as a critical mediator connecting accumulation and aggregation of unfolded proteins in the ER and oxidative stress (Figure 2). In vitro tissue analysis points out the direct evidence and demonstrates strong CHOP expression in advanced lesions (43, 57). CHOP commonly induces, through ATF6 and PERK, UPR pathways during the pathological process of atherosclerosis (58, 59). The short-term induction of CHOP is beneficial for protective UPR, whereas prolonged activation of CHOP is closely correlated with cell survival, including apoptosis, proliferation of VSMCs (57, 60), and apoptosis of ECs (61), as well as driving macrophage-derived foam cell apoptosis (62). These data significantly implicate the CHOP pathway in ER stress-induced atherosclerosis, especially in regulating cell apoptosis. Although the complete mechanism by which CHOP mediates apoptosis is unknown, it has been shown to activate the transcription of several genes, including GADD34 (63), TRB3(64), Bcl-2 (65), and DR5 (death receptor 5) (66), which may facilitate apoptosis. Among these, GADD34 is a gene that encodes a subunit of protein phosphatase 2C that enhances dephosphorylation of eukaryotic Initiation Factor 2 (eIF2) and promotes persistent protein synthesis, by which it chronically activates the UPR during periods of ER stress. Increased expression of DR5, a receptor for tumor necrosis factor α-related apoptosis-inducing ligand (TRAIL) can promote the development of VSMCs in atherosclerotic plaques (67). Also, Bcl-2 is a critical mediator for prolonged ER stress-induced apoptosis (68-70). In addition, the mechanism underlying CHOP-induced apoptosis has been explored in cultured cells, including the generation of reactive oxygen species and Toll-like receptors (TLR)-TRIF-dependent translational control pathway (71).

The promotion of apoptosis in macrophages induced by ER stress has been shown to be relevant to advanced atherosclerosis and extensive studies point out a genotype-phenotype correlation between CHOP and macrophage apoptosis. Genetic deletion of CHOP can attenuate macrophage death, both in in vivo and in vitro cultured cells (43, 62, 72), and also protect plaques from rupture in mice (73). Herein, three molecular mechanisms of CHOP-induced macrophage cell apoptosis are introduced. One recognized mechanism involves the increased ER oxidase 1α (ERO1α) by CHOP in ER stressed-macrophages. This inactivated pathway leads to the release of Ca2+ into the cytosol, which is mediated by activating the inositol triphosphate receptor (IP3R). The accumulation of cytosolic Ca2+ drives Ca2+-dependent signaling activation and triggers apoptosis execution pathways. These pathways include stimulation of the Fas death receptor (74) and mitochondrial release of apoptogens, as well as activation in the pro-apoptotic pathway such as activation of transcription-1 (STAT1), and reactive oxygen species ROS production. CHOP also regulates apoptosis by controlling the expression of anti-apoptosis and pro-apoptosis members of the Bcl family. CHOP down-regulates the anti-apoptotic Bcl family member protein Bcl-2 and Bcl-2 transduction of these cells rescues the cells from both oxidative stress and apoptosis (75-78). As one abundantly expressed member of Bcl-2, Bcl-x inactivation enhances macrophage apoptosis in Apoe(-/-) mice as well as accelerates the progression of

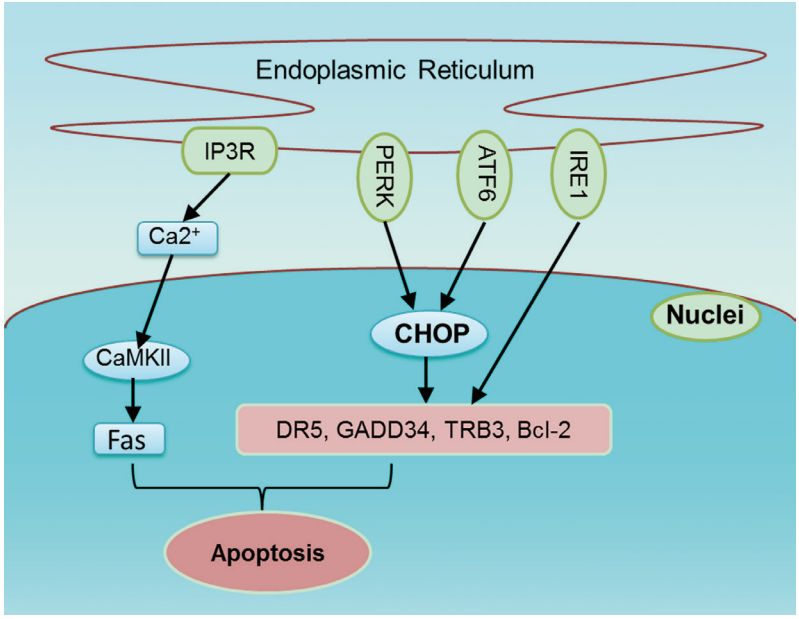

Figure 2. ER stress-induced proapoptotic signaling. During prolonged activation of the UPR, activation of PERK and ATF6 leads to induction of CHOP, which in turn can cause changes in apoptosis-associated gene expression, as well as activate calcium signaling pathways, to cause cell death. Activation of IRE1 can also induce apoptosis mediated by Bcl-2.

advanced atherosclerotic lesions (79). In addition, CHOP can activate the UPR via inducing the expression of its transcriptional target GADD34 in ER stress-induced macrophage apoptosis (63).

Although the mechanism of ER stress-induced apoptosis in VSMCs is not clear, the protection of VSMCs from apoptosis in plaques has become a potentially important therapeutic target for atherosclerotic plaque stabilization (80, 81). In vivo hydrogen peroxide-incubated VSMCs have a deficiency of the novel survival factor, Wnt1-inducible secreted protein-1 (WISP-1) in intimal VSMCs of unstable coronary plaques; this suggests that there is altered Wnt/β-catenin/T-cell factor signaling with progressive atherosclerosis. Restoration of the WISP-1 protein might be an effective stabilization factor for vulnerable atherosclerotic plaques (81) under conditions of oxidative stress. Pro178 and Pro183, belonging to essential residues of Selenoprotein S, play pivotal roles in the progression of ER-associated degradation via interacting with p97 (valosin-containing protein) (VCP) (82). Additionally, depletion of Selenoprotein S-enhanced ER stress in VSMCs involves ER chaperone GRP78, ER stress transducer phosphorylated protein kinase RNA, such as PERK and CHOP. Thus, much more work is needed to understand the mechanisms and consequences of ER stress-induced VSMC survival in atherosclerosis.

In in vitro ER stress-activated ECs, two branches of the UPR cascades, including PERK and IRE1, are activated, thereby contributing to apoptosis in ECs (59, 61). All these processes involve CHOP pathway-mediated cell apoptosis. Experimental incubation with toxic, oxidized LDLs increases expression of CHOP and XBP2; this effectively activates ER stress sensors (phosphorylation of IRE1alpha and PERK, nuclear translocation of ATF6) and induces ER stress-induced endothelial HMEC-1 apoptosis, as well as promotes plaque progression (83, 84). Although cultured ECs are triggered into apoptosis, in vivo evidence connecting EC death to atherosclerotic plaque formation is unavailable.

The content that ER stress/CHOP-induced macrophage, VSMC, and EC apoptosis is a critical pathological cell basis for necrotic plaque formation, and cytologic and histopathologic evidence, shows particular relevance to the rapidly growing epidemic of atherothrombotic vascular disease driven by risk factors. These phenomena attract the attention of researchers and up to now have been recognized in numerous studies in vitro. However, evidence for a dominant pro-apoptotic mechanism in vivo is lacking and further study is required.

ER-stress induced inflammations in atherosclerosis

Atherosclerosis is a pathological, chronic inflammatory reaction of anatomical ECs and VSMCs in the arterial wall (85-87), which is largely mediated by macrophage activation. Initially, ER stress-induced inflammation primarily serves to limit the formation of plaques and facilitate lesion repair. Along with aggregation in unfolded proteins in cells, inflammation develops into an uncontrolled state; that is, abnormal cell death-induced necrosis formation. It is noted that macrophages are observed to abundantly aggregate in plaques and are proven to be involved in the formation of arterial lesions during atherosclerosis, combining with sporadic inflammatory cells including dendritic cells (88), T cells, B cells, and NK cells (89-91). The initiation step in atherosclerosis is activation of ECs in response to circulatory risk factors and inflammatory mediators that induce the release of interleukin cytokines (IL-4, IL-12, IL-6) and chemokines (92, 93). To date, increasing evidence indicates that there are signaling links between the UPR and inflammatory reactions through various mechanisms. The dominant inflammatory pathway mediator, NF-κB, is activated by PERK and IRE1 branches of the ER stress-triggered UPR (94). Also, the IRE1/α-TRAF2 complex recruits and activates IκB kinase (IKK), thereby leading to IκB degradation and activation of NF-κB. The integration of ATF4 with

XBP1 stimulates the production of inflammatory cytokines IL-8 and IL-6 (95). Another inflammatory mediator, AP1 transcriptional factor, is activated in response to oxidative stress (96).

Convincing proof has accumulated in cultured ECs that supports a connection between ER stress and inflammation in atherosclerosis. Studies using human aortic ECs found that inflammation-related genes IL-8, IL-6, monocyte chemoattractant protein 1 (MCP1), and the chemokine CXC motif ligand 3 (CXCL3) were induced by the UPR activator tunicamycin (95). A histological identification in vivo supported this link by determining a finding that activated UPR is shown in areas of human oxidized phospholipid-enriched endothelium lesions. High concentrations of oxidized phospholipids (OxPLs) that are commonly identified in atherosclerotic lesions can activate UPR in ECs, which is associated with genetic variation in a locus affecting the action of USP16 (ubiquitin-specific protease 16), a histone H2A deubiquitinase (97).

Calciumion

The ER serves as the Ca2+ store for free Ca2+ ions in humans, and the main function is to maintain the balance of cellular Ca2+ in response to a variety of cellular signals. Disorders of Ca2+ represent dysfunction in ER, thereby triggering cardiovascular diseases (98, 99). Evidence indicates that various risk factors for atherosclerosis, such as diabetes mellitus, hypertension, and hyperlipidemia, can induce lower Ca2+ in the ER of VSMCs, macrophages, and platelets, suggesting the essential role of ER Ca2+ in the pathological process of atherosclerosis (100-102). The depletion of ER Ca2+ in aortic smooth muscle induces ER stress, and also accelerates atherosclerosis in homocysteine patients. The downstream of Ca2+ is correlated with activated Ca2+ dependent signaling which includes Ca2+-/calmodulin-dependent protein kinase II (CaMKII) (103). As mentioned above, CaMKII functions as a downstream initiator of CHOP and is involved in cholesterol-induced macrophage death (104). Depletion of Ca2+/calmodulin-dependent protein kinase kinase (CaMKK) β in ECs increased atherosclerosis both in atheroprone and in atheroprotective areas (105). Dysregulation of Ca2+ transport during the progression of the UPR in ER stressed VSMCs has been considered as a characteristic of the late onset of cellular stress response, and occurs prior to the initiation of the UPR, rather than as a result of its many corrective pathways (49). This review has previously stated the evidence in a recognized mechanism of EC, VSMC, and macrophage apoptosis by unresolved ER stress with the subsequent persistent activation of the UPR. As in cultured cells, Ca2+ influx into endothelial cells can promote ER stress and/or contribute to mechanisms associated with it. Human Coronary Artery Endothelial Cells' (HCAECs) activation of the UPR and subsequent ER stress-induced apoptosis exhibit a strong requirement for constitutive Ca2+ influx and transient receptor potential canonical 3 (TRPC3) contributes to this process. Evidence has been obtained in studies indicating that, in accordance with the roles of Ca2+ in non-endothelial cells, CaMKII participates in ER stress-induced apoptosis in ECs (55, 106, 107).

Summary and Perspective

Increasing individuals in modern societies have numerous atherosclerotic lesions in their coronary, carotid, and other susceptible peripheral arteries. A small portion of these lesions will develop into pathogenic plaques that tend to lead to obstructive vascular disease. The primary task of the current therapeutic strategy in preventing this deterioration is acquirement of comprehensive knowledge of the progression between advanced plaque morphology and pathophysiology of plaque progression. Plaque progression involves a number of complex processes, including the topics of this review (ER stress-induced macrophage cell death and VSMC/EC injury and defective efferocytosis) but also includes other forms of macrophage death, death of intimal smooth muscle cells, and possibly endothelium, and roles played by living macrophages in advanced plaques.

Within the focus of this review, the hope is to comprehend the knowledge of how the combination of ER stress-induced cell physiological changes in ECs, VSMCs, and macrophages, and effectively release ER stress-induced dysfunctional cells, will provide a valid therapeutic strategy for atherosclerosis. In the initiation of therapeutic agents targeting ER stress-induced pathology, referred to as chemical chaperones, are increasingly to be investigated as therapeutic agents; this is accomplished by alleviating ER stress by facilitating proper protein folding, decreasing the accumulation of misfolded proteins, inhibiting CHOP signaling, and reducing the inflammatory response, therefore resulting in the suppression of atheromatous plaque formation in ECs and macrophages (31, 108, 109). However, there are some limitations that threaten the therapeutic efficiency, since many questions addressing the mechanism of ER stress-induced atherosclerosis remain unanswered. In summary, coordinated developments in the domain of advanced plaque formation, and the cellular biology of lesion/plaque progression, will provide the best prospect of realizing therapeutic purposes.

Conflict of Interest

All authors declare that there is no conflict of interest.

References

1. Meyer ML, Tanaka H, Palta P, Patel MD, Camplain R, Couper D, et al. Repeatability of Central and Peripheral Pulse Wave Velocity Measures: The Atherosclerosis Risk in Communities (ARIC) Study. American journal of hypertension. 2015.
2. Tabas I, Williams KJ, Boren J. Subendothelial lipoprotein retention as the initiating process in atherosclerosis: update and therapeutic implications. Circulation. 2007;116(16):1832-44.
3. Curcio CA, Johnson M, Huang JD, Rudolf M. Apoli-

poprotein B-containing lipoproteins in retinal aging and age-related macular degeneration. Journal of lipid research. 2010;51(3):451-67.
4. Tiniakou I, Drakos E, Sinatkas V, Van Eck M, Zannis VI, Boumpas D, et al. High-density lipoprotein attenuates Th1 and th17 autoimmune responses by modulating dendritic cell maturation and function. Journal of immunology. 2015;194(10):4676-87.
5. Jung MY, Kim HS, Hong HJ, Youn BS, Kim TS. Adiponectin induces dendritic cell activation via PLCgamma/JNK/NF-kappaB pathways, leading to Th1 and Th17 polarization. Journal of immunology. 2012;188(6):2592-601.
6. Scipione CA, Sayegh SE, Romagnuolo R, Tsimikas S, Marcovina SM, Boffa MB, et al. Mechanistic insights into lipoprotein(a)-induced interleukin-8 expression: a role for oxidized phospholipid modification of apolipoprotein(a). Journal of lipid research. 2015.
7. Alasoo K, Martinez FO, Hale C, Gordon S, Powrie F, Dougan G, et al. Transcriptional profiling of macrophages derived from monocytes and iPS cells identifies a conserved response to LPS and novel alternative transcription. Scientific reports. 2015;5:12524.
8. Eligini S, Brioschi M, Fiorelli S, Tremoli E, Colli S, Banfi C. Data for proteomic analysis of Human monocyte-derived macrophages. Data in brief. 2015;4:177-9.
9. Thomas AC, Eijgelaar WJ, Daemen MJ, Newby AC. Foam Cell Formation In Vivo Converts Macrophages to a Pro-Fibrotic Phenotype. PloS one. 2015;10(7):e0128163.
10. McLaren JE, Michael DR, Ashlin TG, Ramji DP. Cytokines, macrophage lipid metabolism and foam cells: implications for cardiovascular disease therapy. Progress in lipid research. 2011;50(4):331-47.
11. Cheng F, Torzewski M, Degreif A, Rossmann H, Canisius A, Lackner KJ. Impact of glutathione peroxidase-1 deficiency on macrophage foam cell formation and proliferation: implications for atherogenesis. PloS one. 2013;8(8):e72063.
12. Ucar R, Arslan S, Turkmen K, Caliskaner AZ. Accelerated atherosclerosis in patients with common variable immunodeficiency: Is it overlooked or absent? Medical hypotheses. 2015.
13. Protogerou AD, Fransen J, Zampeli E, Argyris AA, Aissopou E, Arida A, et al. The Additive Value of Femoral Ultrasound for Subclinical Atherosclerosis Assessment in a Single Center Cohort of 962 Adults, Including High Risk Patients with Rheumatoid Arthritis, Human Immunodeficiency Virus Infection and Type 2 Diabetes Mellitus. PloS one. 2015;7:e0132307.
14. Anderson TJ. New Hope for Lipid-Lowering Beyond Statins: Effect of IMPROVE-IT on Understanding and Implementation of Atherosclerosis Prevention. The Canadian journal of cardiology. 2015;31(5):585-7.
15. Geraci G, Mule G, Costanza G, Mogavero M, Geraci C, Cottone S. Relationship Between Carotid Atherosclerosis and Pulse Pressure with Renal Hemodynamics in Hypertensive Patients. American journal of hypertension. 2015.
16. Torres N, Guevara-Cruz M, Velazquez-Villegas LA, Tovar AR. Nutrition and Atherosclerosis. Archives of medical research. 2015;46(5):408-26.
17. Csordas A, Kreutmayer S, Ploner C, Braun PR, Karlas A, Backovic A, et al. Cigarette smoke extract induces prolonged endoplasmic reticulum stress and autophagic cell death in human umbilical vein endothelial cells. Cardiovascular research. 2011;92(1):141-8.
18. Johnson JS, Kono T, Tong X, Yamamoto WR, Zarain-Herzberg A, Merrins MJ, et al. Pancreatic and duodenal homeobox protein 1 (Pdx-1) maintains endoplasmic reticulum calcium levels through transcriptional regulation of sarco-endoplasmic reticulum calcium ATPase 2b (SERCA2b) in the islet beta cell. The Journal of biological chemistry. 2014;289(47):32798-810.
19. Perez-Linero AM, Muniz M. Membrane trafficking: returning to the fold(ER). Current biology : CB. 2015;25(7):R288-90.
20. Koc M, Mayerova V, Kracmerova J, Mairal A, Malisova L, Stich V, et al. Stress of endoplasmic reticulum modulates differentiation and lipogenesis of human adipocytes. Biochemical and biophysical research communications. 2015;460(3):684-90.
21. Diaz-Villanueva JF, Diaz-Molina R, Garcia-Gonzalez V. Protein Folding and Mechanisms of Proteostasis. International journal of molecular sciences. 2015;16(8):17193-230.
22. Hiramatsu N, Chiang WC, Kurt TD, Sigurdson CJ, Lin JH. Multiple Mechanisms of Unfolded Protein Response-Induced Cell Death. The American journal of pathology. 2015;185(7):1800-8.
23. Ren S, Lu G, Ota A, Zhou ZH, Vondriska TM, Lane TF, et al. IRE1 phosphatase PP2Ce regulates adaptive ER stress response in the postpartum mammary gland. PloS one. 2014;9(11):e111606.
24. Rajapaksa G, Nikolos F, Bado I, Clarke R, Gustafsson JA, Thomas C. ERbeta decreases breast cancer cell survival by regulating the IRE1/XBP-1 pathway. Oncogene. 2015;34(31):4130-41.
25. Cunard R. Endoplasmic Reticulum Stress in the Diabetic Kidney, the Good, the Bad and the Ugly. Journal of clinical medicine. 2015;4(4):715-40.
26. Volgyi K, Juhasz G, Kovacs Z, Penke B. Dysfunction of Endoplasmic Reticulum (ER) and Mitochondria (MT) in Alzheimer's Disease: The Role of the ER-MT Cross-Talk. Current Alzheimer research. 2015;12(7):655-72.
27. Inacio P, Zuzarte-Luis V, Ruivo MT, Falkard B, Nagaraj N, Rooijers K, et al. Parasite-induced ER stress response in hepatocytes facilitates Plasmodium liver stage infection. EMBO reports. 2015.
28. Mozzini C, Fratta Pasini A, Garbin U, Stranieri C, Pasini A, Vallerio P, et al. Increased endoplasmic reticulum stress and Nrf2 repression in peripheral blood mononuclear cells of patients with stable coronary artery disease. Free radical biology & medicine. 2014;68:178-85.

29. Cominacini L, Garbin U, Mozzini C, Stranieri C, Pasini A, Solani E, et al. The atherosclerotic plaque vulnerability: focus on the oxidative and endoplasmic reticulum stress in orchestrating the macrophage apoptosis in the formation of the necrotic core. Current medicinal chemistry. 2015;22(13):1565-72.
30. Zhang J, Zhou HJ, Ji W, Min W. AIP1-mediated stress signaling in atherosclerosis and arteriosclerosis. Current atherosclerosis reports. 2015;17(5):503.
31. Chung J, Kim KH, Lee SC, An SH, Kwon K. Ursodeoxycholic Acid (UDCA) Exerts Anti-Atherogenic Effects by Inhibiting Endoplasmic Reticulum (ER) Stress Induced by Disturbed Flow. Molecules and cells. 2015;38(10):851-8.
32. Wu X, Qi YF, Chang JR, Lu WW, Zhang JS, Wang SP, et al. Possible role of fibroblast growth factor 21 on atherosclerosis via amelioration of endoplasmic reticulum stress-mediated apoptosis in apoE(-/-) mice. Heart and vessels. 2015;30(5):657-68.
33. Zavar Reza J, Nahangi H, Mansouri R, Dehghani A, Mojarrad M, Fathi M, et al. The Effect of Unsaturated Fatty Acids on Molecular Markers of Cholesterol Homeostasis in THP-1 Macrophages. Iranian Red Crescent medical journal. 2013;15(7):554-9.
34. Ross MK, Borazjani A, Mangum LC, Wang R, Crow JA. Effects of toxicologically relevant xenobiotics and the lipid-derived electrophile 4-hydroxynonenal on macrophage cholesterol efflux: silencing carboxylesterase 1 has paradoxical effects on cholesterol uptake and efflux. Chemical research in toxicology. 2014;27(10):1743-56.
35. Brown AJ, Mander EL, Gelissen IC, Kritharides L, Dean RT, Jessup W. Cholesterol and oxysterol metabolism and subcellular distribution in macrophage foam cells. Accumulation of oxidized esters in lysosomes. Journal of lipid research. 2000;41(2):226-37.
36. Schrijvers DM, De Meyer GR, Kockx MM, Herman AG, Martinet W. Phagocytosis of apoptotic cells by macrophages is impaired in atherosclerosis. Arteriosclerosis, thrombosis, and vascular biology. 2005;25(6):1256-61.
37. Nurgazieva D, Mickley A, Moganti K, Ming W, Ovsyi I, Popova A, et al. TGF-beta1, but not bone morphogenetic proteins, activates Smad1/5 pathway in primary human macrophages and induces expression of proatherogenic genes. Journal of immunology. 2015;194(2):709-18.
38. Metghalchi S, Ponnuswamy P, Simon T, Haddad Y, Laurans L, Clement M, et al. Indoleamine 2,3-Dioxygenase Fine-Tunes Immune Homeostasis in Atherosclerosis and Colitis through Repression of Interleukin-10 Production. Cell metabolism. 2015.
39. Nurnberg ST, Cheng K, Raiesdana A, Kundu R, Miller CL, Kim JB, et al. Coronary Artery Disease Associated Transcription Factor TCF21 Regulates Smooth Muscle Precursor Cells That Contribute to the Fibrous Cap. PLoS genetics. 2015;11(5):e1005155.
40. Tucka J, Yu H, Gray K, Figg N, Maguire J, Lam B, et al. Akt1 regulates vascular smooth muscle cell apoptosis through FoxO3a and Apaf1 and protects against arterial remodeling and atherosclerosis. Arteriosclerosis, thrombosis, and vascular biology. 2014;34(11):2421-8.
41. Rotllan N, Wanschel AC, Fernandez-Hernando A, Salerno AG, Offermanns S, Sessa WC, et al. Genetic Evidence Supports a Major Role for Akt1 in VSMCs During Atherogenesis. Circulation research. 2015;116(11):1744-52.
42. Pedruzzi E, Guichard C, Ollivier V, Driss F, Fay M, Prunet C, et al. NAD(P)H oxidase Nox-4 mediates 7-ketocholesterol-induced endoplasmic reticulum stress and apoptosis in human aortic smooth muscle cells. Molecular and cellular biology. 2004;24(24):10703-17.
43. Tsukano H, Gotoh T, Endo M, Miyata K, Tazume H, Kadomatsu T, et al. The endoplasmic reticulum stress-C/EBP homologous protein pathway-mediated apoptosis in macrophages contributes to the instability of atherosclerotic plaques. Arteriosclerosis, thrombosis, and vascular biology. 2010;30(10):1925-32.
44. Chigurupati S, Wei Z, Belal C, Vandermey M, Kyriazis GA, Arumugam TV, et al. The homocysteine-inducible endoplasmic reticulum stress protein counteracts calcium store depletion and induction of CCAAT enhancer-binding protein homologous protein in a neurotoxin model of Parkinson disease. The Journal of biological chemistry. 2009;284(27):18323-33.
45. Oliveira SJ, Pinto JP, Picarote G, Costa VM, Carvalho F, Rangel M, et al. ER stress-inducible factor CHOP affects the expression of hepcidin by modulating C/EBPalpha activity. PloS one. 2009;4(8):e6618.
46. Kwartler CS, Chen J, Thakur D, Li S, Baskin K, Wang S, et al. Overexpression of smooth muscle myosin heavy chain leads to activation of the unfolded protein response and autophagic turnover of thick filament-associated proteins in vascular smooth muscle cells. The Journal of biological chemistry. 2014;289(20):14075-88.
47. Kedi X, Ming Y, Yongping W, Yi Y, Xiaoxiang Z. Free cholesterol overloading induced smooth muscle cells death and activated both ER- and mitochondrial-dependent death pathway. Atherosclerosis. 2009;207(1):123-30.
48. Nagayama D, Ishihara N, Bujo H, Shirai K, Tatsuno I. Effects of serotonin on expression of the LDL receptor family member LR11 and 7-ketocholesterol-induced apoptosis in human vascular smooth muscle cells. Biochemical and biophysical research communications. 2014;446(4):906-10.
49. Ziomek G, van Breemen C, Esfandiarei M. Drop in endo/sarcoplasmic calcium precedes the unfolded protein response in Brefeldin A-treated vascular smooth muscle cells. European journal of pharmacology. 2015;764:328-39.
50. Fiorentino TV, Procopio T, Mancuso E, Arcidiacono GP, Andreozzi F, Arturi F, et al. SRT1720 counteracts glucosamine-induced endoplasmic reticulum stress and endothelial dysfunction. Cardiovascular research.

2015;107(2):295-306.
51. Kim EC, Meng H, Jun AS. N-Acetylcysteine increases corneal endothelial cell survival in a mouse model of Fuchs endothelial corneal dystrophy. Experimental eye research. 2014;127:20-5.
52. Gora S, Maouche S, Atout R, Wanherdrick K, Lambeau G, Cambien F, et al. Phospholipolyzed LDL induces an inflammatory response in endothelial cells through endoplasmic reticulum stress signaling. FASEB journal : official publication of the Federation of American Societies for Experimental Biology. 2010;24(9):3284-97.
53. Shinkai Y, Yamamoto C, Kaji T. Lead induces the expression of endoplasmic reticulum chaperones GRP78 and GRP94 in vascular endothelial cells via the JNK-AP-1 pathway. Toxicological sciences : an official journal of the Society of Toxicology. 2010;114(2):378-86.
54. Qiu L, Xu R, Wang S, Li S, Sheng H, Wu J, et al. Honokiol ameliorates endothelial dysfunction through suppression of PTX3 expression, a key mediator of IKK/IkappaB/NF-kappaB, in atherosclerotic cell model. Experimental & molecular medicine. 2015;47:e171.
55. Ampem PT, Smedlund K, Vazquez G. Pharmacological evidence for a role of the transient receptor potential canonical 3 (TRPC3) channel in endoplasmic reticulum stress-induced apoptosis of human coronary artery endothelial cells. Vascular pharmacology. 2015.
56. Durand E, Scoazec A, Lafont A, Boddaert J, Al Hajzen A, Addad F, et al. In vivo induction of endothelial apoptosis leads to vessel thrombosis and endothelial denudation: a clue to the understanding of the mechanisms of thrombotic plaque erosion. Circulation. 2004;109(21):2503-6.
57. Zhou AX, Wang X, Lin CS, Han J, Yong J, Nadolski MJ, et al. C/EBP-Homologous Protein (CHOP) in Vascular Smooth Muscle Cells Regulates Their Proliferation in Aortic Explants and Atherosclerotic Lesions. Circulation research. 2015;116(11):1736-43.
58. Bi X, He X, Xu M, Zhao M, Yu X, Lu X, et al. Acetylcholine ameliorates endoplasmic reticulum stress in endothelial cells after hypoxia/reoxygenation via M3 AChR-AMPK signaling. Cell cycle. 2015;14(15):2461-72.
59. Kyriakakis E, Philippova M, Joshi MB, Pfaff D, Bochkov V, Afonyushkin T, et al. T-cadherin attenuates the PERK branch of the unfolded protein response and protects vascular endothelial cells from endoplasmic reticulum stress-induced apoptosis. Cellular signalling. 2010;22(9):1308-16.
60. Ye Y, Fu F, Li X, Yang J, Liu H. Selenoprotein S is highly expressed in the blood vessels and prevents vascular smooth muscle cells from apoptosis. Journal of cellular biochemistry. 2015.
61. Hong D, Bai YP, Gao HC, Wang X, Li LF, Zhang GG, et al. Ox-LDL induces endothelial cell apoptosis via the LOX-1-dependent endoplasmic reticulum stress pathway. Atherosclerosis. 2014;235(2):310-7.
62. Yao S, Tian H, Miao C, Zhang DW, Zhao L, Li Y, et al. D4F alleviates macrophage-derived foam cell apoptosis by inhibiting CD36 expression and ER stress-CHOP pathway. Journal of lipid research. 2015;56(4):836-47.
63. Iwasaki N, Sugiyama Y, Miyazaki S, Nakagawa H, Nishimura K, Matsuo S. An ATF4-Signal-Modulating Machine Other Than GADD34 Acts in ATF4-to-CHOP Signaling to Block CHOP Expression in ER-Stress-Related Autophagy. Journal of cellular biochemistry. 2015;116(7):1300-9.
64. Ohoka N, Yoshii S, Hattori T, Onozaki K, Hayashi H. TRB3, a novel ER stress-inducible gene, is induced via ATF4-CHOP pathway and is involved in cell death. The EMBO journal. 2005;24(6):1243-55.
65. Galehdar Z, Swan P, Fuerth B, Callaghan SM, Park DS, Cregan SP. Neuronal apoptosis induced by endoplasmic reticulum stress is regulated by ATF4-CHOP-mediated induction of the Bcl-2 homology 3-only member PUMA. The Journal of neuroscience : the official journal of the Society for Neuroscience. 2010;30(50):16938-48.
66. Trivedi R, Maurya R, Mishra DP. Medicarpin, a legume phytoalexin sensitizes myeloid leukemia cells to TRAIL-induced apoptosis through the induction of DR5 and activation of the ROS-JNK-CHOP pathway. Cell death & disease. 2014;5:e1465.
67. Sato K, Niessner A, Kopecky SL, Frye RL, Goronzy JJ, Weyand CM. TRAIL-expressing T cells induce apoptosis of vascular smooth muscle cells in the atherosclerotic plaque. The Journal of experimental medicine. 2006;203(1):239-50.
68. Kikuchi H, Kuribayashi F, Mimuro H, Imajoh-Ohmi S, Nakayama M, Takami Y, et al. Lack of GCN5 remarkably enhances the resistance against prolonged endoplasmic reticulum stress-induced apoptosis through up-regulation of Bcl-2 gene expression. Biochemical and biophysical research communications. 2015;463(4):870-5.
69. Litwak SA, Wali JA, Pappas EG, Saadi H, Stanley WJ, Varanasi LC, et al. Lipotoxic Stress Induces Pancreatic beta-Cell Apoptosis through Modulation of Bcl-2 Proteins by the Ubiquitin-Proteasome System. Journal of diabetes research. 2015;2015:280615.
70. Carpio MA, Michaud M, Zhou W, Fisher JK, Walensky LD, Katz SG. BCL-2 family member BOK promotes apoptosis in response to endoplasmic reticulum stress. Proceedings of the National Academy of Sciences of the United States of America. 2015;112(23):7201-6.
71. Woo CW, Kutzler L, Kimball SR, Tabas I. Toll-like receptor activation suppresses ER stress factor CHOP and translation inhibition through activation of eIF2B. Nature cell biology. 2012;14(2):192-200.
72. Yu X, Wang Y, Zhao W, Zhou H, Yang W, Guan X. Toll-like receptor 7 promotes the apoptosis of THP-1-derived macrophages through the CHOP-dependent pathway. International journal of molecular medicine. 2014;34(3):886-93.
73. Malhi H, Kropp EM, Clavo VF, Kobrossi CR, Han J, Mauer AS, et al. C/EBP homologous protein-induced macrophage apoptosis protects mice from

steatohepatitis. The Journal of biological chemistry. 2013;288(26):18624-42.
74. Roe ND, Ren J. Oxidative activation of Ca(2+)/calmodulin-activated kinase II mediates ER stress-induced cardiac dysfunction and apoptosis. American journal of physiology Heart and circulatory physiology. 2013;304(6):H828-39.
75. Qin W, Lu Y, Zhan C, Shen T, Dou L, Man Y, et al. Simvastatin suppresses apoptosis in vulnerable atherosclerotic plaques through regulating the expression of p(53), Bcl-2 and Bcl-xL. Cardiovascular drugs and therapy / sponsored by the International Society of Cardiovascular Pharmacotherapy. 2012;26(1):23-30.
76. Thorp E, Li Y, Bao L, Yao PM, Kuriakose G, Rong J, et al. Brief report: increased apoptosis in advanced atherosclerotic lesions of Apoe-/- mice lacking macrophage Bcl-2. Arteriosclerosis, thrombosis, and vascular biology. 2009;29(2):169-72.
77. Patro SC, Pal S, Bi Y, Lynn K, Mounzer KC, Kostman JR, et al. Shift in monocyte apoptosis with increasing viral load and change in apoptosis-related ISG/Bcl2 family gene expression in chronically HIV-1-infected subjects. Journal of virology. 2015;89(1):799-810.
78. Guo G, Meng Y, Tan W, Xia Y, Cheng C, Chen X, et al. Induction of Apoptosis Coupled to Endoplasmic Reticulum Stress through Regulation of CHOP and JNK in Bone Marrow Mesenchymal Stem Cells from Patients with Systemic Lupus Erythematosus. Journal of immunology research. 2015;2015:183738.
79. Shearn AI, Deswaerte V, Gautier EL, Saint-Charles F, Pirault J, Bouchareychas L, et al. Bcl-x inactivation in macrophages accelerates progression of advanced atherosclerotic lesions in Apoe(-/-) mice. Arteriosclerosis, thrombosis, and vascular biology. 2012;32(5):1142-9.
80. French CJ, Zaman AK, Sobel BE. The angiotensin receptor blocker, azilsartan medoxomil (TAK-491), suppresses vascular wall expression of plasminogen activator inhibitor type-I protein potentially facilitating the stabilization of atherosclerotic plaques. Journal of cardiovascular pharmacology. 2011;58(2):143-8.
81. Mill C, Monk BA, Williams H, Simmonds SJ, Jeremy JY, Johnson JL, et al. Wnt5a-induced Wnt1-inducible secreted protein-1 suppresses vascular smooth muscle cell apoptosis induced by oxidative stress. Arteriosclerosis, thrombosis, and vascular biology. 2014;34(11):2449-56.
82. Lee JH, Kwon JH, Jeon YH, Ko KY, Lee SR, Kim IY. Pro178 and Pro183 of selenoprotein S are essential residues for interaction with p97(VCP) during endoplasmic reticulum-associated degradation. The Journal of biological chemistry. 2014;289(20):13758-68.
83. Muller C, Bandemer J, Vindis C, Camare C, Mucher E, Gueraud F, et al. Protein disulfide isomerase modification and inhibition contribute to ER stress and apoptosis induced by oxidized low density lipoproteins. Antioxidants & redox signaling. 2013;18(7):731-42.
84. Sanson M, Auge N, Vindis C, Muller C, Bando Y, Thiers JC, et al. Oxidized low-density lipoproteins trigger endoplasmic reticulum stress in vascular cells: prevention by oxygen-regulated protein 150 expression. Circulation research. 2009;104(3):328-36.
85. Craige SM, Kant S, Reif M, Chen K, Pei Y, Angoff R, et al. Endothelial NADPH oxidase 4 protects ApoE-/- mice from atherosclerotic lesions. Free radical biology & medicine. 2015.
86. Yin YW, Liao SQ, Zhang MJ, Liu Y, Li BH, Zhou Y, et al. TLR4-mediated inflammation promotes foam cell formation of vascular smooth muscle cell by upregulating ACAT1 expression. Cell death & disease. 2014;5:e1574.
87. Simoes Sato AY, Bub GL, Campos AH. BMP-2 and -4 produced by vascular smooth muscle cells from atherosclerotic lesions induce monocyte chemotaxis through direct BMPRII activation. Atherosclerosis. 2014;235(1):45-55.
88. Ge J, Yan H, Li S, Nie W, Dong K, Zhang L, et al. Changes in proteomics profile during maturation of marrow-derived dendritic cells treated with oxidized low-density lipoprotein. Proteomics. 2011;11(10):1893-902.
89. Mandl M, Drechsler M, Jansen Y, Neideck C, Noels H, Faussner A, et al. Evaluation of the BDCA2-DTR Transgenic Mouse Model in Chronic and Acute Inflammation. PloS one. 2015;10(8):e0134176.
90. Cochain C, Zernecke A. Macrophages and immune cells in atherosclerosis: recent advances and novel concepts. Basic research in cardiology. 2015;110(4):34.
91. Yang L, Du C, Chen T, Li S, Nie W, Zhu W, et al. Distinct MAPK pathways are involved in IL-23 production in dendritic cells cocultured with NK cells in the absence or presence of angiotensin II. Molecular immunology. 2012;51(1):51-6.
92. Velsko IM, Chukkapalli SS, Rivera-Kweh MF, Chen H, Zheng D, Bhattacharyya I, et al. Fusobacterium nucleatum Alters Atherosclerosis Risk Factors and Enhances Inflammatory Markers with an Atheroprotective Immune Response in ApoEnull Mice. PloS one. 2015;10(6):e0129795.
93. van der Vorst EP, Doring Y, Weber C. Chemokines and their receptors in Atherosclerosis. Journal of molecular medicine. 2015.
94. Tam AB, Mercado EL, Hoffmann A, Niwa M. ER stress activates NF-kappaB by integrating functions of basal IKK activity, IRE1 and PERK. PloS one. 2012;7(10):e45078.
95. Gargalovic PS, Gharavi NM, Clark MJ, Pagnon J, Yang WP, He A, et al. The unfolded protein response is an important regulator of inflammatory genes in endothelial cells. Arteriosclerosis, thrombosis, and vascular biology. 2006;26(11):2490-6.
96. Van-Assche T, Huygelen V, Crabtree MJ, Antoniades C. Gene therapy targeting inflammation in atherosclerosis. Current pharmaceutical design. 2011;17(37):4210-23.
97. Afonyushkin T, Oskolkova OV, Bochkov VN. Permissive role of miR-663 in induction of VEGF and activa-

tion of the ATF4 branch of unfolded protein response in endothelial cells by oxidized phospholipids. Atherosclerosis. 2012;225(1):50-5.
98. Gassett AJ, Sheppard L, McClelland RL, Olives C, Kronmal R, Blaha MJ, et al. Risk Factors for Long-Term Coronary Artery Calcium Progression in the Multi-Ethnic Study of Atherosclerosis. Journal of the American Heart Association. 2015;4(8).
99. Al Rifai M, McEvoy JW, Nasir K, Rumberger J, Feldman D, Budoff MJ, et al. Traditional cardiovascular disease risk factors associated with one-year all-cause mortality among those with coronary artery calcium scores >/=400. Atherosclerosis. 2015;241(2):495-7.
100. Groves DW, Krantz MJ, Hokanson JE, Johnson LR, Eckel RH, Kinney GL, et al. Comparison of Frequency and Duration of Periodontal Disease With Progression of Coronary Artery Calcium in Patients With and Without Type 1 Diabetes Mellitus. The American journal of cardiology. 2015.
101. Chatterjee S, Bedja D, Mishra S, Amuzie C, Avolio A, Kass DA, et al. Inhibition of glycosphingolipid synthesis ameliorates atherosclerosis and arterial stiffness in apolipoprotein E-/- mice and rabbits fed a high-fat and -cholesterol diet. Circulation. 2014;129(23):2403-13.
102. Balkanci ZD, Pehlivanoglu B, Bayrak S, Karabulut I, Karaismailoglu S, Erdem A. The effect of hypercholesterolemia on carbachol-induced contractions of the detrusor smooth muscle in rats: increased role of L-type Ca2+ channels. Naunyn-Schmiedeberg's archives of pharmacology. 2012;385(11):1141-8.
103. Cipolletta E, Monaco S, Maione AS, Vitiello L, Campiglia P, Pastore L, et al. Calmodulin-dependent kinase II mediates vascular smooth muscle cell proliferation and is potentiated by extracellular signal regulated kinase. Endocrinology. 2010;151(6):2747-59.
104. Timmins JM, Ozcan L, Seimon TA, Li G, Malagelada C, Backs J, et al. Calcium/calmodulin-dependent protein kinase II links ER stress with Fas and mitochondrial apoptosis pathways. The Journal of clinical investigation. 2009;119(10):2925-41.
105. Wen L, Chen Z, Zhang F, Cui X, Sun W, Geary GG, et al. Ca2+/calmodulin-dependent protein kinase kinase beta phosphorylation of Sirtuin 1 in endothelium is atheroprotective. Proceedings of the National Academy of Sciences of the United States of America. 2013;110(26):E2420-7.
106. Toussaint F, Charbel C, Blanchette A, Ledoux J. CaMKII regulates intracellular Ca(2+) dynamics in native endothelial cells. Cell calcium. 2015;58(3):275-85.
107. Li J, Wang P, Yu S, Zheng Z, Xu X. Calcium entry mediates hyperglycemia-induced apoptosis through Ca(2+)/calmodulin-dependent kinase II in retinal capillary endothelial cells. Molecular vision. 2012;18:2371-9.
108. Kawanami D, Matoba K, Okada R, Tsukamoto M, Kinoshita J, Ishizawa S, et al. Fasudil inhibits ER stress-induced VCAM-1 expression by modulating unfolded protein response in endothelial cells. Biochemical and biophysical research communications. 2013;435(2):171-5.
109. Castilho G, Okuda LS, Pinto RS, Iborra RT, Nakandakare ER, Santos CX, et al. ER stress is associated with reduced ABCA-1 protein levels in macrophages treated with advanced glycated albumin - reversal by a chemical chaperone. The international journal of biochemistry & cell biology. 2012;44(7):1078-86.

Lipid and Cardiovascular Research. 2015;**01**(1):12-22
http://www.enochpublisher.com/LCR

ARTICLE

LncRNA *HOTAIR* Promotes Atherosclerosis through Regulating the Expression of PCSK9 in Macrophages

Hong-Jun Zhu[1], De-Guo Wang[2], Ji Yan[1], Jian Xu[1], Xian-Lin Sun[1]*

Abstract

Atherosclerosis is a chronic inflammatory disorder, resulting in the accumulation of lipoproteins and the formation of atherosclerotic plaques. The pathological role of lncRNA *HOTAIR* in the development of atherosclerosis is still unclear. This study aims to investigate the biological role and mechanism of *HOTAIR* in the development of atherosclerosis. Aortic atherosclerotic plaques were collected from 16 patients, and normal aortas were collected from 18 normal patients. The aortas of apolipoprotein E deficient (ApoE-/-) mice fed a high-fat diet (HFD) for a period of six weeks were also obtained. LncRNA *HOTAIR* gene expression analyzed by qRT-PCR and proprotein convertase subtilisin/kexin type 9 (PCSK9) protein expression measured by western blotting were significantly elevated in human aortic atherosclerotic plaques and in the aortas of mice fed the HFD. Acetylated low-density lipoprotein(LDL) and oxidized LDL dose-dependently upregulated HOTAIR gene and PCSK9 protein expression in THP-1 and RAW264.7 macrophages. HOTAIR and PCSK9 increased cholesterol levels determined by high-performance liquid chromatography and inhibited cholesterol efflux and phospholipid efflux in THP-1 macrophages detected by liquid scintillation counting assays. Besides, PCSK9 interference reversed the HOTAIR-induced downregulation of the ATP-binding cassette transporter A1 (ABCA1) expression. Moreover, RNA pull-down and RNA immunoprecipitation (RIP) assays showed that HOTAIR associated with PCSK9 and elevated PCSK9 levels by enhancing PCSK9 protein stability. HOTAIR interference significantly reduced the lesion area, dramatically inhibited PCSK9 protein expression, and remarkably elevated ABCA1 protein expression in the aortas of ApoE-/- mice. These results indicated that lncRNA HOTAIR-mediated promotion of atherosclerosis may be due to the upregulation of PCSK9 expression in macrophages.

Keywords: LncRNA *HOTAIR*, atherosclerosis, proprotein convertase subtilisin/kexin type 9

Introduction

Atherosclerosis is the underlying cause of cardiovascular disease (CVD), which is initiated by the accumulation of lipids, mainly cholesterol and cholesterol esters, and by fibrous elements in the neointima of medium and large arteries, in addition to the infiltration of inflammatory cells, particularly macrophages and T cells(1,2). CVD continues to be the leading cause of death in developed countries, and its incidence is rapidly increasing in developing countries(3,4).

Proprotein convertase subtilisin/kexin type 9 (PCSK9) is primarily expressed in the liver and intestines, and is tightly regulated by intracellular cholesterol, hormones, and metabolic status(5,6). The biochemical relationship between PCSK9 and low-density lipoprotein cholesterol (LDL-C) has been described in detail. It is known that PCSK9 plays an important role in the regulation of cholesterol homeostasis and the modulation of LDL-C metabolism(7), which is an important therapeutic target for the reduction of circulating LDL-C concentrations(8). PCSK9 plays a key role in the regulation of hepatic LDL receptor (LDL-R) activity(9), and inhibits the LDL-R pathway in a posttranscriptional manner(10). Indeed, it is believed that PCSK9 increases circulating LDL-C concentrations via the promotion of LDL-R degradation when bound(11,12).

Long non-coding RNAs (lncRNAs), a recently discovered class of non-protein coding transcribed RNA molecules with more than 200 nucleotides, have increasingly been shown to be involved in the regulation of a wide variety of important physiological processes(13). It is known that aberrant lncRNA expression is associated with human diseases such as cancer, Alzheimer's, and CVD(14-16). Recently, lncRNAs have been recognized to play an important role in cardiac development(17,18) and to be associated with susceptibility to coronary artery disease(19,20). Previous studies showed that lncRNAs were involved in

[1] Department of Cardiology, Anhui Provincial Hospital affiliated to Anhui Medical University, Hefei 230001, P.R. China
[2] Department of Gerontology, Yijishan Hospital of Wannan Medical College, Wuhu 241001, P.R. China

* Corresponding author: De-Guo Wang, Ph.D
Mailing address: 2nd zheshan western road, Jinghu District, Wuhu 241001, Anhui, P. R. China
Tel: +86-553-5739308; Fax: +86-553-5739308
E-mail: wangdeguo2005@hotmail.com

Received: 8 October 2015 / Accepted: 19 November 2015
Published online: 29 December 2015

the regulation of cholesterol metabolism(13,21). However, whether *HOTAIR*, an lncRNA, plays an important role in the development of atherosclerosis is still unclear.

HOTAIR associates with the polycomb repressive complex 2 (PRC2) and is reported to reprogram chromatin organization and to promote tumor progression(22). Although numerous studies have demonstrated the critical functions of *HOTAIR* in tumor development and metastasis, little is known about the roles of this gene in the development of atherosclerosis.

To better understand the role of *HOTAIR* in atherosclerosis development and progression, we investigated the expression pattern of *HOTAIR* in aortic atherosclerotic plaques in apolipoprotein E deficient (ApoE-/-) mice fed a high-fat diet (HFD) and its effect on macrophages, and analyzed its role in cholesterol metabolism. We also explored the effects of *HOTAIR* on atherosclerotic lesions in the aorta, as well as on PCSK9 and the ATP-binding cassette transporter A1(ABCA1) expression.

Materials and Methods

Tissue samples

Aortic atherosclerotic plaques and normal aorta specimens were collected after obtaining informed consent from 16 patients and 18 normal cases at Anhui Provincial Hospital, affiliated with Anhui Medical University. All animal experiments were performed in accordance with the Guidelines for the Care and Use of Animals at the Southeast University Laboratory Animal Center. Our study protocols were approved by the Animal Care and Use Committee of Anhui Medical University.

Cell cultures

The human monocyte cell line (THP-1) was obtained from the American Type Culture Collection (ATCC, no. TIB-202, Manassas, VA, USA). The THP-1 cells were cultured in Roswell Park Memorial Institute (RPMI) 1640 medium supplemented with 10% fetal calf serum (FCS), 2 mmol/l glutamine, 100 U/ml penicillin, and 100 μg/ml streptomycin, and then differentiated for 72 h with 100 nM PMA. The differentiated THP-1 macrophages were washed extensively with phosphate-buffered saline (PBS) before use. The macrophages were then transformed into foam cells. After the addition of different concentrations of oxidized low density lipoprotein (Ox-LDL) or acetylated low density lipoprotein (Ac-LDL) (0, 25, 50, and 100 μg/mL), the cells were incubated in serum-free RPMI 1640 medium containing 0.3% bovine serum albumin (BSA) for 48 h. The cells were incubated at 37 °C with a humidified atmosphere of 5% CO2. The cells were seeded in 12-well plates and grown to 80% confluence before being used in the experiments. The human lipoproteins (Ac-LDL and Ox-LDL) were purchased from Biomedical Technologies, Inc. (Stoughton, MA, USA). All reagents for the cell cultures were purchased from Sigma-Aldrich (St. Louis, MO, USA) unless otherwise noted.

Animals and diets

Fourteen-week-old male ApoE-/- mice with a C57BL/6 background were obtained from the Laboratory Animal Center of Peking University (Beijing, China) and maintained five per cage at 25 °C on a 12 h light/dark cycle under pathogen-free conditions. To detect the effect of *HOTAIR* interference on atherosclerotic lesions, the ApoE-/- mice were randomized into two groups and injected via the tail vein with control siRNAs (si-control, n=15) or siRNA-interfering mouse *HOTAIR* (si-*HOTAIR*, n=15), respectively. To investigate the expression levels of *HOTAIR* and PCSK9 protein in the aortas of ApoE-/- mice fed a HFD compared to a normal diet, the mice were fed the HFD for six weeks, to be used as a model for spontaneous atherosclerotic development(23). The diet was commercially prepared mouse food supplemented with 21% (w/w) butterfat, 0.15% (w/w) cholesterol, and 19.5% (w/w) casein (Beijing Keao Xieli Feed Co., Ltd., Beijing, China). After six weeks, the mice were anesthetized, and 1 ml of blood was collected via cardiac puncture before they were euthanized by cervical dislocation.

Plasmid construction and cell transfection

To create a *HOTAIR* expression vector, we amplified a full-length *HOTAIR* fragment by PCR using *HOTAIR* primers (Table 1). Oligonucleotides were designed to incorporate external HindIII and XhoI sites, respectively. The *HOTAIR* gene was verified and subcloned into the mammalian expression vector pcDNA3.1(+) (Invitrogen, USA) by PCR. The individual small interfering RNA (siRNA) and scrambled negative control siRNA (si-NC) were purchased from GenePharma (Shanghai, China). The siRNAs targeting *HOTAIR* or siRNA/control are shown in Table 1. Cultured THP-1 and RAW264.7 macrophages were seeded into 6-well plates to confluency, and transfected either with pCDNA3.1-*HOTAIR* or pCDNA3.1-NC using Lipofectamine 2000® (Invitrogen), according to the manufacturer's instructions. *HOTAIR* siRNA or si-NC was injected via the tail vein into the ApoE-/- mice. Forty-eight hours after transfection,

Table 1. Sequences for plasmid construction and cell transfection

Genes	Primers	Sequences(5'-3')
HOTAIR	Sense	5'-CATGGATCCACATTCTGCCCTGATTTCCGGAACC-3'
	Antisense	5'-ACTCTCGAGCCACCACACACACACAACCTACAC-3'
siRNA/HOTAIR	-	5'-UUUUCUACCAGGUCGGUAC-3'
siRNA/control	-	5'-CUACAACAGCCACAACGUCdTdT-3'

qRT-PCR or western blot were performed.

Measurement of intracellular cholesterol

Intracellular cholesterol was assessed as previously described(24). THP-1 macrophages transfected with si-*HOTAIR* or si-control were cultured in the serum-free experimental medium for 24 h. The cells were then washed twice in PBS. Subsequently, intracellular lipids were extracted in a chloroform/methanol (2:1) mix and dried under vacuum. Finally, the total cellular cholesterol (TC), free cholesterol (FC), and cholesterol ester (CE) contents were determined with high-performance liquid chromatography (HPLC).

Cellular cholesterol efflux assay

Cellular cholesterol efflux experiments in BHK cells were performed as previously described, with minor modifications(25). Briefly, THP-1 macrophages seeded into 24-well plates were labeled with 0.2 μCi/ml (3H)cholesterol (35-50 Ci/mmol, Amersham Biosciences) in complete DMEM medium. After 48 h, the cells were subsequently washed three times with PBS and incubated overnight in RPMI 1640 medium containing 0.1% (w/v) BSA to allow equilibration of (3H)cholesterol overnight in DMEM containing 0.2% fatty-acid-free BSA (DMEM-BSA). The equilibrated (3H) cholesterol-labeled cells were incubated overnight in 2 ml of efflux medium containing RPMI 1640 medium and 0.1% BSA with 25 g/ml human plasma ApoA-I for 12 h. Following incubation, samples of efflux medium were collected at designated times, and centrifuged to remove detached cells. Adherent cells were washed twice in PBS at 4 °C. Radioactivity in the media was measured directly in a Packard β liquid scintillation counter. Cellular lipids were extracted with hexane/isopropyl alcohol (3:2 v/v) for 30 min at room temperature. Radioactivity in the medium and cell-associated (3H)cholesterol was then measured by liquid scintillation counting. Efflux of cellular (3H)cholesterol to media was calculated by the following equation: (total media counts/(total cellular counts + total media counts)) × 100%.

Phospholipid efflux assay

Using the same experimental protocol, cells were cultured as indicated above and phospholipid efflux was measured by radiolabeling the cells with 2 μCi/ml of (3H)choline chloride (Dupont NEN). After 72 h, cells were subsequently washed with PBS and incubated overnight in RPMI 1640 medium containing 0.1% (w/v) BSA. After 6 h of incubation in the presence of 10 mg/ml ApoA-I, the efflux medium was collected and centrifuged to remove the cell debris as above, and separate wells were then used to determine the initial cell (3H)choline phospholipid and cell choline phospholipid mass (Boehringer Mannheim kit). Phospholipids were extracted from the medium and separated by silica gel TLC with developing solvents of chloroform/methanol/ammonia (25% w/v)/water (50:65:5:4 by volume). Phospholipid spots were run in parallel, visualized by iodine vapors, and identified by co-migration with standards. The spots, scraped directly into vials, were then mixed with scintillation fluid, and relative radioactivity was measured by Phosphor Screen and quantified by PhosphorImager (Molecular Dynamics, Inc.). Phospholipid efflux was expressed as a percentage of the supernatant versus the total count for each individual lipid.

Quantification of atherosclerotic plaques

To quantify the extent of atherosclerotic lesions, immediately after the mice were euthanized, the whole length of each aorta was excised and fixed in 10% buffered formalin for quantification of the plaque area by Oil Red O staining of lipid deposits, as previously described(26). Briefly, after carefully removing the adventitial tissue, the aorta was opened longitudinally, pinned on a blue wax surface, and incubated for 45 min with Oil Red O (0.5% in 60% isopropyl alcohol) (Sigma, St. Louis, MO, USA). Excess stain was removed with 60% isopropyl alcohol. Images of en face preparations of the whole mounted aorta were obtained with a stereomicroscope (SZX12; Olympus, Tokyo, Japan) equipped with a digital camera (Dxm1200, Nikon, Tokyo, Japan). The percentage of plaques in relation to the entire aortic surface was calculated as the plaque score using the public domain software, Image J (NIH Image, Bethesda, MD, USA).

RNA extraction and quantitative real-time PCR (qRT-PCR) analysis

Total RNA was extracted from tissues or cultured cells using TRIzol reagent (Invitrogen, CA, USA) and reverse-transcribed to cDNA using a Sensiscript RT Kit (Qiagen, Hilden, Germany) according to the manufacturer's protocols. The qRT-PCR assays were performed to detect *HOTAIR* expression using SYBR Green master mix (Applied Biosystems, CA, USA) and ABI GeneAmp 7500 Sequence Detection System (Applied Biosystems), as recommended by the manufacturer's protocols. The primers used are summarized in Table 2. The qRT-PCR and data collections were performed on an ABI 7500 Fast Sequence Detection System and software (Applied Biosystems) using the 2-ΔΔCT method normalized to the expression of β-actin.

Western blot

Western blot analyses were performed for the determination of PCSK9 and ABCA1. Protein extracted from the cultured cells was lysed in cell lysis buffer containing 1 mm of phenylmethanesulfonyl fluoride (PMSF). The extracted proteins were separated using 12% SDS-PAGE and then electrically transferred to polyvinylidene difluoride (PVDF) membranes by 2 h of electroblotting. Membranes were blocked with TBST containing 5% BSA overnight at 4°C, probed with anti-PCSK9 antibody (Abcam, CA, USA), anti-ABCA1 antibody (Abcam), or anti-β-Actin antibody (Abcam), and then incubated with horseradish peroxidase-conjugated

secondary antibodies (Boster, Wuhan, China) diluted at 1:2000 for 1h in 5% milk/1×TBST. The immune complexes were visualized with an enhanced chemiluminescence kit (Amersham Biosciences, NJ, USA) according to the manufacturer's instructions.

Table 2. Primer sequences of quantitative real-time PCR.

Genes	Primers	Sequences(5'-3')
HOTAIR	Forward	5'-CAGTGGGGAACTCTGACTCG-3'
	Reverse	5'-GTGCCTGGTGCTCTCTTACC-3'
GAPDH	Forward	5'-GGGA GCCAAAAGGGTCAT-3'
	Reverse	5'-GAGTCCTTCCACGATACCAA-3'

RNA pull-down assay

HOTAIR and its antisense RNA (NC) were in vitro transcribed and biotin-labeled using a biotin RNA labeling mix (Roche, Indianapolis, IN, USA) and T7/SP6 RNA polymerase (Roche), then treated with RNase-free DNase I (Roche) and purified using an RNeasy mini kit (Qiagen, Valencia, CA, USA). One milligram of protein from THP-1 macrophage extract was mixed with 50 pmol biotinylated RNA, incubated with streptavidin agarose beads (Invitrogen), and washed three times with NaCl/Pi at room temperature. The retrieved proteins were detected using a standard western blot technique.

RNA immunoprecipitation (RIP)

RIP experiments were performed using the Magna RIPTM RNA-binding protein immunoprecipitation kit (Millipore, Bedford, MA, USA) according to the manufacturer's instructions. The antibody for RIP assays of PCSK9 (Cell Signaling Technology) was diluted at 1:50. Co-precipitated RNAs were detected by quantitative RT-PCR.

Statistical analysis

Data are expressed as mean ± standard deviation (SD). Comparison between groups was performed with the unpaired t-test using SPSS v17.0 statistical software (SPSS, Inc., Chicago, IL, USA). P values of <0.05 were considered statistically significant.

Results

LncRNA *HOTAIR* gene and PCSK9 protein expressions are significantly elevated in human aortic atherosclerotic plaques and in aortas of mice fed a HFD

Studies have shown that lncRNAs play an essential role in CVD(16). Moreover, PCSK9 has long been considered a potential atherogenic risk marker (27). In this study, to explore possible changes in lncRNA *HOTAIR* gene and PCSK9 protein expression in aortic atherosclerotic plaques, such plaques from 16 patients and the normal aortas of 18 normal cases were collected. ApoE is synthesized by the liver and by macrophages, and has several important anti-atherogenic functions(28). We also detected possible changes in *HOTAIR* gene and PCSK9 protein expression in the aortas of ApoE-/- mice fed a HFD for six weeks. Our data revealed that *HOTAIR* gene and PCSK9 protein expressions were significantly increased in aortic atherosclerotic plaques (Figure 1A and 1B) and in the aortas of mice fed a HFD (Figure 1C and 1D).

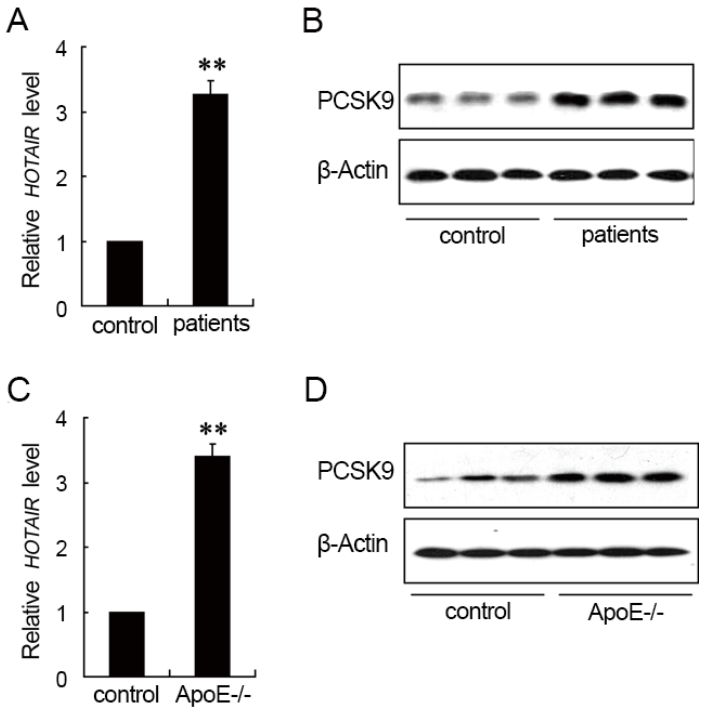

Figure 1. LncRNA HOTAIR gene and PCSK9 protein expression in aortic atherosclerotic plaques and in the aortas of mice fed a HFD. HOTAIR gene expression was analyzed with qRT-PCR. PCSK9 protein expression was assessed by western blot. **P<0.01 vs. control.

Ac-LDL/Ox-LDL upregulates lncRNA *HOTAIR* gene and PCSK9 protein expression in THP-1 and RAW264.7 macrophages in a dose-dependent manner

Modified LDLs, including Ac-LDL and Ox-LDL, are considered the main source of cholesterol that accumulates in monocyte-derived macrophages within atherosclerotic plaques(29). Macrophages play a very important role in the pathogenesis of atherosclerosis and are one of the major cell types that transform into lipid-laden foam cells(30). To further investigate possible

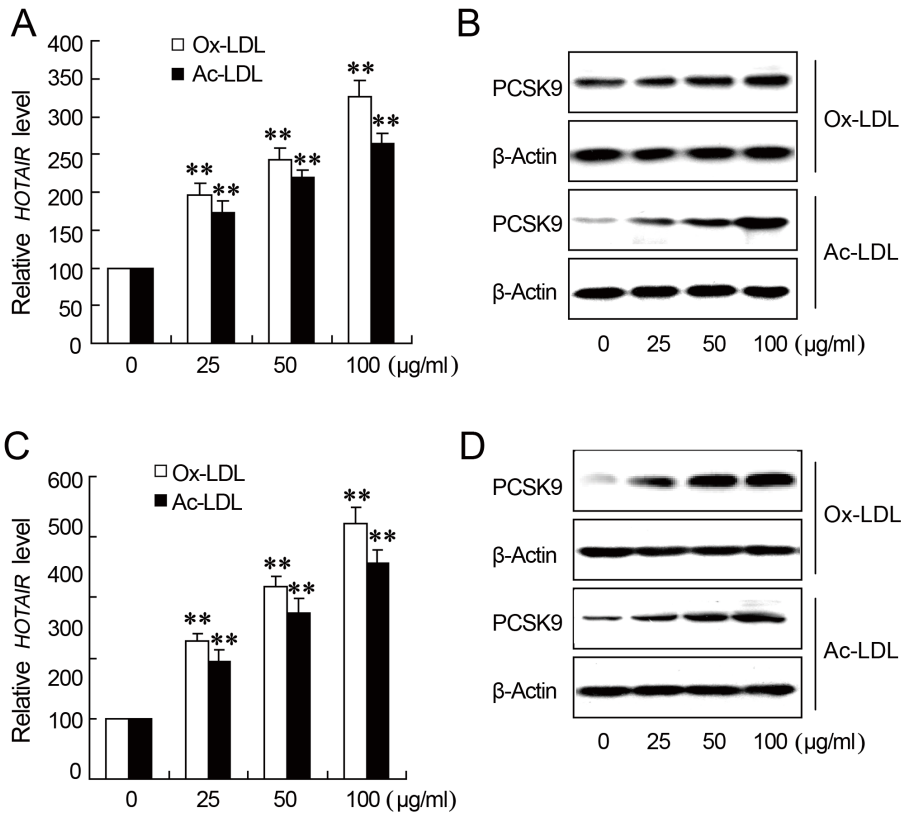

Figure 2. Dose-dependent effects of Ox-LDL/Ac-LDL on lncRNA HOTAIR gene and PCSK9 protein expression in THP-1 and RAW264.7 macrophages. THP-1 and RAW264.7 macrophages were treated with different concentrations of Ac-LDL/Ox-LDL (0, 25, 50, and 100 μg/mL). After 48 h of cultivation, HOTAIR gene expression was evaluated with qRT-PCR, and PCSK9 protein expression was detected with western blot. **P<0.01 vs. control.

changes in lncRNA *HOTAIR* gene and PCSK9 protein expression in THP-1 and RAW264.7 macrophages in the presence of Ac-LDL or Ox-LDL, we performed qRT-PCR and western blot analyses. THP-1 and RAW264.7 macrophages were treated with different concentrations of Ac-LDL/Ox-LDL (0, 25, 50, and 100 μg/mL) for 48 h. The results demonstrated that Ac-LDL/Ox-LDL dose-dependently elevated *HOTAIR* gene and PCSK9 protein expressions in THP-1 (Figure 2A and 2B) and RAW264.7 (Figure 2C and 2D) macrophages.

The effect of lncRNA *HOTAIR* and PCSK9 on cholesterol metabolism

Atherosclerosis can be considered both a lipid metabolism disorder and a complex, chronic inflammatory disease that involves many cell types and circulating mediators, resulting in an inflammatory state(31). PCSK9 concentration was reported to be correlated with LDL-C, TC, and triglycerides(5,8,32-34), and has been considered a potential novel predictor of cardiovascular risk and a target for lipid-lowering therapy(8). To determine whether lncRNA *HOTAIR* and PCSK9 affect cholesterol metabolism, we first examined the effect of lncRNA *HOTAIR* and PCSK9 on cholesterol metabolism in THP-1 macrophages. The plasmid vector pcDNA3.1-*HOTAIR* was created and transfected into THP-1 macrophages. We found that *HOTAIR* overexpression significantly increased TC, FC, and CE levels (Figure 3A). However, the elevated cholesterol content was further reversed by PCSK9 interference. The defect in lipidation of ApoA-I has been considered a major cause of the impaired ability to stimulate cholesterol efflux from Tangier cells(35). To confirm that this process was also regulated by lncRNA *HOTAIR* and PCSK9, we further investigated ApoA-I-mediated cholesterol efflux and phospholipid efflux in THP-1 macrophages. As shown in Figure 3C and 3D, the efflux of cholesterol and phospholipids was decreased significantly when lncRNA *HOTAIR* was overexpressed in THP-1 macrophages. Interestingly, the reductions in cholesterol efflux and phospholipid efflux were also further recovered by PCSK9 interference (Figure 3C and 3D). These results suggest that lncRNA *HOTAIR* and PCSK9 increase cholesterol levels and inhibit cholesterol efflux and phospholipid efflux in THP-1 macrophages.

PCSK9 interference reverses lncRNA *HOTAIR*-induced downregulation of ABCA1 expression

ABCA1 is a member of a family of highly conserved transmembrane transport proteins that plays a crucial role in cholesterol metabolism, for example, in reverse cholesterol transport (RCT)(36,37). Here, we showed that lncRNA *HOTAIR* and PCSK9 could affect cholesterol metabolism and inflammation. Therefore, we hypothesized that lncRNA *HOTAIR* and PCSK9 might be involved in regulating the expression of ABCA1. We then examined the effect of lncRNA *HOTAIR* and PCSK9 on ABCA1 expression in THP-1 (Figure 4A) and RAW264.7 (Figure 4B) macrophages. Our data documented that overexpression of lncRNA *HOTAIR* significantly reduced ABCA1 protein expression levels. Similarly, the reduction of ABCA1 expression levels could be further rescued by PCSK9 interference.

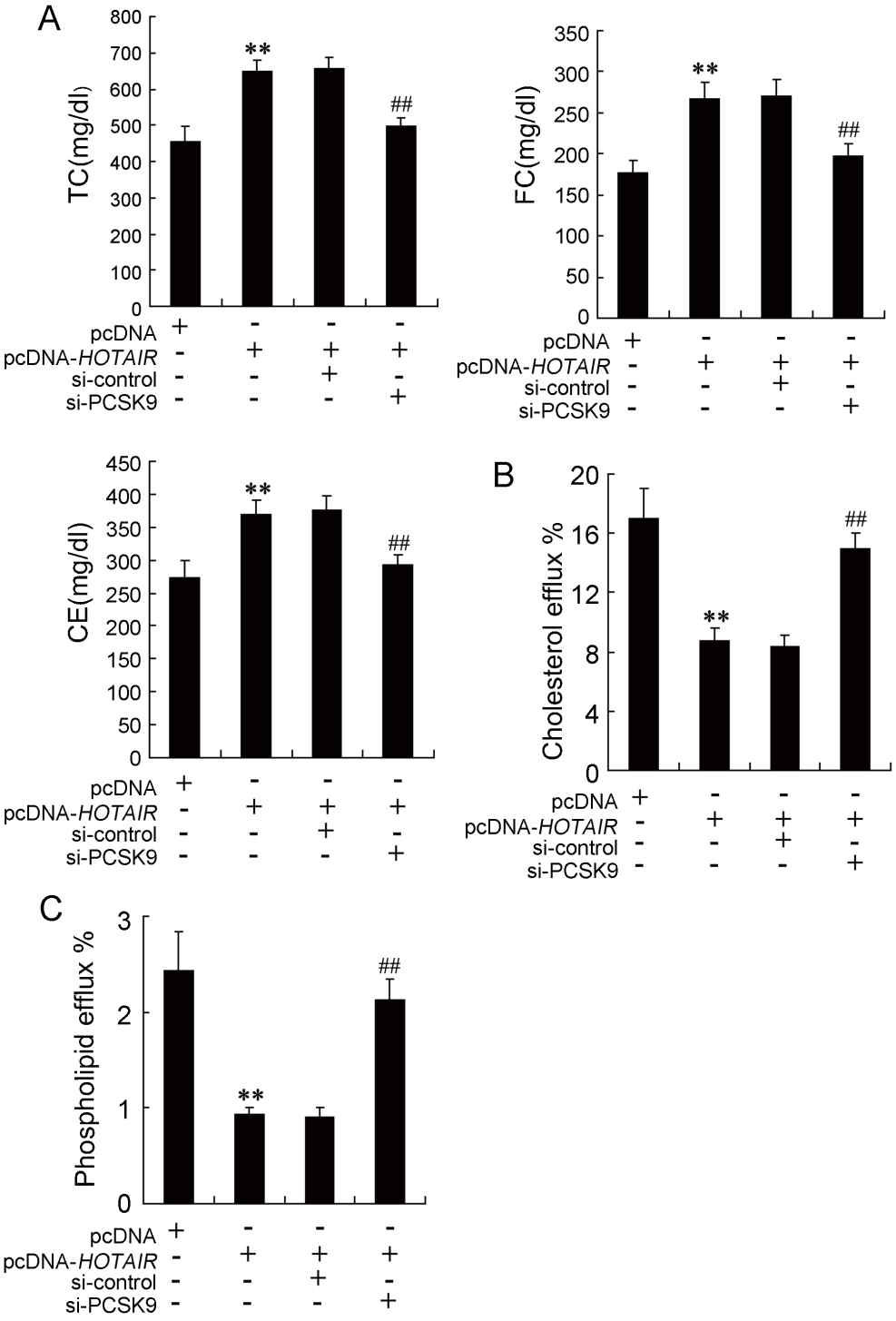

Figure 3. Effects of lncRNA HOTAIR and PCSK9 on cholesterol content and inflammation in THP-1 macrophages. THP-1 macrophages were transfected with empty pcDNA3.1 vector or plasmid vector pcDNA3.1-HOTAIR. (A) Cellular TC, FC, and CE were determined by HPLC. (B, C) The cells were labeled with 0.2 μCi/ml [^{3}H]cholesterol for 48 h or 2 μCi/ml of [^{3}H]choline chloride for 72 h, and then liquid scintillation counting assays were carried out to analyze ApoA-I-mediated cellular cholesterol efflux and phospholipid efflux. Data are expressed as mean ± SD. All experiments were performed in triplicate.

LncRNA *HOTAIR* associates with PCSK9 and elevates PCSK9 levels by enhancing PCSK9 protein stability

Because PCSK9 is an RNA-binding protein, we speculated that lncRNA *HOTAIR* may also bind PCSK9 and influence PCSK9 protein stability. To test this hypothesis, THP-1 macrophages were transfected with pcDNA-*HOTAIR* or empty pcDNA vector and an RNA pull-down experiment was performed. Figure 5A shows a significant enrichment of PCSK9 in the presence of *HOTAIR* RNA compared with antisense

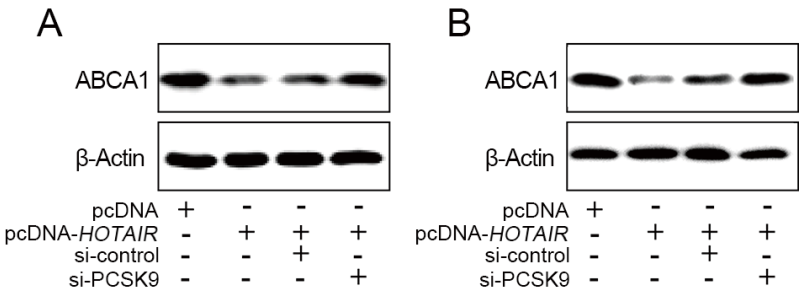

Figure 4. Effects of lncRNA HOTAIR and PCSK9 on ABCA1 expression in THP-1 and RAW264.7 macrophages. THP-1 (A) and RAW264.7 (B) macrophages were transfected with empty pcDNA3.1 vector or plasmid vector pcDNA3.1-HOTAIR. Western blot assays were performed to detect ABCA1 protein expression. All results are presented as mean ± SD (n=5) from three independent experiments, each performed in triplicate.

RNA (negative control). To further confirm the association between *HOTAIR* and PCSK9, we performed RNA immunoprecipitation (RIP) with an antibody directed against PCSK9 using cell extracts from THP-1 macrophages. We found a significant enrichment of *HOTAIR* mRNA using the PCSK9 antibody compared with the IgG control antibody (Figure 5B).

Moreover, we examined the effects of cycloheximide (CHX) and MG132 on PCSK9 protein expression. Our results showed that CHX, a protein synthesis inhibitor, dramatically decreased PCSK9 protein expression in *HOTAIR*-overexpressed THP-1 macrophages, whereas the proteasome inhibitor MG132 significantly elevated PCSK9 protein expression levels in *HOTAIR*-overexpressed THP-1 macrophages (Figure 5C). These results demonstrated a specific association between *HOTAIR* and PCSK9.

Assessment of atherosclerotic lesions in the aorta

Six weeks of the HFD caused increased atherosclerotic plaques within the aorta as assessed by Oil Red O staining (Figure 6). The lesion areas in aortas from ApoE-/- mice treated with *HOTAIR* interference were significantly reduced in comparison with aortas from ApoE-/- mice treated with si-control (Figure 6A). Moreover, *HOTAIR* interference dramatically inhibited PCSK9 protein expression and remarkably elevated ABCA1 protein expression (Figure 6B) in atherosclerotic plaques within the aorta.

Discussion

Atherosclerosis is a systemic and chronic disease that affects virtually all vascular beds and can remain asymptomatic for decades. Increasing studies have revealed that lncRNAs have emerged as a major class of regulatory molecules involved in a variety of biological processes and complex diseases(38). However, until now there has been limited research focused on the effects of lncRNAs on CVD(39), and the full impact of this field on cardiovascular biology is yet to be realized(40). Therefore, a better understanding of the roles of lncRNAs in the development of atherosclerosis will advance our understanding of cell regulatory and disease mechanisms. In the present study, our aim was to identify whether lncRNA *HOTAIR* might play an important role in cholesterol metabolism and in atherosclerosis. Consequently, this study sought to examine possible changes in *HOTAIR* gene and PCSK9 protein expressions in human aortic atherosclerotic plaques and in the aortas of mice fed a HFD. We found that *HOTAIR* gene and PCSK9 protein expressions were significantly elevated in both tissues (Figure 1).

Macrophages, endothelial cells, and vascular smooth muscle cells are the primary cells that contribute to atherosclerotic lesion formation(41-43). In addition, macrophages could accumulate lipids by taking up large-particle lipoproteins through non-receptor-mediated endocytosis(44). Furthermore, macrophages, whether engorged with lipids or not, play a key role in the internalization of chemically modified lipoproteins, such as Ox-LDL and Ac-LDL, by macrophages, involved in foam-cell formation(45). The formation of macrophage foam cells in the intima is a major hallmark of early-stage atherosclerotic lesions(31). THP-1 and RAW264.7 cells have been used in lipid metabolism investigations(46-49).

Evidence from previous studies demonstrated that Ox-LDL contributed to atherosclerotic plaque formation and progression via several mechanisms, including macrophage foam cell formation. Moreover, Ox-LDL upregulates ABCA1 expression at both protein and mRNA levels(50).

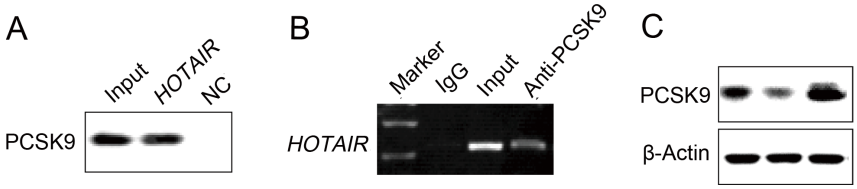

Figure 5. HOTAIR increases PCSK9 levels by enhancing PCSK9 protein stability. (A) An RNA pull-down assay was performed as described in the experimental procedures. HOTAIR or antisense RNA (NC) was incubated with cell extracts, and the PCSK9 protein was assayed with western blot. (B) RIP experiments were performed in THP-1 macrophages using a PCSK9 antibody or nonspecific IgG, and specific primers were used to detect HOTAIR. (C) HOTAIR-overexpressed THP-1 macrophages were treated with CHX and MG132, respectively. After incubation for 4 h, western blot analysis was performed to detect PCSK9 protein expression.

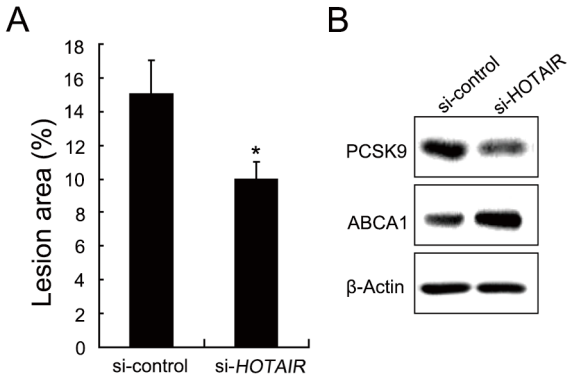

Figure 6. Effects of HOTAIR interference on atherosclerotic lesions in ApoE-/- mice fed HFD. Computerized morphometry was performed to quantify atheroma development in the whole aorta (the aortic arch up to the abdominal aorta). ApoE-/- mice were fed HFD for six weeks and injected with si-HOTAIR or si-control. Arteries were stained with Oil Red O, and the results represent the lesion area (%) relative to total aortic surface (A). PCSK9 and ABCA1 protein expression was evaluated by western blot analysis (B). n=8 mice per group. *P<0.05 vs. si-control.

An interesting study showed that Ox-LDL induces GPR119 expression through lncRNA-DYNLRB2-2 in THP-1 macrophages(13). In the current study, we further investigated the effects of Ac-LDL or Ox-LDL on *HOTAIR* gene and PCSK9 protein expression in THP-1 and RAW264.7 macrophages. Our data revealed that Ac-LDL/Ox-LDL dose-dependently elevated *HOTAIR* gene and PCSK9 protein expression in THP-1 (Figure 2A and 2B) and RAW264.7 (Figure 2C and 2D) macrophages.

PCSK9, which is a crucial modulator of cholesterol metabolism(10), has been recognized for its pivotal role in increasing LDL-R degradation(7). LDL-R is the primary receptor for the binding and internalization of plasma-derived LDL cholesterol, and regulates plasma LDL concentration(51). PCSK9 has emerged as an important factor in fat metabolism since endogenous PCSK9 has been shown to regulate LDL-R concentrations in adipose tissue in mouse models(52). In addition, experiments involving PCSK9 null mice showed that a lack of PCSK9 is protective against postprandial triglyceridemia(53). Furthermore, multiple studies have found that PCSK9 concentrations are correlated with LDL-C concentrations(27,54,55). Genetic association studies have found that subjects with gain-of-function PCSK9 mutations have increased plasma LDL-C levels and premature atherosclerosis(56,57), whereas subjects with loss-of-function PCSK9 mutations have lower LDL-C levels and protection against CVD(27,58), which highlights the importance of clinical applications of PCSK9 inhibition.

Atherosclerosis is characterized by intimal accumulation of lipids(2). Previous studies have suggested that cholesterol and other lipids can be mobilized and excreted to prevent atherosclerosis in a process termed reverse cholesterol transport (RCT)(59). In addition, crosstalk between lipid metabolism and innate immunity pathways plays an important role in the development and/or prevention of atherosclerosis(60). Hypercholesterolemia, which results from abnormalities in lipid metabolism, is one of the key risk factors for the development of atherosclerosis and its pathologic complications. Evidence from several recent studies indicates that reduction of plasma cholesterol levels by dietary and/or pharmacological means leads to a reduction in the risk of death from CVD(61,62). Furthermore, uncontrolled Ox-LDL uptake, excessive cholesterol esterification, and impaired cholesterol release can provoke accumulation of CE stored as cytoplasmic lipid droplets(63). Therefore, we proceeded to investigate the impact of *HOTAIR* and PCSK9 on cholesterol metabolism, and the results showed that elevated cholesterol content induced by *HOTAIR* overexpression was further reversed by PCSK9 interference (Figure 3A), and PCSK9 interference recovered the inhibition effect of *HOTAIR* overexpression on cholesterol efflux and phospholipid efflux (Figure 3B and 3C).

ABCA1 plays an essential role in the efflux of cellular cholesterol to HDL and its apolipoproteins, and affects cellular inflammatory cytokine secretion by modulating cholesterol content(37). In humans, ABCA1 mutations can cause severe HDL-deficiency syndrome, leading to the development of sterol deposits in tissue macrophages, and to premature atherosclerosis(64). Because of its role in macrophage lipid transport, ABCA1 is an important target for the prevention and treatment of atherosclerosis. We discovered that PCSK9 interference could reverse *HOTAIR*-induced downregulation of ABCA1 expression in THP-1 and RAW264.7 macrophages (Figure 4). Therefore, we proposed that lncRNA *HOTAIR* upregulated PCSK9 expression, which decreased ABCA1 expression, resulting in the inhibition of ABCA1-mediated cholesterol efflux and leading to the promotion of atherosclerosis. To confirm this hypothesis, we further uncovered the molecular mechanisms by which *HOTAIR* associates with PCSK9 and elevates PCSK9 levels by enhancing PCSK9 protein stability (Figure 5).

Atherosclerosis is a complex multifactorial disease with numerous pathogeneses that contribute synergistically to the development of atherosclerotic lesions(65). Atherosclerotic lesions are initiated by the focal accumulation of lipoproteins, monocytes/macrophages, smooth muscle cells, and lymphocytes within the arterial wall(37,59). In previous studies on atherosclerosis and its effective therapeutic approaches, the mouse was regarded as the most useful, economical, and validated model to mimic humans metabolically and pathophysiologically(66). In this study, we investigated atherosclerotic lesions in ApoE-/- mice and found that *HOTAIR* interference significantly reduced the lesion area in aortas from these mice (Figure 6A). Indeed, the lesions in ApoE-/- mice resemble their human counterparts and develop over time from initial fatty streaks to complex lesions(67,68). In addition, in this mouse model, *HOTAIR* interference significantly inhibited PCSK9 protein expression and markedly elevated ABCA1 protein expression (Figure 6B) in atherosclerotic plaques within the aortas of ApoE-/- mice.

Conclusion

In conclusion, this study demonstrated that lncRNA *HOTAIR* significantly elevated cholesterol content and dramatically decreased the efflux of cholesterol and phospholipids though regulating the expression of PCSK9 in macrophages. In addition, *HOTAIR* interference significantly reduced the lesion area, dramatically inhibited PCSK9 protein expression, and remarkably elevated ABCA1 protein expression in the aortas of ApoE-/- mice. Together, these results suggested that *HOTAIR* may be a promising target for treating atherosclerotic vascular disease. Although the current study demonstrated that *HOTAIR*-modulated PCSK9 protein expression is a key pathway for regulating cholesterol homeostasis and atherosclerotic lesions, whether atherosclerosis can be affected by *HOTAIR* through other targets remains unclear and needs to be further explored.

Acknowledgement

This study was supported by National Natural Science Foundation of China (81200142).

Conflict of Interest

All authors declare that there is no conflict of interest.

References

1. Lusis AJ. Atherosclerosis. Nature. 2000;407(6801):233-41.
2. Weber C, Noels H. Atherosclerosis: current pathogenesis and therapeutic options. Nature medicine. 2011;17(11):1410-22.
3. Peters SA, den Ruijter HM, Bots ML, Moons KG. Improvements in risk stratification for the occurrence of cardiovascular disease by imaging subclinical atherosclerosis: a systematic review. Heart. 2012;98(3):177-84.
4. Hamamdzic D, Wilensky RL. Porcine models of accelerated coronary atherosclerosis: role of diabetes mellitus and hypercholesterolemia. Journal of diabetes research. 2013;2013:761415.
5. Baass A, Dubuc G, Tremblay M, Delvin EE, O'Loughlin J, Levy E, et al. Plasma PCSK9 is associated with age, sex, and multiple metabolic markers in a population-based sample of children and adolescents. Clinical chemistry. 2009;55(9):1637-45.
6. Costet P, Cariou B, Lambert G, Lalanne F, Lardeux B, Jarnoux AL, et al. Hepatic PCSK9 expression is regulated by nutritional status via insulin and sterol regulatory element-binding protein 1c. The Journal of biological chemistry. 2006;281(10):6211-8.
7. Cariou B, Ouguerram K, Zair Y, Guerois R, Langhi C, Kourimate S, et al. PCSK9 dominant negative mutant results in increased LDL catabolic rate and familial hypobetalipoproteinemia. Arteriosclerosis, thrombosis, and vascular biology. 2009;29(12):2191-7.
8. Zhu YM, Anderson TJ, Sikdar K, Fung M, McQueen MJ, Lonn EM, et al. Association of Proprotein Convertase Subtilisin/Kexin Type 9 (PCSK9) With Cardiovascular Risk in Primary Prevention. Arteriosclerosis, thrombosis, and vascular biology. 2015;35(10):2254-9.
9. Park SW, Moon YA, Horton JD. Post-transcriptional regulation of low density lipoprotein receptor protein by proprotein convertase subtilisin/kexin type 9a in mouse liver. The Journal of biological chemistry. 2004;279(48):50630-8.
10. Costet P, Krempf M, Cariou B. PCSK9 and LDL cholesterol: unravelling the target to design the bullet. Trends in biochemical sciences. 2008;33(9):426-34.
11. Cohen J, Pertsemlidis A, Kotowski IK, Graham R, Garcia CK, Hobbs HH. Low LDL cholesterol in individuals of African descent resulting from frequent nonsense mutations in PCSK9. Nature genetics. 2005;37(2):161-5.
12. Lagace TA, Curtis DE, Garuti R, McNutt MC, Park SW, Prather HB, et al. Secreted PCSK9 decreases the number of LDL receptors in hepatocytes and in livers of parabiotic mice. The Journal of clinical investigation. 2006;116(11):2995-3005.
13. Hu YW, Yang JY, Ma X, Chen ZP, Hu YR, Zhao JY, et al. A lincRNA-DYNLRB2-2/GPR119/GLP-1R/ABCA1-dependent signal transduction pathway is essential for the regulation of cholesterol homeostasis. Journal of lipid research. 2014;55(4):681-97.
14. Zhang H, Chen Z, Wang X, Huang Z, He Z, Chen Y. Long non-coding RNA: a new player in cancer. Journal of hematology & oncology. 2013;6:37.
15. Qureshi IA, Mehler MF. Long non-coding RNAs: novel targets for nervous system disease diagnosis and therapy. Neurotherapeutics : the journal of the American Society for Experimental NeuroTherapeutics. 2013;10(4):632-46.
16. Scheuermann JC, Boyer LA. Getting to the heart of the matter: long non-coding RNAs in cardiac development and disease. The EMBO journal. 2013;32(13):1805-16.
17. Klattenhoff CA, Scheuermann JC, Surface LE, Bradley RK, Fields PA, Steinhauser ML, et al. Braveheart, a long noncoding RNA required for cardiovascular lineage commitment. Cell. 2013;152(3):570-83.
18. Grote P, Wittler L, Hendrix D, Koch F, Wahrisch S, Beisaw A, et al. The tissue-specific lncRNA Fendrr is an essential regulator of heart and body wall development in the mouse. Developmental cell. 2013;24(2):206-14.
19. Holdt LM, Beutner F, Scholz M, Gielen S, Gabel G, Bergert H, et al. ANRIL expression is associated with atherosclerosis risk at chromosome 9p21. Arteriosclerosis, thrombosis, and vascular biology. 2010;30(3):620-7.
20. Burd CE, Jeck WR, Liu Y, Sanoff HK, Wang Z, Sharpless NE. Expression of linear and novel circular forms of an INK4/ARF-associated non-coding RNA correlates with atherosclerosis risk. PLoS genetics. 2010;6(12):e1001233.
21. Liu G, Zheng X, Xu Y, Lu J, Chen J, Huang X. Long

non-coding RNAs expression profile in HepG2 cells reveals the potential role of long non-coding RNAs in the cholesterol metabolism. Chinese medical journal. 2015;128(1):91-7.
22. Liu Z, Sun M, Lu K, Liu J, Zhang M, Wu W, et al. The long noncoding RNA HOTAIR contributes to cisplatin resistance of human lung adenocarcinoma cells via downregualtion of p21(WAF1/CIP1) expression. PloS one. 2013;8(10):e77293.
23. Bond AR, Jackson CL. The fat-fed apolipoprotein E knockout mouse brachiocephalic artery in the study of atherosclerotic plaque rupture. Journal of biomedicine & biotechnology. 2011;2011:379069.
24. Hu YW, Yang JY, Ma X, Chen ZP, Hu YR, Zhao JY, et al. A lincRNA-DYNLRB2-2/GPR119/GLP-1R/ABCA1-dependent Signal Transduction Pathway Is Essential for the Regulation of Cholesterol Homeostasis and Inflammatory Reactions. Journal of lipid research. 2014;55(4):681-97.
25. Francis GA, Knopp RH, Oram JF. Defective removal of cellular cholesterol and phospholipids by apolipoprotein A-I in Tangier Disease. The Journal of clinical investigation. 1995;96(1):78-87.
26. Koga M, Kai H, Yasukawa H, Yamamoto T, Kawai Y, Kato S, et al. Inhibition of progression and stabilization of plaques by postnatal interferon-gamma function blocking in ApoE-knockout mice. Circulation research. 2007;101(4):348-56.
27. Cohen JC, Boerwinkle E, Mosley TH, Jr., Hobbs HH. Sequence variations in PCSK9, low LDL, and protection against coronary heart disease. The New England journal of medicine. 2006;354(12):1264-72.
28. Curtiss LK, Boisvert WA. Apolipoprotein E and atherosclerosis. Current opinion in lipidology. 2000;11(3):243-51.
29. Kruth HS, Huang W, Ishii I, Zhang WY. Macrophage foam cell formation with native low density lipoprotein. The Journal of biological chemistry. 2002;277(37):34573-80.
30. De Winther MP, Gijbels MJ, Van Dijk KW, Havekes LM, Hofker MH. Transgenic mouse models to study the role of the macrophage scavenger receptor class A in atherosclerosis. International journal of tissue reactions. 2000;22(2-3):85-91.
31. Osterud B, Bjorklid E. Role of monocytes in atherogenesis. Physiological reviews. 2003;83(4):1069-112.
32. Lakoski SG, Lagace TA, Cohen JC, Horton JD, Hobbs HH. Genetic and metabolic determinants of plasma PCSK9 levels. The Journal of clinical endocrinology and metabolism. 2009;94(7):2537-43.
33. Cui Q, Ju X, Yang T, Zhang M, Tang W, Chen Q, et al. Serum PCSK9 is associated with multiple metabolic factors in a large Han Chinese population. Atherosclerosis. 2010;213(2):632-6.
34. Dubuc G, Tremblay M, Pare G, Jacques H, Hamelin J, Benjannet S, et al. A new method for measurement of total plasma PCSK9: clinical applications. Journal of lipid research. 2010;51(1):140-9.
35. Lawn RM, Wade DP, Garvin MR, Wang X, Schwartz K, Porter JG, et al. The Tangier disease gene product ABC1 controls the cellular apolipoprotein-mediated lipid removal pathway. The Journal of clinical investigation. 1999;104(8):R25-31.
36. Ye D, Lammers B, Zhao Y, Meurs I, Van Berkel TJ, Van Eck M. ATP-binding cassette transporters A1 and G1, HDL metabolism, cholesterol efflux, and inflammation: important targets for the treatment of atherosclerosis. Current drug targets. 2011;12(5):647-60.
37. Yin K, Liao DF, Tang CK. ATP-binding membrane cassette transporter A1 (ABCA1): a possible link between inflammation and reverse cholesterol transport. Molecular medicine. 2010;16(9-10):438-49.
38. Ponting CP, Oliver PL, Reik W. Evolution and functions of long noncoding RNAs. Cell. 2009;136(4):629-41.
39. Harries LW. Long non-coding RNAs and human disease. Biochemical Society transactions. 2012;40(4):902-6.
40. Schonrock N, Harvey RP, Mattick JS. Long noncoding RNAs in cardiac development and pathophysiology. Circulation research. 2012;111(10):1349-62.
41. Onat D, Brillon D, Colombo PC, Schmidt AM. Human vascular endothelial cells: a model system for studying vascular inflammation in diabetes and atherosclerosis. Current diabetes reports. 2011;11(3):193-202.
42. Ho-Tin-Noe B, Michel JB. Initiation of angiogenesis in atherosclerosis: smooth muscle cells as mediators of the angiogenic response to atheroma formation. Trends in cardiovascular medicine. 2011;21(7):183-7.
43. Martinet W, Schrijvers DM, De Meyer GR. Molecular and cellular mechanisms of macrophage survival in atherosclerosis. Basic research in cardiology. 2012;107(6):297.
44. Liu B, Xie C, Richardson JA, Turley SD, Dietschy JM. Receptor-mediated and bulk-phase endocytosis cause macrophage and cholesterol accumulation in Niemann-Pick C disease. Journal of lipid research. 2007;48(8):1710-23.
45. Ye Q, Chen Y, Lei H, Liu Q, Moorhead JF, Varghese Z, et al. Inflammatory stress increases unmodified LDL uptake via LDL receptor: an alternative pathway for macrophage foam-cell formation. Inflammation research : official journal of the European Histamine Research Society [et al]. 2009;58(11):809-18.
46. Peng H, Wu X, Zhao L, Feng Y. Dynamic analysis of phospholipid metabolism of mouse macrophages treated with common non-steroidal anti-inflammatory drugs. Molecular and cellular biochemistry. 2015.
47. Gao B, Li L, Zhu P, Zhang M, Hou L, Sun Y, et al. Chronic administration of methamphetamine promotes atherosclerosis formation in ApoE-/- knockout mice fed normal diet. Atherosclerosis. 2015;243(1):268-77.
48. Mikita T, Porter G, Lawn RM, Shiffman D. Oxidized low density lipoprotein exposure alters the transcriptional response of macrophages to inflamma-

tory stimulus. The Journal of biological chemistry. 2001;276(49):45729-39.
49. Yang L, Yang JB, Chen J, Yu GY, Zhou P, Lei L, et al. Enhancement of human ACAT1 gene expression to promote the macrophage-derived foam cell formation by dexamethasone. Cell research. 2004;14(4):315-23.
50. Hui DY, Labonte ED, Howles PN. Development and physiological regulation of intestinal lipid absorption. III. Intestinal transporters and cholesterol absorption. American journal of physiology Gastrointestinal and liver physiology. 2008;294(4):G839-43.
51. Smith JR, Osborne TF, Goldstein JL, Brown MS. Identification of nucleotides responsible for enhancer activity of sterol regulatory element in low density lipoprotein receptor gene. The Journal of biological chemistry. 1990;265(4):2306-10.
52. Roubtsova A, Munkonda MN, Awan Z, Marcinkiewicz J, Chamberland A, Lazure C, et al. Circulating proprotein convertase subtilisin/kexin 9 (PCSK9) regulates VLDLR protein and triglyceride accumulation in visceral adipose tissue. Arteriosclerosis, thrombosis, and vascular biology. 2011;31(4):785-91.
53. Le May C, Kourimate S, Langhi C, Chetiveaux M, Jarry A, Comera C, et al. Proprotein convertase subtilisin kexin type 9 null mice are protected from postprandial triglyceridemia. Arteriosclerosis, thrombosis, and vascular biology. 2009;29(5):684-90.
54. Lambert G, Ancellin N, Charlton F, Comas D, Pilot J, Keech A, et al. Plasma PCSK9 concentrations correlate with LDL and total cholesterol in diabetic patients and are decreased by fenofibrate treatment. Clinical chemistry. 2008;54(6):1038-45.
55. Mayne J, Raymond A, Chaplin A, Cousins M, Kaefer N, Gyamera-Acheampong C, et al. Plasma PCSK9 levels correlate with cholesterol in men but not in women. Biochemical and biophysical research communications. 2007;361(2):451-6.
56. Abifadel M, Varret M, Rabes JP, Allard D, Ouguerram K, Devillers M, et al. Mutations in PCSK9 cause autosomal dominant hypercholesterolemia. Nature genetics. 2003;34(2):154-6.
57. Allard D, Amsellem S, Abifadel M, Trillard M, Devillers M, Luc G, et al. Novel mutations of the PCSK9 gene cause variable phenotype of autosomal dominant hypercholesterolemia. Human mutation. 2005;26(5):497.
58. Berge KE, Ose L, Leren TP. Missense mutations in the PCSK9 gene are associated with hypocholesterolemia and possibly increased response to statin therapy. Arteriosclerosis, thrombosis, and vascular biology. 2006;26(5):1094-100.
59. Burnett JR. Lipids, lipoproteins, atherosclerosis and cardiovascular disease. The Clinical biochemist Reviews / Australian Association of Clinical Biochemists. 2004;25(1):2.
60. Shibata N, Glass CK. Regulation of macrophage function in inflammation and atherosclerosis. Journal of lipid research. 2009;50 Suppl:S277-81.
61. Shepherd J, Cobbe SM, Ford I, Isles CG, Lorimer AR, MacFarlane PW, et al. Prevention of coronary heart disease with pravastatin in men with hypercholesterolemia. 1995. Atherosclerosis Supplements. 2004;5(3):91-7.
62. Panel AP. Reducing residual cardiovascular risk: the relevance of raising high-density lipoprotein cholesterol in patients on cholesterol-lowering treatment. Diabetes & vascular disease research. 2006;3(2):S1-S12.
63. Hu YW, Zheng L, Wang Q. Regulation of cholesterol homeostasis by liver X receptors. Clinica chimica acta; international journal of clinical chemistry. 2010;411(9-10):617-25.
64. Oram JF, Lawn RM. ABCA1. The gatekeeper for eliminating excess tissue cholesterol. Journal of lipid research. 2001;42(8):1173-9.
65. Zadelaar S, Kleemann R, Verschuren L, de Vries-Van der Weij J, van der Hoorn J, Princen HM, et al. Mouse models for atherosclerosis and pharmaceutical modifiers. Arteriosclerosis, thrombosis, and vascular biology. 2007;27(8):1706-21.
66. Getz GS, Reardon CA. Animal models of atherosclerosis. Arteriosclerosis, thrombosis, and vascular biology. 2012;32(5):1104-15.
67. Nakashima Y, Plump AS, Raines EW, Breslow JL, Ross R. ApoE-deficient mice develop lesions of all phases of atherosclerosis throughout the arterial tree. Arteriosclerosis and thrombosis : a journal of vascular biology / American Heart Association. 1994;14(1):133-40.
68. Meir KS, Leitersdorf E. Atherosclerosis in the apolipoprotein-E-deficient mouse: a decade of progress. Arteriosclerosis, thrombosis, and vascular biology. 2004;24(6):1006-14.

Lipid and Cardiovascular Research. 2015;**01**(1):23-29
http://www.enochpublisher.com/LCR

ENOCH PUBLISHING CORPORATION

ARTICLE

Rosuvastatin Inhibits Vascular Smooth Muscle Cell Inflammation Pathways through Promotion of MiR-146a Expression

Xiao-Fei Li, Hong-Zhuan Sheng, Dong-Dong Zhen, Min Pan, Hai-Xia Xu*

Abstract

Objective: The vascular smooth muscle cell (VSMC) inflammatory response is the main pathological characteristic of atherosclerosis (AS). This study was conducted to evaluate the effect of rosuvastatin on the inflammatory pathway of VSMCs.
Methods: A total of 20 atherosclerosis patients were recruited for analysis of differential miR-146a expression, and 20 persons with no visible coronary atherosclerotic plaque were analyzed as a control. Cellular miR-146a was manipulated by transfection of miR-146a mimic or miR-146a inhibitor in VSMCs that were isolated from Wistar neonate rats. In vitro inflammatory response of the VSMCs was stimulated by lipopolysaccharide (LPS) (100nM). The expression levels of Phosphoryl-p65 (P-p65), total p65, and toll-like receptor 4-tumor necrosis factor receptor (TRAF6) were determined using Western blotting.
Results: AS patients were characterized by a low high-density lipoprotein(HDL) to low-density lipoprotein (LDL) ratio and had lower serum levels of miR-146. Manipulation of cellular miR-146a in VSMCs negatively regulated inflammation-related signals and P-p65 and TRAF6 expression. MiR-146a expression was enhanced with increasing treatment concentration and processing time of rosuvastatin. rosuvastatin dose-dependently suppressed LPS-induced P-p65 and TRAF6 expression in VSMCs, whereas this inhibitory action was abrogated by miR-146 silencing.
Conclusion: MiR-146a mediated the anti-inflammatory action of rosuvastatin in VSMCs.

Keywords: miR-146a, vascular smooth muscle cell , nuclear factor kappa B, toll-like receptor four-tumor necrosis factor receptor

Introduction

As one of the inflammatory joint diseases, atherosclerosis (AS) and its cardiovascular complications remain the leading causes of death worldwide (1). AS is facilitated by a number of cellular events, including inflammatory response, cell dysfunction, and death of essential vascular cells (2). According to hypotheses regarding the development of AS, the progressive inflammatory impairment of vascular smooth muscle cell (VSMC) function is an important step in the development of atherosclerotic plaques (3). Therefore, inhibition of VSMCs' dysfunctional response to inflammation is increasingly proposed as an important mediator of atherosclerotic regression.

Department of Cardiology, Affiliated Hospital of Nantong University, Nantong 226001, China

* Corresponding author: Xiao-Fei Li
Department of Cardiology, Affiliated Hospital of Nantong University, No.20 Xisi Road, Chongchuan District, Nantong 226001, China
Tel: +86-0513-85052504; Fax: +86-0513-85052504
E-mail: sofia_l@163.com

Received: 26 August 2015 / Accepted: 12 October 2015
Published online: 29 December 2015

Rosuvastatin is clinically prescribed to lower cholesterol and triglyceride levels, and it is used to potentially cure coronary heart disease secondary to AS (4, 5). Well-established studies have pointed out that the anti-atherosclerotic action of rosuvastatin increases high-density lipoprotein (HDL) production, reduces endothelial dysfunction (4), stabilizes atherosclerotic aortic plague (6), and inhibits atherosclerotic inflammation-related events (7). The therapeutic effects of rosuvastatin on AS possibly depend on its inhibitory effect on the activation of certain inflammatory factors, such as NF-κB (nuclear factor kappa B) and tumor necrosis factor (TNF)-α (8). However, the exact anti-AS mechanism of rosuvastatin is still poorly understood, especially in terms of its action on VSMC inflammation.

MicroRNA (miRNA) is a family of non-coding RNAs that consist of 20~22 nucleotides and are responsible for post-transcriptional and cell type-specific repressors of gene expression under both normal and pathological conditions (9). MiRNA expression of different cell types involved in the inflammation of the vascular system has already been widely studied. The inflammation-related miRNA expression profile of atheromatous plaques (10) and serum of AS (11) have also been observed. As the new regulatory layer, several miRNAs have been found to modulate the function of endothelial cells (ECs), smooth muscle cells, and

macrophages by controlling the expression levels of chemokines, thereby affecting different stages in the progression of AS. Among these, miRNA-146a mediates the pathologic processes of AS by involving the inflammatory response of VSMCs (12). It has also been proven to regulate the maturation and proliferation of VSMCs in AS (13, 14), and this process might also be mediated by miR-146a targeting the expression of NF-κB, a critical inflammation-related transcriptional factor (15). Moreover, miR-146a has another inflammatory factor target: toll-like receptor four-tumor necrosis factor receptor 6 (TRAF6), a gene that is essential for maintaining immune tolerance (16). As a signal transductor for TNFs, TNF6 signaling is activated in AS and functions as an inflammatory mediator (17).

Thus, the aim of the current study was initially to assess the anti-inflammatory effects of rosuvastatin in VSMCs, and especially to explore the essential role of miR-146a associated with its downstream signals in this process.

Materials and Methods

Subjects

Twenty coronary artery atherosclerotic patients in Affiliated Hospital of Nantong University were selected for this study between January and December, 2013. The subjects selected had less than 50% vascular stenosis evaluated with coronary artery arteriography. Another 20 participants with no visible coronary atherosclerotic plaque were recruited as a control group. All participants provided written informed consent before participating in the experiments. This study was approved by the Research Ethics Committee of Affiliated Hospital of Nantong University. Participants were invited to participate in a preliminary appointment during which a clinical evaluation was performed in order to obtain general information. During this baseline visit, the height and weight of all participants were measured using a digital bathroom scale (TZ-150; Shanghai, China) and height and weight measurements were used to calculate body mass index (BMI). Systolic blood pressure and diastolic blood pressure were monitored using a hematomanometer. Blood samples were collected for subsequent biochemical analysis.

Biochemical analysis

Blood samples (10mL) were collected and were distributed in different tubes, as follows: (1) no anticoagulant (10mL) for triglyceride, cholesterol, glucose, HDL, and low-density lipoprotein (LDL) analysis and (2) EDTA (5mL) for RNA extraction. Serum and plasma were separated by centrifugation for 15 minutes at 3,500g at 4°C. Samples were stored at 4°C and were analyzed within a 12 hour after samples collection. According to the manufactures' instructions, Olympus laboratory kits were used to measure total cholesterol, triglycerides, HDL, LDL, and glucose using an AU400 chemical analyzer (Olympus, Tokyo, Japan).

VSMC culture

The male and female Wister rats (within 24 hours after birth) were provided by the Animal Center of Nantong University. Animals were sacrificed for VSMC culture. After sacrifice, the aortas were immediately collected and washed with ice-cold phosphate buffered saline (PBS). The clean aortas were carefully sheared into 1mm×1mm fragments and subsequently arranged evenly on the bottom of a culture vessel with 3cm of clearance between tissues. Three ml of high glucose dulbecco's modified eagle medium (DMEM) supplied with 15% fetal calf serum and 0.1 mmol/L of 5-Bromodeoxyuridine (Brdu) were added to the vessel, and the vessel was shaken slightly until tissue infiltration was achieved, then cultured at a constant temperature of 37°C in a 5% CO2 incubator. After one to two hours of incubation, the vessel was turned around, enabling the tissue fragments to become soaked in the culture medium for continuous static cultivation. The first passage was carried out when cells were observed to be stretched out around the tissue fragments and gradually was confluent 85% overspreading the bottom. For passage, tissue fragments were gently removed, and 1mL of 0.1% trypsinase was added. After about two to five minutes of digestion, cells were placed under a microscope. Trypsinase was extracted when cells demonstrated cell retraction and increased gap. Five to 10mL of culture medium containing 0.1mmol/L of Brdu was added to the cells, and cells were passaged every five to seven days. Cells that underwent three or four passages were used for further experiments.

Experimental protocols

Based on the aim of the drug intervention, VSMCs were classified into two experimental procedures: dosage-dependent analysis (treated with one, five, or 10μM doses of rosuvastatin for 24 hours) and time-dependent analysis (treated with 5μM doses of rosuvastatin for 12, 24, or 48 hours). To evaluate the anti-inflammatory effects of rosuvastatin, cells were pretreated with 100nM LPS (lipopolysaccharide) for 24 hours before rosuvastatin treatment.

Quantitative RT-PCR

Total RNA was isolated from VSMCs using a Trizol kit. After being quantified by a spectrophotometer, 2μg of RNA was synthesized to cDNA using the High Capacity cDNA Reverse Transcription Kit (Applied Biosystems, Foster City, CA, USA), according to the manufacturer's protocols. The cDNA product was harvested and stored at -20°C until analysis in real time quantitative reverse transcription-PCR (RT-qPCR). The procedure of RT-PCR was as follows: a homogenized 50μl reaction mixture was created using cDNA product, primers, probes (Applied Biosystems), a dNTP mixture, and Tap DNA polymerase. The procedure was then carried out based on the manufacturer's instructions for use of the Applied Biosystems ABI7500 Real Time PCR Instrument. Relative expression of miR-146a was normalized to U6 and calculated using the $2^{-\Delta\Delta CT}$ method; results are presented as the fold change from the control group mean

values, in which the Ct did not show a significant variation between groups.

Transfection

VSMCs were transfected with commercially available synthetic miRNA mimics for miR-146a, miR-146a mimic control, miRNA inhibitor for miR-146a, or scramble miR-146a inhibitor control (Ambion, Carlsbad, CA, USA) using the Oligofectamine® 2000 transfection reagent (Invitrogen, Chicago, IL, USA) according to the manufacturer's protocols. VSMCs were grown to 85% confluence and incubated with miR-146a mimic or miR-146a inhibitor or controls for 48 hours.

Western blotting

Phosphoryl-p65 (P-p65), total p65, and TRAF6 protein levels were detected via Western blot analysis. Cells from experimental groups were homogenized and made into protein lysate. After being quantified by a BCA Protein Assay kit, 30μg of protein were separated by sodium dodecyl sulfate-polyacrylamide gel electrophoresis (SDS-PAGE) and then transferred to a polyvinylidene fluoride (PVDF) membrane (Millipore, USA). The filters were blocked with 5% milk in Tris-buffered saline, followed by incubation with polyclonal antibodies raised against P-p65 (1:2,000 dilution; Abcam), total p65 (1:500 dilution; Abcam), TRAP6 (1:500 dilution; Abcam), or GAPDH (1:5,000 dilution; Abcam). After overnight incubation at 4°C, the membranes were washed with buffer solution and then incubated with peroxidase-conjugated secondary antibodies (diluted 1:1,000) in Tris-buffered saline with 0.01% Tween-20. The ECL chemiluminescent substrate (Beyotime, Shanghai, China) was used to detect the peroxidase-conjugated antibodies using a SmartGel 600 transilluminator. The intensity of the bands was evaluated with Lane 1DTM analysis software (Beijing Sage).The intensity of the protein bands was quantified relative to the GAPDH bands.

Statistical analysis

All data analyses were performed using the SPSS version 16.0 software. The significant differences between groups were analyzed by the one-way analysis of variance with Bonferroni's multiple comparisons test. Data are presented as mean ± standard deviation. P values < 0.05 were considered to be statistically significant.

Results

Differential expression of miR-146a in atherosclerotic patients

We characterized the parameters of both AS patients and controls in Table 1. Participants in the two study groups had similar characteristics in terms of age, sex, and body mass index. Systolic blood pressure, diastolic blood pressure, and mean arterial blood pressure were significantly or non-significantly higher in AS patients than in controls; however, these three parameters were maintained at the normal physiological levels indicating that AS patients were with atherosclerotic cardiomyopathy. On the other hand, markers for AS—significantly reduced HDL level (P = 0.005) and significantly elevated LDL level (P = 0.008)—were observed. A substantial decrease in the HDL to LDL ratio (P = 0.003) was also observed in atherosclerotic patients. Serum triglyceride and cholesterol levels were slightly lower, but this difference was not statistically significant.

The results of qRT-PCR showed that atherosclerotic patients (n = 20) had significantly lower miR-146a expression in peripheral blood than the 20 controls (P = 0.0004) (Figure 1).

MiR-146a regulates the expression of inflammation-related signaling proteins

To evaluate the potential role of miR-146a in inflammation-related signaling in VSMCs, we manipulated cellular miR-146a by miR-146a mimic or miR-146a inhibitor transfection in order to analyze the expression of inflammation-related signaling proteins. Results from Western blotting showed that phosphoryl-p65 (P-p65) was downreg-

Table 1. Characteristics of the control and patient groups.

	Control Group (N = 20)	Atherosclerotic Patients (N = 20)	p-Value
Age (years)	52.14±6.28	51.75±9.59	0.419
Body Mass Index	23.45±6.18	26.01±12.49	0.079
Systolic Blood Pressure	123.54±8.51	130.21±15.29	0.039
Diastolic Blood Pressure	81.39±4.59	82.13±11.15	0.205
Mean Arterial Blood Pressure	91.34±6.42	97.69±13.25	0.009
Random Blood Glucose Level (mg/dl)	85.29±5.14	137.77±71.28	0.0001
Triglyceride Level (mg/dl)	91.42±27.92	92.07±46.35	0.752
Cholesterol Level (mg/dl)	139.52±20.18	141.29±43.37	0.513
HDL Level (mg/dl)	34.22±4.08	27.41±6.16	0.005
LDL Level (mg/dl)	87.54±21.36	99.59±33.19	0.008
HDL/LDL	0.42±0.25	0.25±0.13	0.003

HDL, high-density lipoprotein; LDL, low density lipoprotein.

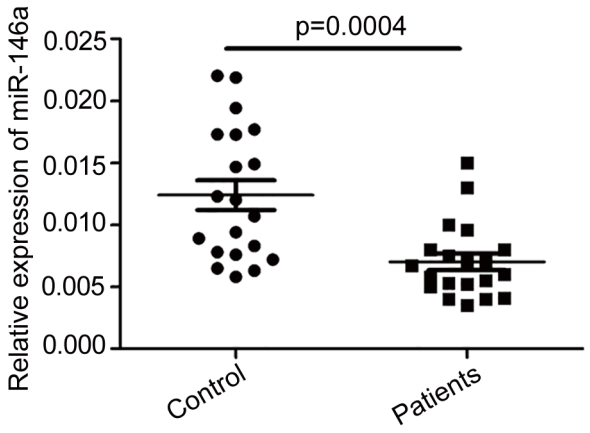

Figure 1. MiR-146a levels in the peripheral blood of atherosclerotic patients in comparison to controls.

ulated in response to miR-146a overexpression, whereas it was upregulated in response to miR-146a silencing, suggesting a negatively regulatory action of miR-146a on NF-κB activation (Figure 2A). In addition, TRAF6 expression was attenuated by miR-146 overexpression and was enhanced by miR-146a silencing (Figure 2B).

Rosuvastatin dose-dependently and efficiently promotes miR-146a expression in VSMCs

We then examined the differential expression of miR-146a in response to rosuvastatin treatment. The results showed that rosuvastatin at doses of one, five, and 10μM effectively strengthened miR-146a expression, and this effect emerged in a dose-dependent manner (Figure 3A). In addition, the relative expression of miR-146a was enhanced by increased processing time in response to the 5μM dose of rosuvastatin (Figure 3B).

Rosuvastatin inhibits inflammatory response mediated by miR-146a in VSMCs

To explore the anti-inflammatory action of rosuvastatin, we treated VSMCs with one, five, and 10μM doses of rosuvastatin in the presence of an LPS-induced inflammatory response in order to evaluate the expression of inflammatory signaling proteins. As shown in Figures 4A and 4B, rosuvastatin dose-dependently attenuated P-p65 and TRAF6 expression. MiR-146a pretreatment effectively abrogated expressional inhibition of rosuvastatin on P-p65 (Figure 4C) and TRAF6 (Figure 4D), suggesting the involvement of miR-146a in the anti-inflammatory action of rosuvastatin.

Discussion

It is well established that people with AS often have the complications of abnormal blood pressure, low HDL levels and elevated LDL levels (Table 1), suggesting the role of chronic inflammation in the development of atherosclerotic plaques (18, 19). One of the inflammatory pathological basics of atherosclerosis is the activation of inflammatory signaling pathways in VSMCs (20). Therefore, therapeutic immunosuppression of VSMCs is a possible strategy for treating AS. In the present study, we showed that rosuvastatin inhibited the NF-κB and TRAF-6 inflammatory signals of VSMCs by enhancing miR-146a expression.

AS is often associated with aberrant miRNA expression and miRNA-regulated target pathways (21). In the present study, we found that plasma miR-146a was downregulated in the peripheral blood of AS patients. Previous studies have shown that high expression of miR-146a associating with its target genes was beneficial for suppressing inflammation and AS (12, 22). We thereby speculated that miR-146a might function as a regulator for inflammation-related gene expression in VSMCs. NF-κB (15) and TRAF6 (16, 23) were regarded as the targets of miR-146a in inflammatory disease in various cells in previous studies. These two proteins are essential molecules for the immune system. TRAF6 mediated signals have proven critical to the development, homeostasis, and activation of immune cells. NF-κB and the signals that it controls regulate cellular oxidative stress and inflammation (24). Furthermore, TRAF6 and NF-κB have been proven to be activated in AS, inducing inflammatory mediators. These situations are shown in Figure 2, which shows the negative alteration of phosphoryl-p65 expression (a subunit of NF-κB) and presents its activation as indicated by phosphorylation level (25) and the expression of TRAF6

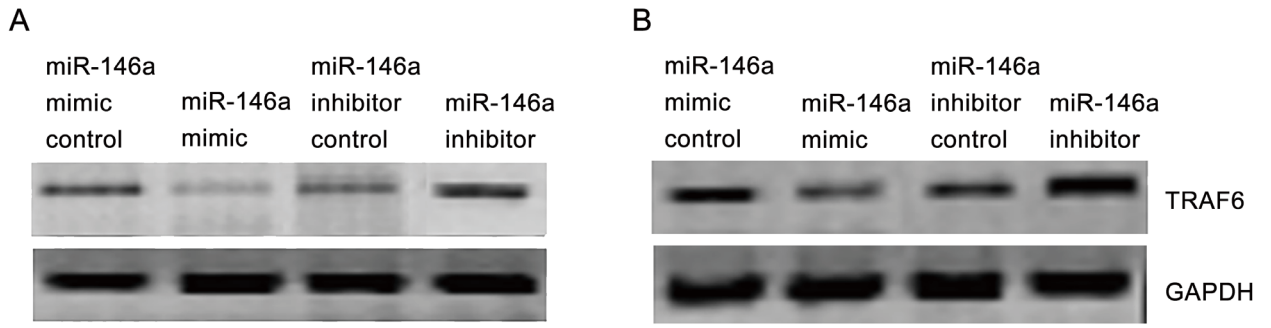

Figure 2. Expression of inflammation-related signals in VSMCs mediated by miR-146a. (A) Representation of phosphoryl-p65 (P-p65) and total p65, and (B) TRAF6 in miR-146a mimic- or miR-146a inhibitor-transfected VSMCs by Western blotting.

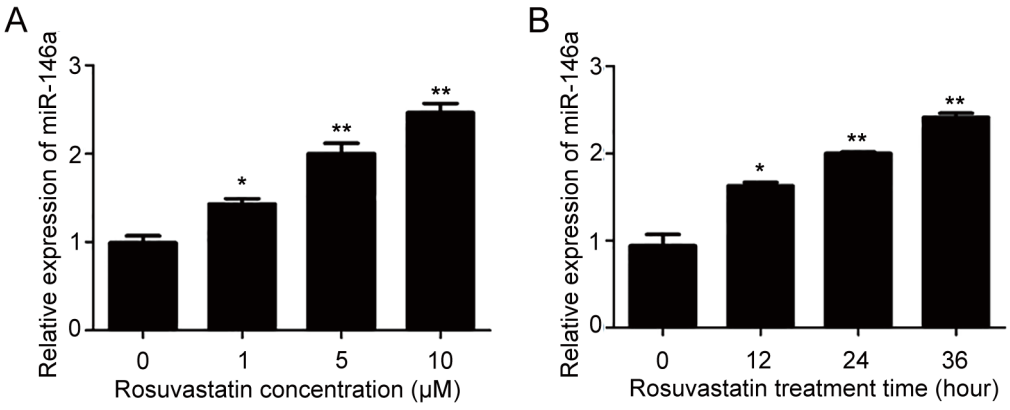

Figure 3. Effect of rosuvastatin on miR-146a expression in VSMCs. Relative expression of miR-146a was determined (A) after a 24 hour period of treatment with one, five, or 10μM of rosuvastatin and (B) after a 5μM dose of rosuvastatin after 12, 24, or 36 hours treatment. Data are presented as mean ± standard deviation. $^{*}p < 0.05$, $^{**}p < 0.01$ compared with no rosuvastatin treatment.

by enrichment or silence of cellular miR-146a in VSMCs. These data suggest the miR-146a/NF-κB/TRAF6 axis in VSMCs.

In addition, the anti-atherogenic drug rosuvastatin was shown to efficiently and dose-dependently enhance miR-146a expression in VSMCs in the present study, indicating the involvement of miR-146a in the anti-inflammatory action of rosuvastatin. Rosuvastatin is commonly regarded as a 3-hydroxy-3-methylglutaryl coenzyme reductase inhibitor, and it is clinically and experimentally used in pleiotropic therapy for anti-inflammation and anti-AS. The benefit derived from rosuvastatin is primarily a result of achieving low LDL cholesterol levels and enhancing the stability of atherosclerotic plaques. The pharmacological effects of rosuvastatin have been evaluated through both in vivo animal studies and more abstract analysis of clinical data. The clinical data appear to indicated that rosuvastatin had anti-proliferation and anti-migration effects on VSMCs (26); however, there is little evidence focusing on its role in the inflammatory response. Therefore, further research is required to evaluate the anti-inflammatory benefits of rosuvastatin and to optimize its potential to treat and prevent cardiovascular disease.

This study examined whether miR-146a is involved in the

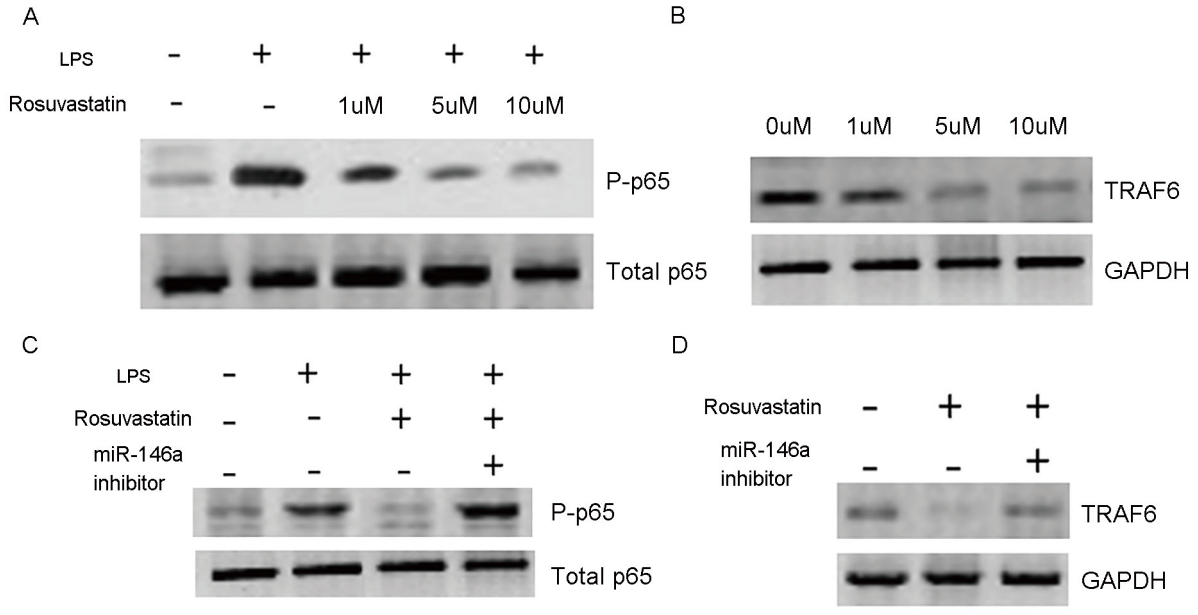

Figure 4. Rosuvastatin inhibits inflammatory response mediated by miR-146a in VSMCs. (A) Expression levels of P-p65 and total p65, and (B) TRAF6 in VSMCs that have experienced a 12 hour period of treatment with one, five, or 10μM rosuvastatin and a 12 hour period of treatment with 100nM LPS. (C) P-p65 and total p65, and (D) TRAF6 expression were found in VSMCs that were treated with both rosuvastatin and miR-146a inhibitor.

anti-inflammatory action of rosuvastatin in VSMCs. MiR-146 was first identified as a negative regulator in innate immune and inflammatory responses induced by LPS (27). LPS-induced upregulation of P-p65 and TRAF6 expression are gradually attenuated by increasing the dose of rosuvastatin in VSMCs. The anti-inflammatory response of rosuvastatin was reversed by miR-146a silencing. Several studies in the clinical and experimental setting have investigated the effects of rosuvastatin on the pathogenesis of AS-related disease, including its ability to alter HLD concentration, improve endothelial function, and stabilize atherosclerotic aortic plaques (6), although it does not appear to improve the function of VSMCs. Rosuvastatin can ameliorate the inflammation response through inactivation of NF-κB (28).

In conclusion, rosuvastatin, the well-known treatment used in AS diseases, was found to have an anti-inflammatory effect on LPS-induced VSMCs by affecting the miR-146a/NF-κB/TRAF6 signaling pathway. Our study provides strong evidence for direct, beneficial anti-inflammatory effects of rosuvastatin in AS-effected VSMCs.

Conflict of Interest

All authors declare that there is no conflict of interest.

References

1. Celermajer DS, Chow CK, Marijon E, Anstey NM, Woo KS. Cardiovascular disease in the developing world: prevalences, patterns, and the potential of early disease detection. Journal of the American College of Cardiology. 2012;60(14):1207-16.
2. Hemerich D, van der Laan SW, Tragante V, den Ruijter HM, de Borst GJ, Pasterkamp G, et al. Impact of carotid atherosclerosis loci on cardiovascular events. Atherosclerosis. 2015;243(2):466-8.
3. Gardner SE, Humphry M, Bennett MR, Clarke MC. Senescent Vascular Smooth Muscle Cells Drive Inflammation Through an Interleukin-1alpha-Dependent Senescence-Associated Secretory Phenotype. Arteriosclerosis, thrombosis, and vascular biology. 2015;35(9):1963-74.
4. Ikdahl E, Hisdal J, Rollefstad S, Olsen IC, Kvien TK, Pedersen TR, et al. Rosuvastatin improves endothelial function in patients with inflammatory joint diseases, longitudinal associations with atherosclerosis and arteriosclerosis: results from the RORA-AS statin intervention study. Arthritis research & therapy. 2015;17:279.
5. Masuda J, Tanigawa T, Yamada T, Nishimura Y, Sasou T, Nakata T, et al. Effect of combination therapy of ezetimibe and rosuvastatin on regression of coronary atherosclerosis in patients with coronary artery disease. International heart journal. 2015;56(3):278-85.
6. Ueno Y, Yamashiro K, Tanaka Y, Watanabe M, Miyamoto N, Shimada Y, et al. Rosuvastatin may stabilize atherosclerotic aortic plaque: transesophageal echocardiographic study in the EPISTEME trial. Atherosclerosis. 2015;239(2):476-82.
7. Aydin MU, Aygul N, Altunkeser BB, Unlu A, Taner A. Comparative effects of high-dose atorvastatin versus moderate-dose rosuvastatin on lipid parameters, oxidized-LDL and inflammatory markers in ST elevation myocardial infarction. Atherosclerosis. 2015;239(2):439-43.
8. Wang JA, Chen WA, Wang Y, Zhang S, Bi H, Hong B, et al. Statins exert differential effects on angiotensin II-induced atherosclerosis, but no benefit for abdominal aortic aneurysms. Atherosclerosis. 2011;217(1):90-6.
9. Kotsinas A, Sigala F, Garbis SD, Galyfos G, Filis K, Vougas K, et al. MicroRNAs Determining Inflammation as Novel Biomarkers and Potential Therapeutic Targets. Current medicinal chemistry. 2015;22(22):2666-79.
10. Raitoharju E, Oksala N, Lehtimaki T. MicroRNAs in the atherosclerotic plaque. Clinical chemistry. 2013;59(12):1708-21.
11. Wang J, Pei Y, Zhong Y, Jiang S, Shao J, Gong J. Altered serum microRNAs as novel diagnostic biomarkers for atypical coronary artery disease. PloS one. 2014;9(9):e107012.
12. Chen LJ, Chuang L, Huang YH, Zhou J, Lim SH, Lee CI, et al. MicroRNA mediation of endothelial inflammatory response to smooth muscle cells and its inhibition by atheroprotective shear stress. Circulation research. 2015;116(7):1157-69.
13. Joshi SR, Comer BS, McLendon JM, Gerthoffer WT. MicroRNA Regulation of Smooth Muscle Phenotype. Molecular and cellular pharmacology. 2012;4(1):1-16.
14. Sun SG, Zheng B, Han M, Fang XM, Li HX, Miao SB, et al. miR-146a and Kruppel-like factor 4 form a feedback loop to participate in vascular smooth muscle cell proliferation. EMBO reports. 2011;12(1):56-62.
15. Dong S, Xiong W, Yuan J, Li J, Liu J, Xu X. MiRNA-146a regulates the maturation and differentiation of vascular smooth muscle cells by targeting NF-kappaB expression. Molecular medicine reports. 2013;8(2):407-12.
16. Walsh MC, Lee J, Choi Y. Tumor necrosis factor receptor- associated factor 6 (TRAF6) regulation of development, function, and homeostasis of the immune system. Immunological reviews. 2015;266(1):72-92.
17. Wu XD, Zeng K, Liu WL, Gao YG, Gong CS, Zhang CX, et al. Effect of aerobic exercise on miRNA-TLR4 signaling in atherosclerosis. International journal of sports medicine. 2014;35(4):344-50.
18. Rosenson RS, Brewer HB, Jr., Ansell BJ, Barter P, Chapman MJ, Heinecke JW, et al. Dysfunctional HDL and atherosclerotic cardiovascular disease. Nature reviews Cardiology. 2015.
19. Yang RH, Liu YF, Wang XJ, Liang JG, Liu JC. Correlation between high density lipoprotein and monocyte subpopulations among stable coronary atherosclerotic heart disease patients. International journal of clinical and experimental medicine. 2015;8(9):16969-77.
20. Chistiakov DA, Orekhov AN, Bobryshev YV. Vascular smooth muscle cell in atherosclerosis. Acta physiologi-

ca. 2015;214(1):33-50.
21. Julio MM, Noemi R, Aranda JF, Carlos FH. MicroRNAs and atherosclerosis. Current atherosclerosis reports. 2013.
22. Li K, Ching D, Luk FS, Raffai RL. Apolipoprotein E enhances microRNA-146a in monocytes and macrophages to suppress nuclear factor-kappaB-driven inflammation and atherosclerosis. Circulation research. 2015;117(1):e1-e11.
23. Gao M, Wang X, Zhang X, Ha T, Ma H, Liu L, et al. Attenuation of Cardiac Dysfunction in Polymicrobial Sepsis by MicroRNA-146a Is Mediated via Targeting of IRAK1 and TRAF6 Expression. Journal of immunology. 2015;195(2):672-82.
24. Morgan MJ, Liu ZG. Crosstalk of reactive oxygen species and NF-kappaB signaling. Cell research. 2011;21(1):103-15.
25. Shishodia S, Majumdar S, Banerjee S, Aggarwal BB. Ursolic acid inhibits nuclear factor-kappaB activation induced by carcinogenic agents through suppression of IkappaBalpha kinase and p65 phosphorylation: correlation with down-regulation of cyclooxygenase 2, matrix metalloproteinase 9, and cyclin D1. Cancer research. 2003;63(15):4375-83.
26. Kiyan J, Kusch A, Tkachuk S, Kramer J, Haller H, Dietz R, et al. Rosuvastatin regulates vascular smooth muscle cell phenotypic modulation in vascular remodeling: role for the urokinase receptor. Atherosclerosis. 2007;195(2):254-61.
27. Baltimore D, Boldin M, Taganov K. Modulation of innate immunity receptors' signaling by microRNAs miR-146a and miR-146b. US; 2014.
28. Kim YS, Ahn Y, Hong MH, Kim KH, Park HW, Hong YJ, et al. Rosuvastatin suppresses the inflammatory responses through inhibition of c-Jun N-terminal kinase and Nuclear Factor-kappaB in endothelial cells. Journal of cardiovascular pharmacology. 2007;49(6):376-83.

ARTICLE

Lipid and Cardiovascular Research. 2015;**01**(1):30-36
http://www.enochpublisher.com/LCR

ENOCH PUBLISHING CORPORATION

The Impact of Total Bilirubin on Prognosis Among No-reflow Patients Presenting with Acute ST-segment Elevation Myocardial Infarction During Primary Coronary Angioplasty: An 11 Year Follow-up Study

Jian-Feng Liu[1], Chang-Hua Wang[3], Jin-Wen Wang[3], Jing Wang[2], Jun-Jie Yang[2], Feng Tian[2], Shan-Shan Zhou[2], Yun-Dai Chen[2]*

Abstract

Total bilirubin (TB) is reversely associated with in-hospital outcomes of acute ST-segment elevation myocardial infarction (STEMI) patients during primary percutaneous coronary intervention (PCI). However, whether high TB exerts favorable effects on the prognosis for no-reflow patients remains in need of further investigation. A total of 135 consecutive no-reflow patients were enrolled in the study. Patients were divided into two groups based on TB concentrations (0.9 mg/dl). No-reflow was diagnosed using two different methods: Thrombolysis in myocardial infarction (TIMI) flow grade ≤ 2 or TIMI flow grade 3 with a TIMI myocardial perfusion grade (TMPG) ≤ 1. The primary clinical endpoints were all-cause death and cardiovascular outcomes. The in-hospital cardiovascular mortality of the high TB group was lower than that of the low TB group (1.4% vs. 12.7%, p = 0.013). By multivariate logistic regression analysis, high TB levels were a significant predictor of in-hospital cardiovascular mortality (odds ratio (OR) 0.083, 95% confidence intervals (CI) 0.007–0.977, p = 0.048). In the receiver operating characteristic curve (ROC) analysis, TB > 0.9 mg/dl was a significant indicator of no-reflow patients for in-hospital cardiovascular mortality (area under the curve 0.802, 95% CI; 0.613–0.990, p = 0.003). The conclusion of the study is that high TB level is an independent predictor of in-hospital outcomes among no-reflow patients.

Keywords: total bilirubin, myocardial infarction, primary percutaneous coronary intervention, no-reflow, mortality

Introduction

The no-reflow phenomenon occurs in patients with ST-segment elevation myocardial infarction (STEMI) undergoing percutaneous coronary intervention (PCI), which hinders myocardial reperfusion, results in persistent myocardial ischemia and irreversible cell loss, and further leads to deteriorative cardiac function and increased mortality. The underlying cause of no-reflow is microvascular obstruction, which includes amplifying inflammatory response and excessive reactive oxygen species (ROS) (1, 2). These factors might induce disruption of endothelial cells, vasospasm, downstream microembolization, and, ultimately, adverse clinical events.

The literature to this point has suggested that total bilirubin (TB) possesses potent antioxidant and anti-inflammatory properties (3-6). It has been reported that the TB level in plasma is inversely related to the risk of cardiovascular disease (CVD) (7-13). Although a high serum TB concentration after primary PCI has been reported to be inversely associated with in-hospital adverse outcomes in patients with STEMI who undergo primary PCI (14), none of the studies provide evidence showing an association between TB level and the prognosis for no-reflow patients treated by primary PCI. The study was performed to assess the impact of TB levels after primary PCI on in-hospital and long-term cardiovascular mortality in no-reflow patients.

Patients and Methods

Selection of Patients

Between January 2003 and June 2009, 134 consecutive no-reflow patients with STEMI, undergoing urgent car-

[1] Department of Geriatric Cardiology, Chinese PLA General Hospital, Beijing 100000, China
[2] Department of Cardiology, Chinese PLA General Hospital, Beijing 100000, China
[3] Department of Cardiology, Anzhen hospital, Beijing 100000, China

[*] Corresponding Author: Yun-Dai Chen
Department of Cardiology, Chinese PLA General Hospital, Beijing 100000, China
E-mail: shenlangliu@sina.com

Received: 18 October2015 / Accepted: 5 December 2015
Published online: 29 December 2015

diac catheterization admitted within 12 hr after the onset of STEMI, were retrospectively evaluated in the Chinese PLA General Hospital. The study protocol was approved by the Ethics Committee of the Chinese PLA General Hospital . The diagnosis of STEMI was based on clinical symptoms, cardiac enzyme concentration, and 12-lead electrocardiogram results. The diagnosis was also in accordance with coronary angiography in such patients.

Primary PCI, angiograp hic analysis, and definition of no-reflow

All patients underwent primary PCI and periprocedural care according to a standard procedure. Antiplatelet therapy consisted of chewable aspirin (300 mg at the start of the procedure and 75–100 mg/day continued indefinitely thereafter) and oral clopidogrel (600 mg as a loading dose followed by a maintenance dosage of 75 mg/day for at least 9–12 months). All patients received intravenously weight-adjusted unfractionated heparin (100 U/kg) before PCI. Primary PCIs were performed in our healthcare centers by experienced investigators. Bare metal stents (BMS) or drug-eluting stents (DES) were successfully implanted in the infarct-related artery (IRA) after the coronary angiography. Angiograms were analyzed using a validated quantitative coronary angiographic system (MEDIS, CMS 4.0, Leiden, the Netherlands) by personnel blinded to the clinical diagnosis. The diagnosis of no-reflow was established according to following criteria: thrombolysis in myocardial infarction (TIMI) flow grade < 3, or TIMI flow grade 3 with final myocardial blush grade (MBG) 0–1 (15, 16), at least 10 min after the end of primary PCI procedure [15,16]. Primary PCI success was defined as residual stenosis < 50% and TIMI grade 3 flow.

Data collection

The demographic and clinical details of the patients were ascertained by two of the investigators from hospital files and electronic medical records. The traditional cardiovascular risk factors included age, smoking history, hypertension, hypercholesterolemia, and diabetes mellitus. Hypertension was defined as systolic pressure > 140 mmHg or diastolic pressure < 90 mmHg on two separate measurements or as having undergone prior antihypertensive treatment. Hypercholesterolemia was defined as a level of total cholesterol in the blood ≥ 5.18 mmol/L, the previous use of lipid-lowering agents, or a previous diagnosis. Diabetes mellitus was defined as having a previous diagnosis, taking oral hypoglycemic drugs, having insulin injection therapy, or having a fasting plasma glucose (FBG) concentration above 7 mmol/L for those previously untreated patients. The fasting antecubital venous blood samples were drawn on the morning after coronary angiography. Peak creatine kinase-MB (CK-MB) and troponin T were determined from blood samples assayed every 4 hr following primary PCI. All biochemistry measurements employed standard methods.

Cardiac functions were evaluated through both clinical Killip classification and left ventricular ejection fraction (LVEF). Cardiogenic shock was defined as sustained hypotension (systolic blood pressure < 80 mmHg for > 30 minutes) with inadequate tissue perfusion, which is secondary to left ventricular dysfunction.

Clinical end points and follow-up

The follow-up deadline was May 18, 2010. The follow-up data was obtained by telephone contact or review of the hospital records. The primary end points of this study included all-cause death, cardiovascular death, and major adverse cardiovascular events (MACE) which are defined as cardiovascular death, non-fatal myocardial infarction (MI), ischemic stroke, rehospitalization for unstable angina, and target vessel revascularization (TVR). Cardiovascular death was defined as sudden death and death from a definitive cardiovascular cause.

Statistical analysis

All continuous variables are described as mean ± standard deviation (SD). All categorical variables are expressed as frequencies (percentages). Comparison of continuous variables between the two independent groups was performed with 2-tailed Student's t test. Statistical analysis was performed by means of the likelihood ratio, chi-square test for categorical variables.. Univariate and multivariate logistic regression analyses were applied to identify the independent predictors of in- hospital mortality. All variables in Table 1 and Table 2 suggesting a significant correlation ($p < 0.05$) with TB concentration in no-reflow patients after primary PCI at univariate analyses were recruited to multivariate a logistic regression model. The receiver operating characteristic (ROC) curves were used to assess the predictive value of TB on in-hospital mortality. Univariate Cox proportional hazards models were performed for all variables in Table 1 and Table 2 to determine the independent predictors of long-term mortality. Next, those with $p < 0.05$ were entered into the multivariate Cox proportional hazards analysis with the backward variable selection method. The cumulative survival curve for long-term mortality was estimated by applying the Kaplan-Meier method and the log-rank test. All analyses were performed by using the SPSS 17.0 (SPSS Inc., Chicago, Illinois, USA) software package. $P < 0.05$ was considered as statistically significant.

Results

The study sample included 134 patients with a mean age of 64.9 ± 12.7 years. Long-term follow-up (mean follow-up time 4.7 ± 2.5 years) endpoints were available for all patients. Patients were stratified into 2 groups according to their TB levels (14). There were 63 patients in the low TB group (TB ≤ 0.9 mg/dl) and 71 patients in the high TB group (TB > 0.9 mg/dl). Baseline clinical and laboratory characteristics of the study population are described in Table 1. Male patients were more often seen in the high TB

Table 1. Baseline clinical and laboratory characteristics in patients with no-reflow

Variable	Low TB (n=63)	High TB (n=71)	P value
Age (yrs)	66.5±11.4	63.5±13.7	0.178
Men	38 (60.3%)	57 (80.3%)	**0.011**
Body mass index (kg/ m^2)	25.0±2.9	25.2±2.7	0.781
Current smoker	18 (28.6%)	26 (36.6%)	0.322
Hypertension	35 (55.6%)	43 (60.6%)	0.557
Hypercholesterolemia	19 (30.2%)	24 (33.8%)	0.692
Diabetes mellitus	22 (34.9%)	16 (22.5%)	0.112
Prior myocardial infarction	6 (9.5%)	3 (4.2%)	**0.023**
Prior percutaneous coronary intervention	7 (11.1%)	3 (4.2%)	0.130
Prior coronary bypass	1 (1.6%)	1 (1.4%)	0.717
Anterior myocardial infarction	28 (44.4%)	36 (50.7%)	0.469
Killip class 2/3	14 (22.2%)	20 (28.2%)	0.430
Admission systolic blood pressure <100 mmHg	19 (30.2%)	20 (28.2%)	0.800
Admissive heart rate >100 beats/min	8 (12.7%)	9 (12.7%)	0.997
Symptom-to-perfusion time	4.75±2.60	5.13±3.32	0.468
AST (U/L)	158.0±270.2	167.6±205.8	0.787
ALT (U/L)	45.5±97.8	49.6±74.8	0.332
Total bilirubin (mg/dL)	0.64±0.15	1.28±0.38	**0.000**
Direct bilirubin (mg/dL)	0.22±0.10	0.31±0.26	**0.006**
Fasting glucose (mmol/L)	8.6±5.1	7.4±2.5	0.066
Total cholesterol (mmol/L)	4.6±1.0	4.4±1.1	0.269
Triglyceride (mmol/L)	1.5±0.9	1.3±0.7	0.449
Low-density lipoprotein (mmol/L)	2.6±0.7	2.4±0.8	0.261
High-density lipoprotein (mmol/L)	1.4±0.9	1.4±0.5	0.967
Creatinine (umol/L)	93.4±58.3	78.2±28.8	0.065
Uric acid (umol/L)	334.4±114.9	336.3±114.7	0.923
White blood cell ($\times 10^9$)	12.1±5.3	11.5±5.4	0.470
Hemoglobin (g/L)	132.5±20.2	141.2±16.5	**0.008**
Peak creatinine kinase-MB (U/L)	284.8±240.7	366.0±325.8	0.101
Peak troponin T (ng/mL)	9.2±11.8	9.5±9.0	0.835
Admission left ventricular ejection fraction (%)	46.2±9.5	47.6±9.1	0.410
Anemia on admission	10 (15.9%)	3 (4.2%)	**0.023**

Data are described as mean ± SD for continuous data and n (%) for categorical variables. AST = aspartic transaminase; ALT = alanine aminotransferase.

group compared with those patients in the low TB group. Prior myocardial infarction was more frequently seen in the low TB group than in the high TB group.

The concentration of serum TB and direct bilirubin on admission was 1.28 ± 0.38 mg/dl and 0.31 ± 0.26 mg/dl for the high TB group and 0.64 ± 0.15 mg/dl and 0.22 ± 0.10 mg/dl for the low TB group (p = 0.000 and p = 0.006, respectively). Patients with high TB levels had higher plasma hemoglobin levels than those with low TB concentration (141.2 ± 16.5 vs. 132.5 ± 20.2, p = 0.008). The prevalence of anemia on admission in the high TB group was lower than that of the low TB group (p = 0.023).

Angiographic and procedural characteristics are stated in Table 2. A lower proportion of patients with 3-vessel disease was observed in the high TB group. In contrast, significantly greater rates of 1 or 2-vessel disease were found in the high TB group (p = 0.037).

In-hospital prognoses based on serum TB levels are shown in Table 3. The incidence of in-hospital death was significantly lower in the high TB group than in the low TB group (1.4% vs. 12.7%, p = 0.013). Serious ventricular arrhythmia in the high TB group was observed less frequently compared with that of the low TB group (p = 0.036). Although no significant difference was found between groups with respect to cardiogenic shock necessitating an intra-aortic balloon pump (IABP) (p = 0.05), a decreasing trend was observed from the low TB group to the high TB group.

As shown in Table 4, none of the long-term MACE (include all-cause mortality, non-fatal infarction, target vessel revascularization, ischemic stroke, rehospitalization for unstable angina), was noted to have any significant difference. Likewise, the Kaplan-Meier survival curve showed that no statistical difference for long-term cardiovascular mortality was observed between the low and high TB groups (p = 0.621; Figure 1).

In order to assess the association of serum TB levels with

Table 2. Angiographic and procedural characteristics in patients with no-reflow

Variable	Low TB (n=63)	High TB (n=71)	P value
Infarct related artery			0.139
Left main	0	0	
Left anterior descending	30 (47.6%)	43 (60.6%)	
Circumflex	4 (6.3%)	7 (9.9%)	
Right coronary artery	29 (46.0%)	21 (29.6%)	
Venous bypass graft	0	0	0.137
Infarct location			
Proximal	30 (47.6%)	35 (49.3%)	
Middle	21 (33.3%)	30 (42.3%)	
Distal	12 (19.0%)	6 (8.5%)	
Narrowed coronary vessels (n)			**0.037**
1	18 (28.6%)	25 (35.2%)	
2	15 (23.8%)	27 (38.0%)	
3	30 (47.6%)	19 (26.8%)	
Stent type			0.109
Drug-eluting stent	45 (71.4%)	42 (59.2%)	
Bare metal stent	14 (22.2%)	27 (38.0%)	
Stent length, average (mm)	19.1±8.6	19.7±8.0	0.694
Stent diameter, average (mm)	3.1±0.4	3.2±0.3	0.114
Thrombus burden			0.390
0	4 (6.3%)	6 (8.5%)	
1	1 (1.6%)	4 (5.6%)	
2	2 (3.2%)	1 (1.4%)	
3	3 (4.8%)	4 (5.6%)	
4	0 (0.0%)	3 (4.2%)	
5	53 (84.1%)	53 (74.6%)	
Preintervention TIMI flow grade			0.356
0-1	53 (84.1%)	54 (76.1%)	
2	1 (1.6%)	4 (5.6%)	
3	9 (14.3%)	13 (18.3%)	
Postintervention TIMI flow grade			0.083
0-1	4 (6.3%)	1 (1.4%)	
2	5 (7.9%)	13 (18.3%)	
3	54 (85.7%)	57 (80.3%)	
Glycoprotein Ⅱb/Ⅲa inhibitor	5 (7.9%)	11 (15.5%)	0.178
Thrombus aspiration	21 (33.3%)	19 (26.8%)	0.407

Data are described as mean ± SD for continuous data and n (%) for categorical variables.

Table 3. In-hospital cardiac events and complications

Variable	Low TB (n=63)	High TB (n=71)	P value
In hospital mortality	8 (12.7%)	1 (1.4%)	**0.013**
Non-fatal MI	1 (1.6%)	2 (2.8%)	0.627
Target vessel revascularization (PCI or CABG)	5 (7.9%)	6 (8.5%)	0.914
Ischemic stroke	0 (0.0%)	1 (1.4%)	0.258
Major adverse cardiac events	13 (20.6%)	11 (15.5%)	0.502
Intra-aortic balloon pump/cardiogenic shock	13 (20.6%)	6 (8.5%)	**0.050**
Serious ventricular arrhythmia	15 (23.8%)	7 (9.9%)	**0.036**
Complete atrioventricular block requiring transient pacemaker	16 (25.4%)	11 (15.5%)	0.196

MACE: In-hospital death, non-fatal MI, target vessel revascularization, ischemic stroke. Data are described as n (%) for categorical variables.

in-hospital mortality, univariate and multivariate logistic regression analyses were performed. After adjustment for

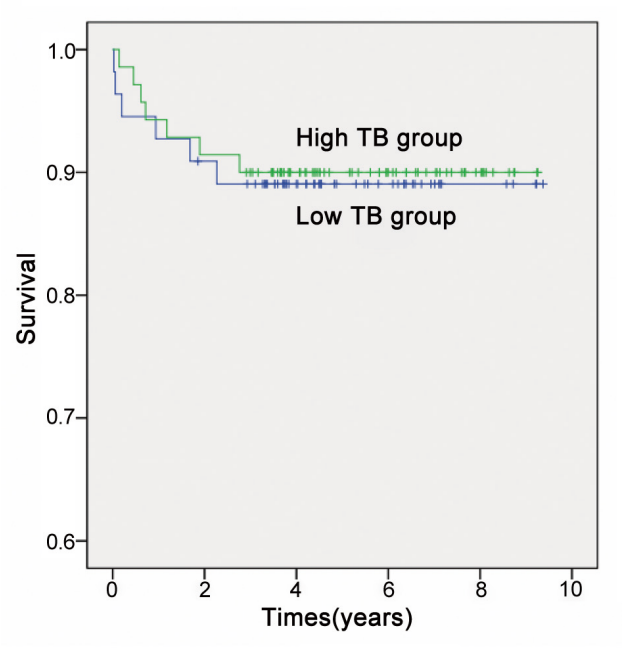

Figure 1. Kaplan-Meier survival curve for long-term survival according to bilirubin levels in entire population of patients. (P = 0.621, log-rank test).

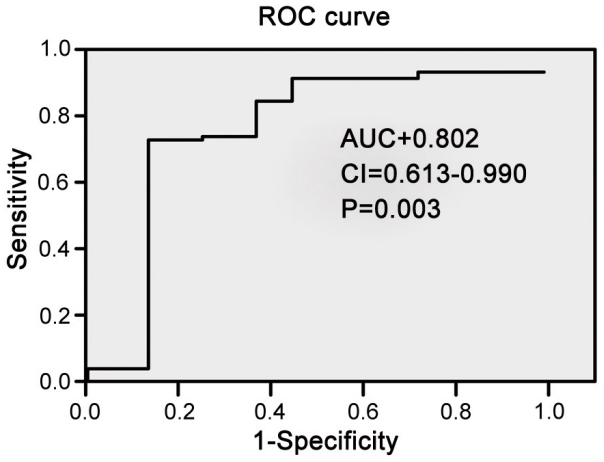

Figure 2. The ROC curve of total bilirubin for predicting in-hospital mortality in no-reflow patients.

heart rate, peak troponin T, TB level > 0.9 mg/dl, and anemia on admission due to a significant difference found in univariate analysis, multivariate logistic analysis showed that the independent predictor of in-hospital mortality in no-reflow patients with STEMI after primary PCI was high TB level (odds ratio (OR) 0.098, 95% confidence intervals (CI) 0.012–0.809, p = 0.031) and anemia (OR 18.281, 95% CI 4.090–81.704, p = 0.000) (Table 5).

The ROC curve analysis further illustrated that the serum TB value > 0.90 mg/dl on admission are a strong indicator of in-hospital cardiovascular mortality in no-reflow patients (area under the curve 0.802, 95% CI 0.613–0.990, p = 0.003; Figure.2).

Discussion

The major findings of the study are as follows: decreased serum TB levels were inversely associated with increased risk of in-hospital cardiovascular events, including cardiovascular mortality and serious ventricular arrhythmia, in no-reflow patients with STEMI after primary PCI. This study demonstrated that high levels of fasting serum TB after primary PCI can independently predict in-hospital cardiovascular outcomes in no-reflow patients. However, serum TB levels cannot serve as an independent predictor of long-term mortality.

No-reflow is a frustrating phenomenon for patients with STEMI during primary PCI due to its poor prognosis, which is defined by the presence of patent epicardial upstream coronary arteries with the onset of severe myocardial tissue hypoperfusion (17). In particular, what is called "reperfusion no-reflow" occurs following primary PCI for revascularization of the infarct related artery (17). An earlier study demonstrated that patients with transient no-reflow had higher in- hospital and 6-month mortality compared with those without transient no-reflow during the procedure (18). It was also reported that no-reflow after primary PCI was associated with increased risk of 1-year mortality (19). Another prospective study on 599 patients who underwent primary PCI for STEMI found that no-reflow is a strong predictor of long-term mortality (20). Given the high risk of the no-reflow phenomenon during primary PCI, considerable attempts should be taken to facilitate clinical risk stratification and to provide a more predictable strategy

Table 4. Follow-up cardiovascular events

Variable	Low TB (n=55)	High TB (n=70)	P value
All cause death	7 (12.7%)	7 (10.0%)	0.631
Cardiovascular mortality	6 (10.9%)	3 (4.3%)	0.155
Non-fatal infarction	3 (5.5%)	1 (1.4%)	0.204
Target vessel revascularization (PCI or CABG)	12 (21.8%)	11 (15.7%)	0.382
Ischemic stroke	1 (1.8%)	4 (5.7%)	0.270
Rehospitalisation for unstable angina	7 (12.7%)	4 (5.7%)	0.169
Major adverse cardiac events	24 (43.6%)	25 (35.7%)	0.368

MACE: All-cause death, non-fatal infarction, target vessel revascularization, ischemic stroke, rehospitalization for unstable angina. Data are described as n (%) for categorical variables.

Table 5. Predictors of in-hospital death in univariable and multivariable logistic regression analysis

Variable	Univariable Analysis			Multivariable-Adjusted Analysis		
	OR	95% CI	P value	OR	95% CI	P value
Admissive HR >100bpm	6.892	1.642-28.937	0.008	4.362	0.660-28.818	0.126
TnT peak value	1.076	1.018-1.137	0.009	1.069	0.978-1.169	0.141
TB >0.9 mg/dl	0.098	0.012-0.809	0.031	0.083	0.007-0.977	0.048
Anemia	18.281	4.090-81.704	0.000	6.315	1.074-37.132	0.041

for the prognosis of no-reflow patients.

In the past decades, many studies have focused on the association between serum bilirubin levels and coronary arterial disease (CAD). It was reported that serum bilirubin levels were significantly inversely related to CAD (7, 11, 13). Higher bilirubin levels could be associated with a better prognosis for patients with cardiac syndrome X at the 5 year follow-up (21). Moreover, elevated serum bilirubin levels provide protection against coronary flow reserve (CFR) impairment and coronary microvascular dysfunction (22). Additionally, increased serum bilirubin levels are related to favorable coronary collateral flow in patients with chronic total coronary occlusion (23). Also, collateral blood flow may predict MBG in acute myocardial infarction patients undergoing primary PCI (24). Moreover, recent research has confirmed that the elevated serum bilirubin levels in patients with acute MI are positively correlated with serum HO-1 levels and that the bilirubin peak level, 15–18 hours after MI, is a favorable biomarker for myocardial injury (25). It is not surprising that high TB is independently related to in-hospital adverse outcomes in patients with STEMI who undergo primary PCI (14). These results suggest that high levels of bilirubin can attenuate endothelial dysfunction.

Although the underlying cause of no-reflow is microvascular obstruction, its etiology appears to be multifactorial, such as endothelial injury, microvascular inflammatory response, reactive oxygen species, vasospasm, intracellular calcium overload (1, 2). It is well known that bilirubin is an end product generated intracellularly during heme catabolism by heme oxygenase (HO), which emerges as a potent antioxidant (3). The antioxidant capacity of bilirubin gives it the ability to scavenge oxygen radicals and provides a protection from oxidation for low-density lipoprotein cholesterol (LDL-C) (26). Moreover, it also has anti-inflammatory and anti-complement properties (27, 28). Considering all of these factors, the results support the concept that bilirubin can potentially provide beneficial effects against the possible pathophysiologic mechanisms associated with the onset of no-reflow.

Study Limitation

There are some limitations of the study that should be noted. First, it was a retrospective, single-center study, and the sample size was relatively small. However, the mean follow-up period of about five years was comparatively long. Second, white blood cells are only one kind of marker for inflammation response, and the other inflammatory and oxidative stress markers were not examined.

Conclusion

In no-reflow patients with STEMI treated by primary coronary angiography, a higher serum TB level was positively associated with in-hospital cardiovascular mortality, but it was not an independent prognostic predictor for long-term mortality. Thus, the TB level may be an available and useful biomarker for risk stratification in these patients. All these findings need to be investigated further in the future through other large-scale, prospective studies.

Acknowledgments

The authors thank professor Sun ZJ, Liu HB, Guo J, Wang SX and Jingjing for technical assistance in images and statistical analysis.

Authors Contribution

Jianfeng Liu developed the original idea and the protocol, wrote the manuscript and analysis and interpretation of data. Changhua Wang, Jinwen Wang and Jing Wang contributed to collecting data. Junjie Yang was responsible for critical revision of the manuscript for important intellectual content. Feng Tian was responsible for Administrative, technical, and material support. Shanshan Zhou was responsible for Statistical analysis. Yundai Chen was responsible for study supervision.

Conflict of Interest

All authors declare that there is no conflict of interest.

Funding

This study was supported by the Beijing Municipal Science and Technology Commission, China (Z121107001012002) and Doctorial Innovation Fund Project of Chinese PLA General Hospital (No. 11BCZ05).

References

1. Jaffe R, Charron T, Puley G, Dick A, Strauss BH. Microvascular obstruction and the no-reflow phenomenon after percutaneous coronary intervention. Circulation. 2008;117(24):3152-6.
2. Bekkers SC, Yazdani SK, Virmani R, Waltenberger J. Microvascular obstruction: underlying pathophysiology and clinical diagnosis. J Am Coll Cardiol.

2010;55(16):1649-60.
3. Stocker R, Yamamoto Y, McDonagh AF, Glazer AN, Ames BN. Bilirubin is an antioxidant of possible physiological importance. Science. 1987;235(4792):1043-6.
4. Vitek L, Jirsa M, Brodanova M, Kalab M, Marecek Z, Danzig V, et al. Gilbert syndrome and ischemic heart disease: a protective effect of elevated bilirubin levels. Atherosclerosis. 2002;160(2):449-56.
5. Vitek L, Schwertner HA. The heme catabolic pathway and its protective effects on oxidative stress-mediated diseases. Adv Clin Chem. 2007;43:1-57.
6. Mazzone GL, Rigato I, Ostrow JD, Bossi F, Bortoluzzi A, Sukowati CH, et al. Bilirubin inhibits the TNFalpha-related induction of three endothelial adhesion molecules. Biochem Biophys Res Commun. 2009;386(2):338-44.
7. Ghem C, Sarmento-Leite RE, de Quadros AS, Rossetto S, Gottschall CA. Serum bilirubin concentration in patients with an established coronary artery disease. Int Heart J. 2010;51(2):86-91.
8. Troughton JA, Woodside JV, Young IS, Arveiler D, Amouyel P, Ferrieres J, et al. Bilirubin and coronary heart disease risk in the Prospective Epidemiological Study of Myocardial Infarction (PRIME). Eur J Cardiovasc Prev Rehabil. 2007;14(1):79-84.
9. Novotny L, Vitek L. Inverse relationship between serum bilirubin and atherosclerosis in men: a meta-analysis of published studies. Exp Biol Med (Maywood). 2003;228(5):568-71.
10. Djousse L, Levy D, Cupples LA, Evans JC, D'Agostino RB, Ellison RC. Total serum bilirubin and risk of cardiovascular disease in the Framingham offspring study. Am J Cardiol. 2001;87(10):1196-200; A4, 7.
11. Mayer M. Association of serum bilirubin concentration with risk of coronary artery disease. Clin Chem. 2000;46(11):1723-7.
12. Hopkins PN, Wu LL, Hunt SC, James BC, Vincent GM, Williams RR. Higher serum bilirubin is associated with decreased risk for early familial coronary artery disease. Arterioscler Thromb Vasc Biol. 1996;16(2):250-5.
13. Schwertner HA, Jackson WG, Tolan G. Association of low serum concentration of bilirubin with increased risk of coronary artery disease. Clin Chem. 1994;40(1):18-23.
14. Gul M, Uyarel H, Ergelen M, Akgul O, Karaca G, Turen S, et al. Prognostic Value of Total Bilirubin in Patients With ST-Segment Elevation Acute Myocardial Infarction Undergoing Primary Coronary Intervention. Am J Cardiol. 2012.
15. Niccoli G, Burzotta F, Galiuto L, Crea F. Myocardial no-reflow in humans. J Am Coll Cardiol. 2009;54(4):281-92.
16. Ndrepepa G, Tiroch K, Fusaro M, Keta D, Seyfarth M, Byrne RA, et al. 5-year prognostic value of no-reflow phenomenon after percutaneous coronary intervention in patients with acute myocardial infarction. J Am Coll Cardiol. 2010;55(21):2383-9.
17. Jaffe R, Dick A, Strauss BH. Prevention and Treatment of Microvascular Obstruction-Related Myocardial Injury and Coronary No-Reflow Following Percutaneous Coronary Intervention A Systematic Approach. Jacc-Cardiovasc Inte. 2010;3(7):695-704.
18. Mehta RH, Harjai KJ, Boura J, Cox D, Stone GW, O'Neill W, et al. Prognostic significance of transient no-reflow during primary percutaneous coronary intervention for ST-elevation acute myocardial infarction. Am J Cardiol. 2003;92(12):1445-7.
19. Ndrepepa G, Tiroch K, Keta D, Fusaro M, Seyfarth M, Pache J, et al. Predictive factors and impact of no reflow after primary percutaneous coronary intervention in patients with acute myocardial infarction. Circ Cardiovasc Interv. 2010;3(1):27-33.
20. Brosh D, Assali AR, Mager A, Porter A, Hasdai D, Teplitsky I, et al. Effect of no-reflow during primary percutaneous coronary intervention for acute myocardial infarction on six-month mortality. Am J Cardiol. 2007;99(4):442-5.
21. Huang SS, Huang PH, Leu HB, Wu TC, Lin SJ, Chen JW. Serum bilirubin predicts long-term clinical outcomes in patients with cardiac syndrome X. Heart. 2010;96(15):1227-32.
22. Gullu H, Erdogan D, Tok D, Topcu S, Caliskan M, Ulus T, et al. High serum bilirubin concentrations preserve coronary flow reserve and coronary microvascular functions. Arterioscler Thromb Vasc Biol. 2005;25(11):2289-94.
23. Erdogan T, Cicek Y, Kocaman SA, Canga A, Cetin M, Durakoglugil E, et al. Increased serum bilirubin level is related to good collateral development in patients with chronic total coronary occlusion. Intern Med. 2012;51(3):249-55.
24. Ilia R, Wolak A, Amit G, Weinstein JM. Collateral blood flow can predict myocardial blush grade in primary coronary intervention. Catheter Cardiovasc Interv. 2012;80(1):67-70.
25. Okuhara K, Kisaka T, Ozono R, Kurisu S, Inoue I, Soga J, et al. Change in bilirubin level following acute myocardial infarction is an index for heme oxygenase activation. South Med J. 2010;103(9):876-81.
26. Wu TW, Fung KP, Yang CC. Unconjugated bilirubin inhibits the oxidation of human low density lipoprotein better than Trolox. Life Sci. 1994;54(25):P477-81.
27. Takamiya R, Murakami M, Kajimura M, Goda N, Makino N, Takamiya Y, et al. Stabilization of mast cells by heme oxygenase-1: an anti-inflammatory role. Am J Physiol Heart Circ Physiol. 2002;283(3):H861-70.
28. Nakagami T, Toyomura K, Kinoshita T, Morisawa S. A beneficial role of bile pigments as an endogenous tissue protector: anti-complement effects of biliverdin and conjugated bilirubin. Biochim Biophys Acta. 1993;1158(2):189-93.

Lipid and Cardiovascular Research. 2015;**01**(1):37-43
http://www.enochpublisher.com/LCR

ENOCH PUBLISHING CORPORATION

ARTICLE

The Correlation between HDL Particle Size and Stable Coronary Heart Disease

*Rui-Xia Xu, Sha Li, Yuan-lin Guo, Jun Liu, Jing Sun, Cheng-Gang Zhu, Li-Xin Jiang, Jian-Jun Li**

Abstract

Compared with healthy controls, the concentration of total high-density lipoprotein cholesterol (HDL-C), large HDL-C, and medium HDL-C particles was significantly reduced in people with Coronary heart disease (CHD) compared to healthy controls [(41.79±10.83)mg/dl vs. (55.88±15.41) mg/dl, p<0.001; (14.01±5.46) mg/dl vs. (23.38±10.67) mg/dl, p<0.001; (21.08±5.26) mg/dl vs. (25.35±5.33) mg/dl, p<0.001], whereas no significant difference was found with regard to the concentration of small HDL-C particles. The percentage of large HDL-C particles, as a percentage of total HDL-C, was decreased, while the percentages of medium HDL-C and small HDL-C particles were elevated. Multivariate logistic regression analysis showed that age and body mass index were independent predictors of CHD. Larger HDL-C particles negatively correlated with CHD occurrence (OR=0.91, 95%CI: 0.836-0.991, p=0.030). Single-factor analysis of variance showed that the percentage of large HDL-C particles was decreased, while the percentage of small HDL-C particles was increased, according to number of coronary artery lesion branches.

Keywords: high-density lipoprotein cholesterol particles, coronary heart disease, risk factors, coronary artery lesion branches

HDL in coronary artery disease

Coronary heart disease (CHD) is defined as vascular cavity stenosis or obstruction-induced myocardial ischemia, hypoxia, or necrosis of the heart, and is commonly caused by a pathological change of coronary arterial atherosclerosis (1). CHD is ranked first in the global disease causes of death, and its occurrence is closely related to abnormal blood lipids. Epidemiologic data has shown that plasma high-density lipoprotein cholesterol (HDL-C) level is negatively correlated with occurrence of coronary heart disease (CHD) (2, 3). Every elevated 1mg/dl HDL-C contributes to a 2–3% decrease in the incidence of CHD (4). Although decreased plasma HDL-C levels are considered as independent risk factors for CAD, as reflected by a working group report (5), studies which focused on HDL-C concentration enrichment indicated that a simple change of HDL-C level does not delay the pathogenesis of atherosclerosis or reduce cardiovascular disease events (6, 7). Conversely, some therapeutic methods that act via improving HDL-C function and promoting reverse cholesterol transport markedly prevent atherosclerosis (8).

HDL-C is a family of heterogeneous lipoproteins of various sizes, densities, and chemical compositions, as well as different physiological functions (9), and is divided according to size into large, medium, and small particles (10). The change in the particle size results from a feasible transformation between them or the product of metabolic pathways. Each HDL-C particle size represents a unique function that is essential for maintaining the normal metabolism of the body (11). Although the details of the correlation between HDL-C particle size and CHD remain unclear, it has been shown that a disorder of particle size increases cardiovascular risk, including myocardial injury, following elective percutaneous coronary intervention, cardiac autonomic neuropathy (12), and acute coronary syndrome (13).

The present study investigated HDL-C particle size in relation to the occurrence and severity of CHD.

Clinical participants

A total of 90 stable CHD patients, who received interventional treatment in the FuWai Hospital and National Center for Cardiovascular Diseases, Beijing, China, from October 2012 to February 2013 were included, and

Division of Dyslipidemia, State Key Laboratory of Cardiovascular Disease, Fu Wai Hospital; National Center for Cardiovascular Diseases, CAMS and PUMC, Beijing 100037, China

* Corresponding author: Jian-Jun Li
Division of Dyslipidemia, State Key Laboratory of Cardiovascular Disease, Fu Wai Hospital; National Center for Cardiovascular Diseases, CAMS and PUMC, Beijing 100037, China
E-mail: lijnjn@yahoo.com.cn

Received: 28 September 2015 / Accepted: 1 December 2015
Published online: 29 December 2015

each participant provided written, informed consent before enrolment. The study was approved by the hospital's ethical review board and complied with the Declaration of Helsinki.

Inclusion criteria: (I) stable CHD diagnosed by coronary angiogram (CAG); (II) the participants were not receiving any statin therapy; (III) left main, left anterior descending branch, swing, right coronary artery, or its main branches of blood vessel diameter stenosis was at least 50% CAG was conducted according to Judkins' methods (14), and the results were interpreted by two independent interventional physicians. If the two physicians did not agree, the results were given to a third physician for analysis.

Exclusion criteria: (I) clinical or CAG data were not available; (II) acute myocardial infarction or unstable angina pectoris; (III) anemic diseases; (IV) inflammatory disease; (V) thyroid disease; (VI) heart failure (left ventricular ejection fraction < 45%); (VII) severe hepatic or renal dysfunction; (VIII) malignant tumor; and (IX) blood diseases.

In addition, 40 healthy adults were recruited as controls.

General information

The participants were aged 56.98±8.38 years and 66.7% were male. Several CHD risk factors were defined as follows:
Hypertension: systolic blood pressure ≥140mmHg (1mmHg=0.133kpa) and/or diastolic pressure ≥90mmHg or undergoing anti-hypertensive therapy.

Diabetes (diagnostic standard of American Diabetes Association): fasting plasma glucose ≥ 7.0mmol/L or plasma glucose ≥11.1 mmol/L at 2 hours post glucose tolerance test or undergoing oral antidiabetic therapy.

Smoking history: at least 1 cigarette per day for over 1 year.

Family history: first-degree relatives with CHD - men aged under 55 years or women aged under 65 years.

Laboratory measurements

A detailed medical history was recorded for all participants, and physical measurements, including height and weight, were taken. The weight index value was calculated according to body mass index (BMI): height (m)/weight (kg).2
EDTA anticoagulant fasting blood specimens were collected on the morning after hospitalization, and serum samples were isolated from the blood for HDL-C particle detection. The cholesterol contents of HDL particles were electrophoretically determined using high-resolution 3% polyacrylamide gel tubes and the Lipoprint HDL System (Quantimetrix Corporation, Redondo Beach, CA, USA) according to the manufacturer's instructions. HDL-C was then divided into 10 sub fractions. Sub fraction 1–3 represented large HDL-C particles, sub fraction 4–7 indicated intermediate HDL-C particles, and sub fraction 8–10 designated small HDL-C particles.

Table 1. The baseline data in participants with CHD and healthy controls

Characteristics	Control (n=40)	CHD (n=90)	P
Age (years)	40.53±13.45	56.98±8.38	< 0.001
Male N (%)	13(32.5)	60(66.7)	< 0.001
Body mass index (kg/m^2)	22.11±2.83	25.86±3.34	< 0.001
Smoking history N (%)	3 (7.5)	43 (47.8)	< 0.001
Hypertension N (%)	5 (12.5)	61 (67.8)	< 0.001
Diabetes N (%)	2 (5)	25 (27.8)	0.007
Family history of premature CHD N (%)	2 (5.0)	23 (25.6)	0.012
HsCRP (mg/l)	0.97±1.15	3.19±3.32	< 0.001
Apolipoprotein A-I (g/L)	1.61±0.32	1.45±0.29	0.006
Apolipoprotein B (g/L)	0.79±0.16	1.07±0.27	< 0.001
Lp (a) (mg/L)	190.72±195.99	264.16±264.79	0.118
Total cholesterol (mmol/L)	4.99±0.57	4.99±1.06	0.978
Triglyceride (mmol/L)	1.26±0.75	3.35±14.49	0.363
LDL-C (mmol/L)	2.65±0.55	3.20±0.89	< 0.001
HDL-C (mg/dL)	55.88±15.41	41.79±10.83	< 0.001
Large particle HDL-C (mg/dL)	23.38±10.67	14.01±5.46	< 0.001
Medium HDL-C (mg/dL)	25.35±5.33	21.08±5.26	< 0.001
Small particle HDL-C (mg/dL)	6.93±1.85	6.77±2.25	0.697
Large particle HDL-C (%)	40.00±9.26	32.77±6.93	< 0.001
Medium HDL-C (%)	46.68±5.75	50.63±4.24	< 0.001
Small particle HDL-C (%)	13.33±4.12	16.48±4.92	< 0.001

Data presented as mean±SD or percentage (%).
Abbreviation: HsCRP, (high sensitivity C reactive protein);Lp (a), Lipoprotein(a); LDL-C, low-density lipoprotein cholesterol; HDL-C, high-density lipoproteincholesterol.

A

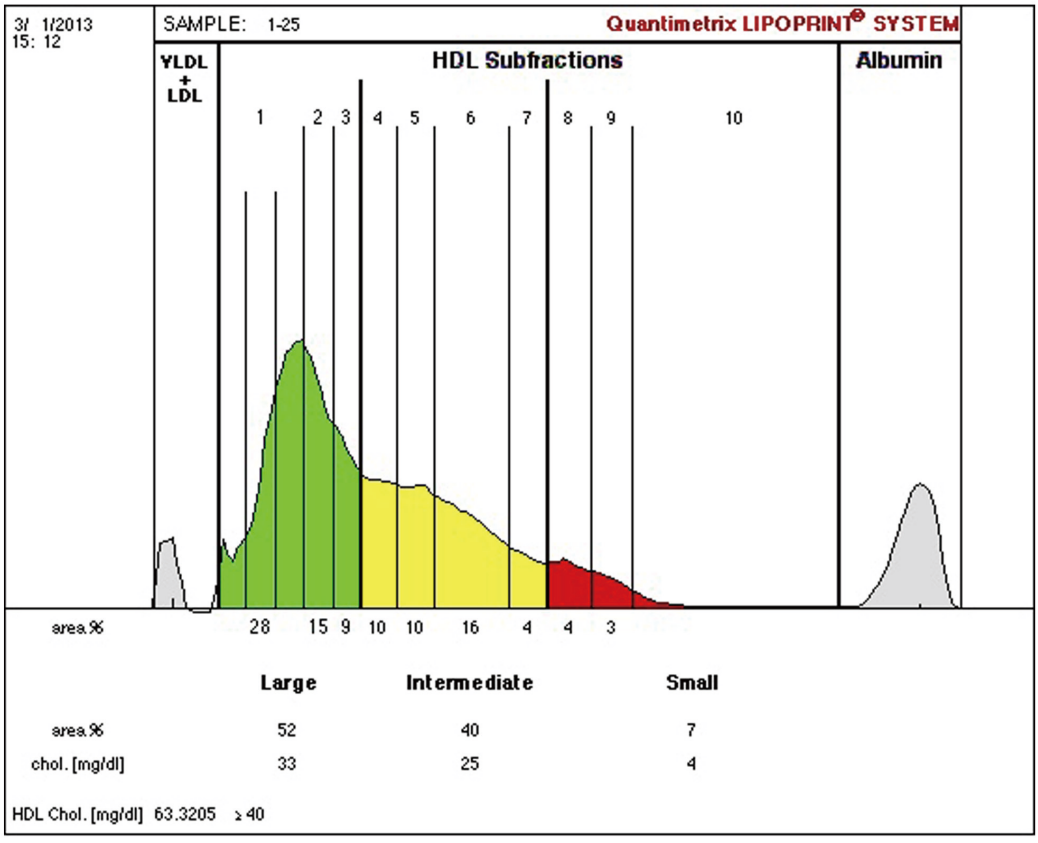

B

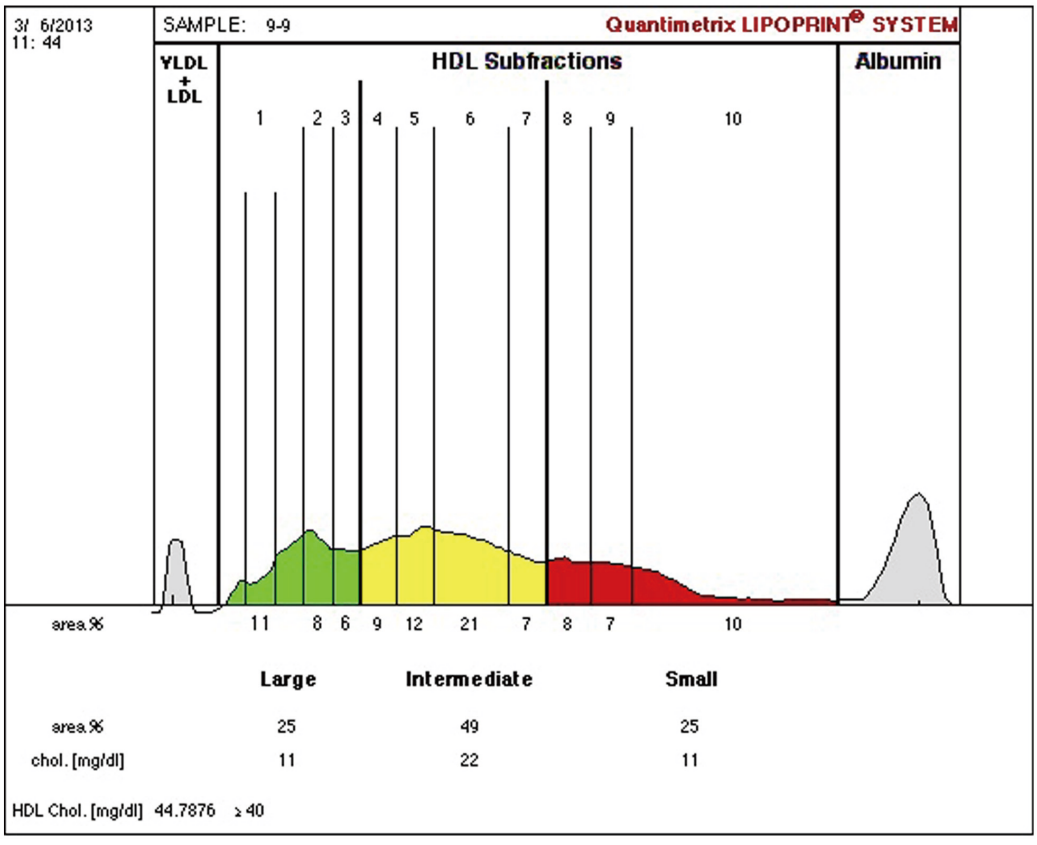

Figure 1. The map of plasma HDL-C particles in a healthy control individual (A) and in a participant with CHD (B) described by the Lipoprint HDL System

Statistical analysis

Statistical Package for the Social Sciences (version 19.0) software (SPSS Inc., Chicago, IL, USA) was used for statistical analysis. An x2 test was used for a between groups comparison of the categorical variables used, a t-test was used to compare continuous variables between the two groups, and a one-way analysis of variance (ANOVA) was used for comparison of three groups. Univariate logistic regression analysis was used to detect the relationship of blood lipid profiles, HDL-C particles, and various traditional CHD risk factors with CHD. Multiple logistic regression analysis was used to determine the independent predictive role of blood lipid profiles, HDL-C particles, and different traditional CHD risk factors with regard to CHD. Statistical significance tests were bilateral, and a difference of $p < 0.05$ was considered statistically significant.

Results

Baseline characteristics

Age, gender, BMI, smoking history, hypertension, diabetes, and family history of CHD differences between participants with CHD and healthy controls were statistically significant ($p<0.05$). Those with CHD had higher plasma levels of high sensitivity C reactive protein, apolipoprotein B, and low-density lipoprotein cholesterol (LDL-C) ($p<0.05$). There was no statistical difference in lipoprotein (a), total cholesterol, and triglyceride level between the two groups ($p>0.05$). The Lipoprint lipoprotein classification results showed that both large and medium HDL-C particles were markedly decreased in participants with CHD, compared to the healthy controls [(23.38±10.67) vs. (14.01±5.46) mg/dl, $p<0.001$; (25.35±5.33) vs. (21.08±5.26) mg/dl, $p<0.001$, respectively]. In addition, the percentage of large HDL-C particles was significantly reduced [(40.00±9.26) vs. (32.77±6.93)%, $p<0.001$], whereas the percentages of medium and small HDL-C particles were elevated, compared to the healthy controls [(46.68±5.75) vs. (50.63±4.24)%, $p<0.001$; (13.33±4.12) vs. (16.48±4.92)%, $p<0.001$]. All of the above data are shown in Table 1.

Figure 1A and 1B respectively show the plasma HDL-C particles map of one healthy control individual and one participant with CHD. In the healthy control, the HDL-C level was 63.32mg/dl, which included 33mg/dl large, 25 mg/dl medium, and 4mg/dl small HDL-C particles. All three classes of particles accounted for 52% (green area), 40% (yellow area), and 7% (red area) of total HDL-C. In the map of the participant with CHD, the HDL-C level was 44.79 mg/dl, which included 11mg/dl large, 22 mg/dl medium, and 11mg/dl small HDL-C particles. All three classes of particles accounted for 25% (green area), 49% (yellow area), and 25% (red area) of total HDL-C. This image shows that healthy people tended to possess more large HDL-C particles, whereas participants with CHD were more likely to have numerous medium and small HDL-C particles.

Association of blood lipid profiles and HDL-C particles with CHD

Atherosclerosis is a pathological, chronic inflammatory reaction of anatomical ECs and VSMCs in the arterial wall [85-87], which is largely mediated by macrophage activation. Initially, ER stress-induced inflammation primarily serves to limit the formation of plaques and facilitate lesion repair. Along with aggregation in unfolded proteins in cells, inflammation develops into an uncontrolled state; that is, abnormal cell death-induced necrosis formation. It is noted that macrophages are observed to abundantly aggregate in plaques and are proven to be involved in the formation of arterial lesions during atherosclerosis, combining with sporadic inflammatory cells including dendritic cells [88], T cells, B cells, and NK cells [89-91]. The initiation step in atherosclerosis is activation of ECs in response to circulatory risk factors and inflammatory mediators that induce the release of interleukin cytokines (IL-4, IL-12, IL-6) and chemokines [92, 93]. To date, increasing evidence indicates that there are signaling links between the UPR and inflammatory reactions through various mechanisms. The dominant inflammatory pathway mediator, NF-κB, is activated by PERK and IRE1 branches of the ER stress-triggered UPR [94]. Also, the IRE1/α-TRAF2 complex recruits and activates IκB kinase (IKK), thereby leading to IκB degrada-

Table 2. The association of lipid profiles and HDL particles with CHD (univariate regression analysis)

Factor	OR	95% CI	P
Total cholesterol (mmol/L)	1.006	0.673-1.503	0.977
Triglyceride (mmol/L)	2.603	1.391-4.869	0.003
LDL-C (mmol/L)	2.512	1.446-4.364	0.001
HDL-C (mg/dL)	0.922	0.891-0.954	< 0.001
Large particle HDL-C (mg/dL)	0.862	0.811-0.915	< 0.001
Medium HDL-C (mg/dL)	0.866	0.803-0.934	< 0.001
Small particle HDL-C (mg/dL)	0.965	0.810-1.151	0.695
Large particle HDL-C (%)	0.892	0.845-0.941	< 0.001
Medium HDL-C (%)	1.179	1.084-1.283	< 0.001
Small particle HDL-C (%)	1.159	1.061-1.266	< 0.001

LDL-C, low-density lipoproteincholesterol; HDL-C, high-density lipoproteincholesterol.

Table 3. Multivariate analysis to determine the independent predictors of CHD

Factor	OR	95% CI	P
Age (years)	1.104	1.042-1.171	0.001
BMI (kg/m^2)	1.228	1.003-1.504	0.046
Large particle HDL-C (mg/dL)	0.91	0.836-0.991	0.030

BMI, body mass index; HDL-C, high-density lipoproteincholesterol.

tion and activation of NF-κB. The integration of ATF4 with XBP1 stimulates the production of inflammatory cytokines IL-8 and IL-6 [95]. Another inflammatory mediator, AP1 transcriptional factor, is activated in response to oxidative stress [96].

Convincing proof has accumulated in cultured ECs that supports a connection between ER stress and inflammation in atherosclerosis. Studies using human aortic ECs found that inflammation-related genes IL-8, IL-6, monocyte chemoattractant protein 1 (MCP1), and the chemokine CXC motif ligand 3 (CXCL3) were induced by the UPR activator tunicamycin [95]. A histological identification in vivo supported this link by determining a finding that activated UPR is shown in areas of human oxidized phospholipid-enriched endothelium lesions. High concentrations of oxidized phospholipids (OxPLs) that are commonly identified in atherosclerotic lesions can activate UPR in ECs, which is associated with genetic variation in a locus affecting the action of USP16 (ubiquitin-specific protease 16), a histone H2A deubiquitinase [97].

Multiple logistic regression analysis to determine the independent predictors of CHD

TIn the multiple logistic regression analysis, lipid profiles, and HDL-C particle components, as well as age, gender, BMI, family history of CHD, and smoking history, were regarded as the independent variables, and CHD was considered the dependent variable. As shown in Table 3, age (OR=1.104, 95%CI: 1.042-1.71, p=0.001), BMI (OR=1.228, 95%CI: 1.003-1.504, p=0.046) and large HDL-C particles (OR=0.91, 95%CI: 0.836-0.991, p=0.030) were independent predictors of CHD.

Correlation of lipid profiles and HDL-C particles with coronary artery lesion branches

Participants with CHD were divided into three groups, namely, single, double, and treble branches, on the basis of coronary artery lesion branches. One-way ANOVA indicated that concentration of large HDL-C particles tended to decline with an increasing number of coronary lesion branches. The comparison of single and double lesion branches revealed an apparent decrease in the level of large HDL-C particles [(16.05±6.31) vs. (12.63±4.75) mg/dl, p<0.05]. In addition, the comparison with lesions with three branches indicated that the level of large HDL-C particles level had a downward trend, but no statistical difference was observed [(16.05±6.31) vs. (13.56±5.06) mg/dl, p>0.05]. In contrast, the percentage of small HDL-C particles reflected an upward trend, as coronary lesions increased. Significantly, the percentage of small HDL-C particles was elevated in participants with CHD with double, compared to single, coronary lesion branches [(14.52±4.57) vs. (18.11±4.39)%, p<0.05]. Participants with three lesion branches had a higher percentage of small HDL-C particles than those with a single lesion, but no statistical difference was found [(16.44±5.31) vs. (14.52±4.57) mg/dl, p>0.05] (Table 4, Figure 2). There was no correlation between all other lipid profiles and coronary artery lesion branches.

Discussion

Table 4. Correlation of lipid profiles and HDL-C particles with coronary artery lesion branches

Factor	Stable coronary disease(Coronary lesion vessels)		
	Single (N=24)	Double (N=27)	Tripl (N=39)
Total cholesterol(mmol/L)	4.69±0.85	5.03±1.21	5.05±1.04
Triglyceride(mmol/L)	1.71±0.84	2.15±1.42	1.68±0.83
LDL-C (mmol/L)	2.92±0.73	3.20±0.97	3.28±0.89
HDL-C (mg/dL)	44.27±11.36	39.53±11.23	41.40±9.76
Large particle HDL-C (mg/dL)	16.05±6.31	12.63±4.75 *	13.56±5.06
Medium HDL-C (mg/dL)	22.09±5.16	20.04±5.68	21.03±4.92
Small particle HDL-C(mg/dL)	6.29±1.79	7.00±2.17	6.77±2.52
Large particle HDL-C (%)	35.09±7.12	31.33±6.45	32.31±7.19
Medium HDL-C (%)	50.09±3.94	50.59±3.85	51.13±4.78
Small particle HDL-C (%)	14.52±4.57	18.11±4.39 *	16.44±5.31

Data presented as mean±SD or percentage (%). *p<0.05 compared with single vessel.
LDL-C, low-density lipoproteincholesterol; HDL-C, high-density lipoproteincholesterol.

HDL-C possesses an atherosclerosis-resistant function and is involved in the process of atherosclerosis regression, via direct protection of the arterial vascular wall and promotion of cholesterol reverse transport (3). It has been conventionally believed that HDL-C is "good cholesterol" and plays a protective role in cardiovascular and cerebrovascular diseases. However, recent studies have pointed out that while certain components of HDL-C are indeed beneficial with regard to cardiovascular diseases, other components might cause atherosclerosis (15). This suggests that HDL-C particle sizes are closely related to function, but the role of different sizes of HDL-C particles in the process of atherosclerosis remains unclear (16).

In the present study, people with CHD had lower levels of total HDL-C, large, and medium HDL-C particles than did healthy control individuals. Of total HDL-C, the percentage rate of large HDL-C particles was significantly reduced, whereas the percentages of both medium and small HDL-C particles were apparently increased. These data indicated that healthy people mainly possess large HDL-C particles, whereas medium and small HDL-C particles are dominant in people with CHD. Our findings are in accordance with those of previous studies (17). Controversially, Kontush et al. pointed out that small HDL-C particles exerted a greater influence on cholesterol reversal than did large HDL-C particles (18), and it is the small, rather than the large, HDL-C particles that play a pivotal role in anti-atherosclerosis (19). Therefore, the changes in concentration and percentage of all sizes of particles might be predictive factors in CHD. We next evaluated possible risk factors for the people with CHD by single-factor logistic regression analysis. The results revealed that the distribution of triglycerides, total LDL-C, medium HDL-C percentage/concentration, and small HDL-C percentage/concentration were significantly different between participants with CHD and healthy controls. Our data also suggested that percentage and concentration of total HDL-C, medium HDL-C, and large HDL-C were negatively correlated with CHD. Multiple logistic regression analysis revealed that age, BMI and large HDL-C particles were independent predictors of CHD. All of our data suggested that large HDL-C particles were negatively correlated with CHD, and therefore large HDL-C particles are considered to be a protective factor.

Since CHD results from coronary artery stenosis or obstruction, we characterized CHD severity by the amount of branches OF coronary arteries lesion (20). We divided participants with CHD into three groups, namely, single, double, and triple branches, on the basis of the coronary angiogram results (21). The one-way ANOVA showed that large HDL-C particles showed a trend toward decline as the number of coronary lesion branches increased. In contrast, the percentage of small HDL-C particles was increased with an increased number of coronary lesion branches. These data indicated that the progression of CHD may relate to decreased large HDL-C particles in plasma, and an elevated level of small HDL-C particles.

In conclusion, our study showed that the plasma level of large HDL-C particles is associated with occurrence of CHD. In addition, a decreased percentage of large HDL-C particles and an elevated percentage of small HDL-C particles are significantly correlated with CHD severity.

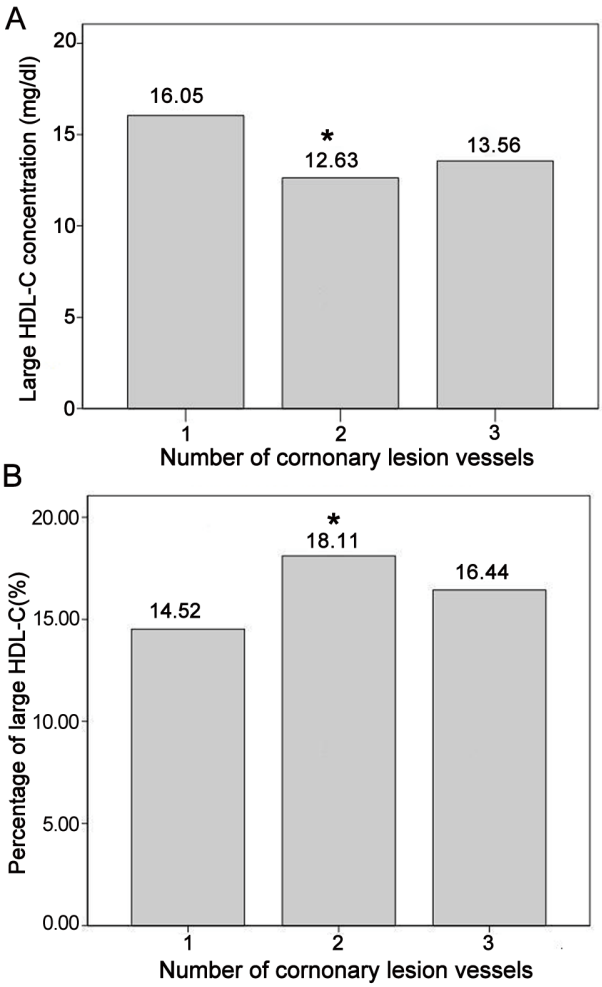

Figure 2. The concentration of large HDL-C particles (A) and larg e HDL-C percentage (B) in patients with single, double, and triple numbers of diseased coronary arteries

Conflict of Interest

All authors declare that there is no conflict of interest.

References

1. Yousuf FA, Iqbal MP. Review: Apolipoprotein E (Apo E) gene polymorphism and coronary heart disease in Asian populations. Pakistan journal of pharmaceutical sciences. 2015;28(4):1439-44.
2. Agarwala AP, Rodrigues A, Risman M, McCoy M, Trindade K, Qu L, et al. High-Density Lipoprotein (HDL) Phospholipid Content and Cholesterol Efflux Capacity Are Reduced in Patients With Very High HDL Cholesterol and Coronary Disease. Arteriosclerosis, thrombosis, and vascular biology. 2015;35(6):1515-9.
3. Vergeer M, Holleboom AG, Kastelein JJ, Kuivenhoven

JA. The HDL hypothesis: does high-density lipoprotein protect from atherosclerosis? Journal of lipid research. 2010;51(8):2058-73.
4. McGrowder D, Riley C, Morrison EY, Gordon L. The role of high-density lipoproteins in reducing the risk of vascular diseases, neurogenerative disorders, and cancer. Cholesterol. 2011;2011:496925.
5. Gotto AM, Jr. Low high-density lipoprotein cholesterol as a risk factor in coronary heart disease: a working group report. Circulation. 2001;103(17):2213-8.
6. Heinecke JW. Small HDL promotes cholesterol efflux by the ABCA1 pathway in macrophages: implications for therapies targeted to HDL. Circulation research. 2015;116(7):1101-3.
7. Do RQ, Nicholls SJ, Schwartz GG. Evolving targets for lipid-modifying therapy. EMBO molecular medicine. 2014;6(10):1215-30.
8. Duffy D, Rader DJ. Emerging therapies targeting high-density lipoprotein metabolism and reverse cholesterol transport. Circulation. 2006;113(8):1140-50.
9. Zhou L, Li C, Gao L, Wang A. High-density lipoprotein synthesis and metabolism (Review). Molecular medicine reports. 2015.
10. Razavi AE, Ani M, Pourfarzam M, Naderi GA. Associations between high density lipoprotein mean particle size and serum paraoxonase-1 activity. Journal of research in medical sciences : the official journal of Isfahan University of Medical Sciences. 2012;17(11):1020-6.
11. German JB, Smilowitz JT, Zivkovic AM. Lipoproteins:
12. Jang EH, Park YM, Hur J, Kim MK, Ko SH, Baek KH, et al. Higher levels of small dense low-density lipoprotein (LDL) are associated with cardiac autonomic neuropathy in patients with type 2 diabetes. Diabetic medicine : a journal of the British Diabetic Association. 2013;30(6):694-701.
13. Emami Razavi A, Basati G, Varshosaz J, Abdi S. Association between HDL particles size and myeloperoxidase/ paraoxonase-1 (MPO/PON1) ratio in patients with acute coronary syndrome. Acta medica Iranica. 2013;51(6):365-71.
14. Scheffel H, Alkadhi H, Plass A, Vachenauer R, Desbiolles L, Gaemperli O, et al. Accuracy of dual-source CT coronary angiography: First experience in a high pretest probability population without heart rate control. European radiology. 2006;16(12):2739-47.
15. Goliasch G, Oravec S, Blessberger H, Dostal E, Hoke M, Wojta J, et al. Relative importance of different lipid risk factors for the development of myocardial infarction at a very young age (</= 40 years of age). European journal of clinical investigation. 2012;42(6):631-6.
16. Florentin M, Liberopoulos EN, Wierzbicki AS, Mikhailidis DP. Multiple actions of high-density lipoprotein. Current opinion in cardiology. 2008;23(4):370-8.
17. Kadi H, Ozyurt H, Ceyhan K, Koc F, Celik A, Burucu T. The relationship between high-density lipoprotein cholesterol and coronary collateral circulation in patients with coronary artery disease. Journal of investigative medicine : the official publication of the American Federation for Clinical Research. 2012;60(5):808-12.
18. Kontush A, Chapman MJ. Antiatherogenic small, dense HDL--guardian angel of the arterial wall? Nature clinical practice Cardiovascular medicine. 2006;3(3):144-53.
19. Hansel B, Giral P, Nobecourt E, Chantepie S, Bruckert E, Chapman MJ, et al. Metabolic syndrome is associated with elevated oxidative stress and dysfunctional dense high-density lipoprotein particles displaying impaired antioxidative activity. The Journal of clinical endocrinology and metabolism. 2004;89(10):4963-71.
20. Scognamiglio G, Babu-Narayan SV, Rubens MB, Gatzoulis MA, Li W. The Essential Role of Imaging in the Evaluation of Patients With Pulmonary Arterial Hypertension in Association With Congenital Heart Disease. Advances in Pulmonary Hypertension. 2013.
21. Corporation HP. Relation of High-Density Lipoprotein Cholesterol and Apoprotein A1 Levels with Presence and Severity of Coronary Obstruction. International Scholarly Research Notices. 2012;2012.

CASE REPORT

Lipid and Cardiovascular Research. 2015;**01**(1):44-47
http://www.enochpublisher.com/LCR

Cyst-like Structure in the Noncoronary Sinus of Valsalva

*Su-Juan Yan, Ren-Qiang Yang, Mei-Zhen Xu,Hai Su, Yan-Na Liu, Qing-Hua Wu, Yan-Qing Wu, Xiao-Shu Cheng, Xing-Hua Jiang**

Abstract

The most common congenital anomaly of the sinus of valsalva is the sinus of valsalva aneurysm (SVA), which can be easily ruptured, causing severe outcomes. In this report, we describe the case of a 65-year-old man who developed a cyst-like structure in the sinus of valsalva, which can be easily misdiagnosed as an SVA. Although the cyst-like mass was thick, its wall was smooth and it had a low risk of rupture. Therefore, it was diagnosed as a benign anomaly.

Keywords: sinus of Valsalva, cyst-like structure, sinus of valsalva aneurysm, benign anomaly

Introduction

The sinuses of valsalva are 3 distinct outpouchings of the aortic wall and are associated with the 3 cusps of the aortic valve. Sinus of valsalva aneurysm (SVA) is a rare cardiac malformation that is congenital in most cases and is usually located at the right coronary or noncoronary sinus(1). Congenital anomalies of the sinus of valsalva are very rare(2) . However, they frequently co-occur with ventricular septal defects (VSD), aortic valve dysfunction, or other cardiac abnormalities. SVA has a higher incidence among Asians, a male preponderance, and it accounts for 0.1% to 3.5% of all congenital heart defects. An autopsy series reported its prevalence to be 0.09% (3). SVA can also be acquired through conditions affecting the aortic wall , such as infections, trauma, or degenerative diseases. Moreover, compression of the left coronary arteries by SVA has been identified as a potentially life-threatening condition (4), as it may lead to refractory angina, persistent myocardial dysfunction, and sudden cardiac death. The clinical manifestations of SVA vary widely. Although both unruptured and ruptured SVAs are associated with potentially life-threatening complications, unruptured SVAs are usually asymptomatic, originate mostly from the right aortic sinus, and are discovered incidentally (5). On the other hand, ruptured SVAs cause symptoms similar to those of heart failure and produce a continuous, mechanical-sounding murmur (6). The rarity of SVA and its scattered multinational incidence make it difficult to track and study. Early diagnosis and immediate surgical treatment can save the patient's life in most cases. In the current study, we report the case of a 65-year-old man who developed a cyst-like structure in the noncoronary sinus of valsalva that was resembled an SVA.

Case Report

A 65-year-old man presented with symptoms of chest distress, breathlessness, and cough. He had been suffering from hypertension for 5 years. Physical examination revealed that the heart had enlarged to the left and inferiorly; a grade 2/6 blowing systolic murmur was heard over the cardiac apex; and moist rales were heard over the left lower lung field. No other abnormalities were detected. Electrocardiogram (ECG) showed a sinus rhythm, ventricular premature beats, and a complete left bundle-branch block. However, the echocardiogram showed a cyst-like structure extending from the right atria to the noncoronary sinus of valsalva; it was 35 × 35 mm in size with a 2.6-mm thick smooth wall. In addition, an enlarged left ventricle and right atrium as well as decreased left ventricular systolic function with an ejection fraction of 31% were noted (Figures 1 and 2). To confirm the echocardiogram findings, we performed percutaneous arterial angiography and found a cyst-like mass connected to the noncoronary sinus and invading the right atrium (Figure 3).

Discussion

SVA is confined to one aortic sinus that stems from incomplete fusion of the aortic media and the aortic valve annulus, a weakness that may result in the rupture of the sinus, a large left-to-right shunt, and severe congestive heart failure (7, 8). SVA may be congenital or acquired, and it consists of a localized diverticular outpouching of the coronary sinus. Approximately two-thirds

Department of Cardiology, Second Affiliated Hospital of Nanchang University, Nanchang 330006, China

* Corresponding author: Xing-Hua Jiang
Department of cardiology, the Second Affiliated Hospital of Nanchang University, Nanchang 330006, China
Tel: +8613197912195
E-mail: jiangxhcq@qq.com

Received: 27 October 2015 / Accepted: 3 December 2015
Published online: 29 December 2015

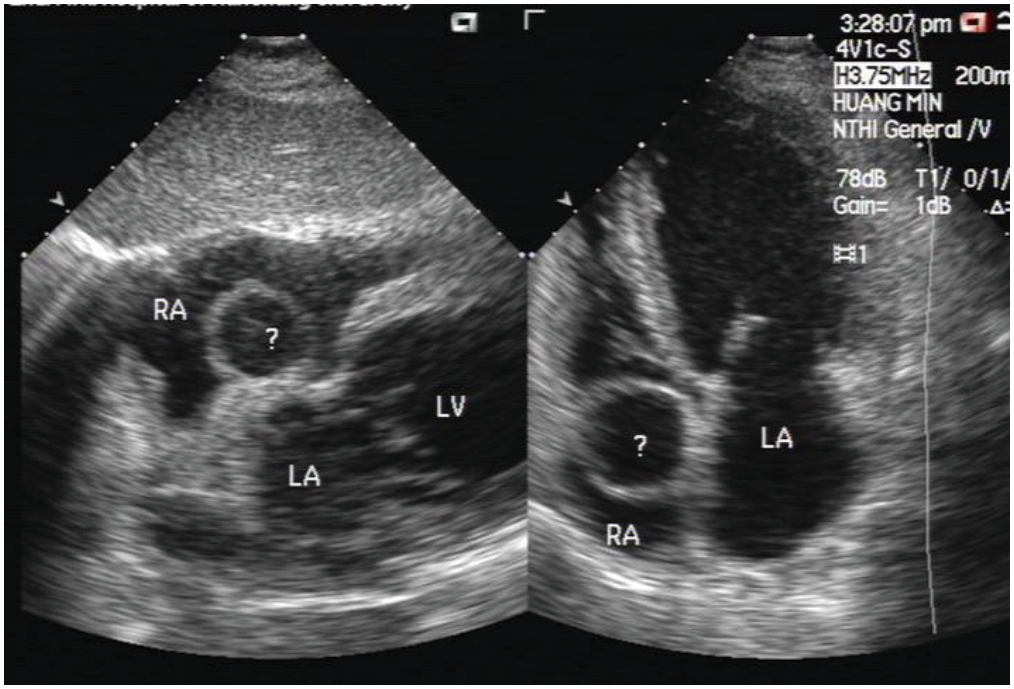

Figure 1. Two 4-chamber echocardiograms show a cyst-like structure in the right atrium. This structure appears to be adhering to the atrial septum

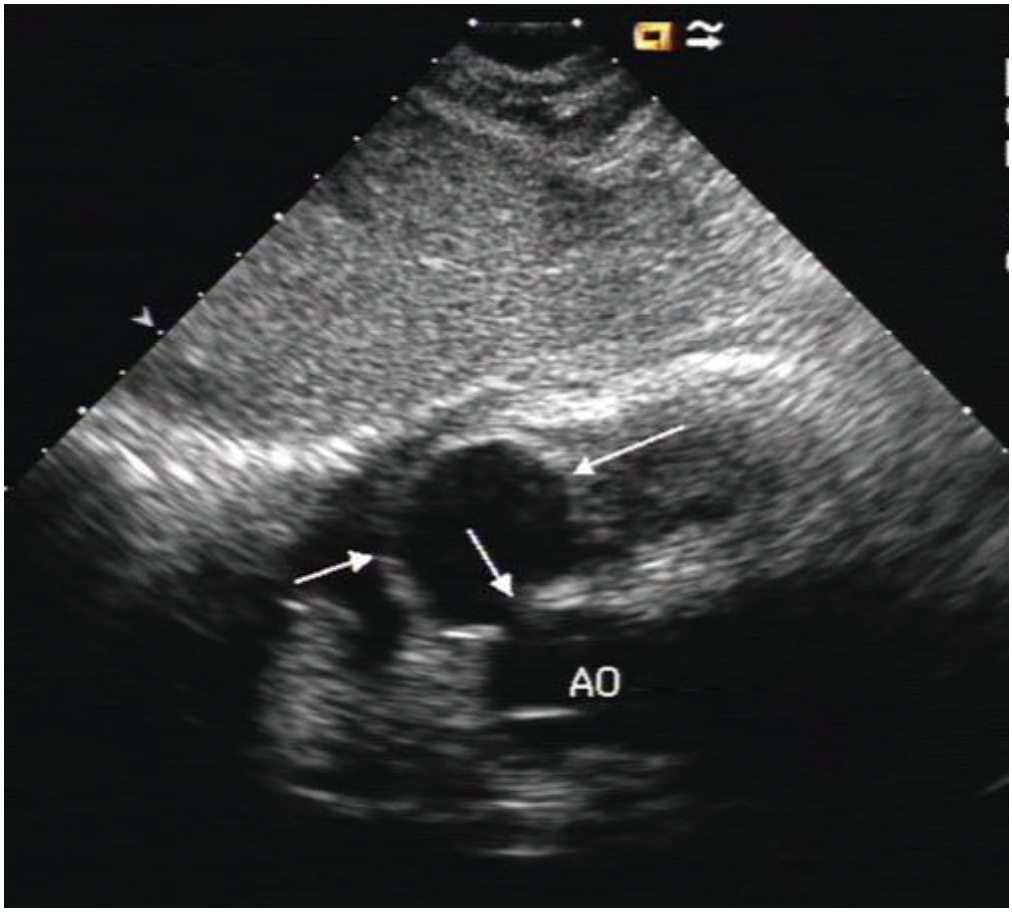

Figure 2. A 4-chamber echocardiogram shows that the cyst-like structure is connected to the aorta.

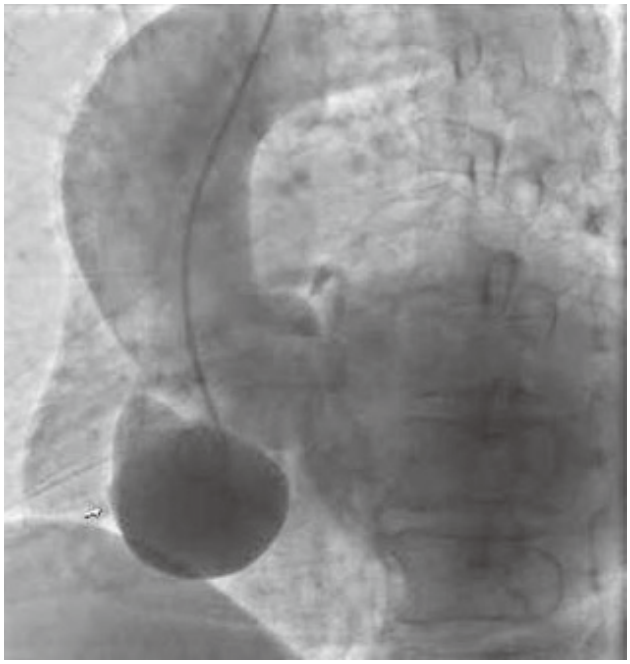

Figure 3. the visualization of percutaneous cardiac catheterization shows that the catheter can goes into the cyst-like structure

of the surgically resected SVA cases are congenital; endocarditis, syphilis, and atherosclerosis are the main causes for acquired cases (9). SVAs may be associated with other congenital anomalies such as VSD and atrial septal defect (10, 11). In particular, associated VSD was found in 15 of 129 patients (11.6%) with SVA. Normally, SVA is asymptomatic if unruptured. Occasionally, overstretching of the left main coronary stem by a large left SVA can cause an acute coronary syndrome or even cardiogenic shock (12, 13), but when the SVA ruptures or a fistula develops, symptoms begin to appear and the patient's condition deteriorates rapidly (6). The rupture of a sinus aneurysm can create an aortocardiac fistula (14). Ruptured SVAs may cause cardiac arrest, congestive heart failure, acute chest pain, ischemic electrocardiographic changes, hypotension, and a sudden onset of lower extremity edema; alternatively, it can be asymptomatic (15). The variations in clinical manifestation and presentation make it difficult to diagnose ruptured SVAs, which are largely dependent on the cardiac chamber in which the aortocardiac fistula develops. However, ruptured SVAs can be relatively easily detected using procedures like transesophageal and transthoracic cardiography, and once detected, timely interventions including surgical repairs and percutaneous closure of the ruptured SVA should be performed as they have low risk and generally an excellent long-term prognosis (16). On the basis of our patient's symptoms and the results of the examinations, we concluded that the cyst-like structure in the noncoronary sinus is congenital, making this a rare case. This structure was quite different from an SVA, which has even smooth wall and low risk of rupture. In addition, its presence does not affect the hemodynamics. Therefore, the structural changes in the left ventricle and other symptoms observed in our patient may have been caused by hypertension.

Conclusion

The cyst-like mass observed in the sinus valsalva was different from an SVA. It was diagnosed as a benign congenital anomaly that did not need special treatment. Hence, only follow-up was prescribed to the patient.

Conflict of Interest

All authors declare that there is no conflict of interest.

References

1. Feldman DN, Roman MJ. Aneurysms of the sinuses of Valsalva. Cardiology. 2006;106(2):73-81.
2. Sachdeva A, Bhatia N, Pau B, Kumar V. Sinus of valsalva aneurysm. The Journal of the Association of Physicians of India. 2013;61(9):655.
3. Troupis JM, Nasis A, Pasricha S, Patel M, Ellims AH, Seneviratne S. Sinus valsalva aneurysm on cardiac CT angiography: assessment and detection. Journal of medical imaging and radiation oncology. 2013;57(4):444-7.
4. de Jesus Perez VA, Haddad F, Vagelos RH, Fearon W, Feinstein J, Zamanian RT. Angina associated with left main coronary artery compression in pulmonary hypertension. The Journal of heart and lung transplantation : the official publication of the International Society for Heart Transplantation. 2009;28(5):527-30.
5. Thankachen R, Gnanamuthu R, Doshi H, Shukla V, Korula RJ. Unruptured aneurysm of the sinus of Valsalva presenting with right ventricular outflow obstruction. Texas Heart Institute journal / from the Texas Heart Institute of St Luke's Episcopal Hospital, Texas Children's Hospital. 2003;30(2):152-4.
6. Ott DA. Aneurysm of the sinus of valsalva. Seminars in thoracic and cardiovascular surgery Pediatric cardiac surgery annual. 2006:165-76.
7. Tong S, Zhong L, Liu J, Yao Q, Guo Y, Shu M, et al. The immediate and follow-up results of transcatheter occlusion of the ruptured sinus of Valsalva aneurysm with duct occluder. The Journal of invasive cardiology. 2014;26(2):55-9.
8. Sivadasanpillai H, Valaparambil A, Sivasubramonian S, Mahadevan KK, Sasidharan B, Namboodiri N, et al. Percutaneous closure of ruptured sinus of Valsalva aneurysms: intermediate term follow-up results. EuroIntervention : journal of EuroPCR in collaboration with the Working Group on Interventional Cardiology of the European Society of Cardiology. 2010;6(2):214-9.
9. Tipoo Sultan FA, Basir N, Fatimi S. Aneurysm of sinus of Valsalva. Journal of the College of Physicians and Surgeons--Pakistan : JCPSP. 2011;21(3):173-5.
10. Mittal K, Dadhania D, Dey AK, Gadewar R, Hira P. Unruptured Noncoronary Sinus of Valsalva Aneurysm Associated with Atrial Septal Defect (ASD). Journal of clinical and diagnostic research : JCDR. 2015;9(8):TD01-2.
11. Das S, Ladha S, Airan B. Unruptured Sinus of Valsalva Aneurysm with Right Ventricular Outflow Tract Ob-

struction and Ventricular Septal Defect--A Rare Combination. Echocardiography. 2015;32(8):1322-4.
12. Martinez-Comendador J, Gualis J, Martin CE, Santamaria A. Left main coronary artery compression by a left sinus of Valsalva aneurysm. Interactive cardiovascular and thoracic surgery. 2013;16(5):713-4.
13. Karvounaris S, Michas G, Karampetsos V, Soteriou M, Foussas S, Mavrommatis P. Giant Unruptured Left Sinus of Valsalva Aneurysm as an Unusual Cause of Ischemic Heart Failure. Hellenic Journal of Cardiology. 2015;56.
14. Marian F, Svatopluk N, Tomas A, Petr N. Ruptured aneurysm of non-coronary sinus of valsalva as a rare cause of chest pain. European Heart Journal. 2014;35(31):2123-.
15. Golzari M, Riebman JB. The four seasons of ruptured sinus of valsalva aneurysms: case presentations and review. The heart surgery forum. 2004;7(6):E577-83.
16. Kuriakose EM, Bhatla P, McElhinney DB. Comparison of reported outcomes with percutaneous versus surgical closure of ruptured sinus of Valsalva aneurysm. The American journal of cardiology. 2015;115(3):392-8.

Enoch Publishing Corporation

EPC, an international publisher of peer-reviewed, open-access journals covering a broad range of science, technology and medicine, was founded by a few scholars and registered in the state of Georgia, USA, and has offices in Doraville in USA and Wuxi in China.

Publishing with EPC

* For associations, we can help you to publish your own journal.
* For old publications, we can help you to improve the editing efficiency, optimize the working quality and maximize your journal's global impact.
* For authors, a wide range of journals can be selected.

EPC currently has 6 journals in launching process and is going to launch more than 10 in the coming future. These journals covered multiple medical subjects including immunology, oncology, digest & gastroenterology, cardiovascular, aging disease, gynaecology and obstetrics, respiratory, endocrinology, translational medicine, etc. Papers across the world are invited to be submitted in the form of original articles, reviews, editorials, letters to the Editor, short communications, case reports, etc.

All the journals published by EPC are working towards being indexed in PubMed, Science Citation IndexExpanded, BIOSIS, Scopus, etc.

Our professional and highly efficient team and Online Manuscript Submission and Peer-review System can ensure that every part of the publishing work from sending invitation to online publication will be perfect.

EPC sincerely welcome publishing partners all over the world!

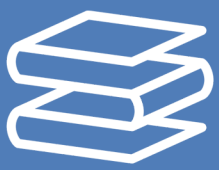

ENOCH PUBLISHING CORPORATION

An international publisher of peer-reviewed, open-access journals covering a broad range of science, technology and medicine

5725 Buford Hwy, Suite 117, Doraville, Georgia 30340, USA

E-mail: service@enochpublisher.com

Http://www.enochpublisher.com